DISSECTING THE SALIVARY GLAND: EPITHELIAL-CENTERED DYSFUNCTION IN PRIMARY SJÖGREN'S SYNDROME

by

Braxton Noll

A dissertation submitted to the faculty of
The University of North Carolina at Charlotte
in partial fulfillment of the requirements
for the degree of Doctor of Philosophy in
Biology

Charlotte

2022

Approved by:

_____
Dr. Valery Grdzelishvili

_____
Dr. Jean-Luc Mougeot

_____
Dr. Farah Mougeot

_____
Dr. Ian Marriott

_____
Dr. Jerry Troutman

ABSTRACT

BRAXTON NOLL. Dissecting The Salivary Gland: Epithelial-Centered Dysfunction in Primary Sjögren's Syndrome. (Under the direction of DR. JEAN-LUC MOUGEOT)

Primary Sjögren's syndrome (pSS) is an autoimmune disease of exocrine tissues causing dry mouth and eyes, mainly affecting women. A culmination of etiologic events leads to the loss of epithelial homeostasis resulting in the MMP9-mediated destruction of the extracellular matrix (ECM). The disease process mainly occurs within the salivary and lacrimal glands and is followed by immune cell infiltration in most cases. Overall, the extent to which the epithelium is involved in the initiation and continuous destruction of glandular structures is supported by a growing body of evidence and is suspected to occur slowly over several years.

Inflammatory mediators and immune cell infiltration were historically the suspected drivers of MMP9 mediated ECM destruction. However, both inflammatory and immune responses that affect salivary/lacrimal glands directly, occur later during disease progression, well after ECM degradation and MMP9 overexpression are observed. Herein, I sought to determine factors capable of regulating MMP9 following the evidential pathogenesis and role of the pSS epithelium.

Using an innovative bioinformatics approach we identified transcription factors, ETS1 and LEF1, as candidate regulators of MMP9 expression. To substantiate these findings, we first determined whether ETS1 and LEF1 are co-overexpressed with MMP9 in pSS labial salivary gland (LSG) biopsies in lieu of infiltrating $CD4^+$ lymphocytes, which also express these factors in pSS. To fully establish a direct *in-vitro* regulatory relationship among ETS1, LEF1 and MMP9, I developed two unique, immortalized salivary gland epithelial cell lines from a pSS (FS=1.8) and a non-pSS "sicca complex" (FS=0.3) patient (Chapter 2). Subsequently, I provided substantial evidence using two salivary gland cancer cell lines and iSGEC line models, regarding the direct regulation of MMP9 by ETS1 in the salivary gland epithelium (Chapter 3). After cloning the MMP9 promoter into a luciferase reporter vector, three significant sites responsible for ETS1

binding were validated *in vitro*. The interaction of ETS1 with the MMP9 promoter was further confirmed by ChIP analysis. ETS1 siRNA mediated knockdown decreased MMP9 mRNA and both intracellular and secreted MMP9 protein levels, overall demonstrating the regulatory effect on MMP9 expression. Taken together, these data suggest that ETS1 regulates MMP9 overexpression in the pSS salivary glands, thereby constituting a significant target for decreasing ECM destruction in pSS, since current MMP9 inhibitors have been proven inadequate.

Many etiologic conditions contributing to the development of pSS have been put forth, including an improper telomere maintenance response after DNA damage, which ultimately leads to senescence associated with telomere shortening in salivary progenitor cells within the pSS epithelium. Beyond functional maintenance of the salivary glands, the ECM regulates repair and re-epithelization by salivary progenitor cells. Disruption of the ECM could be a driving factor related to the excessive replication history and shortened telomeres of pSS salivary progenitor cells. To determine a relationship between ETS1, LEF1, and MMP9 expression, we utilized a PCR-based approach to determine relative telomere length. In Chapter 4**,** I showed that pSS patients had significantly shorter telomeres of saliva DNA compared to healthy controls. Using LSG biopsies of pSS and non-pSS patients, I also determined mRNA overexpression of DNA-damage response mediator, ATM, in pSS patients. These results provided evidence for the impact of DNA damage to the pSS epithelium, suggesting a causal relationship with shortening of salivary telomere DNA, consistent with aging and senescence in peri-menopausal and post-menopausal women. Lastly, telomere shortening significantly correlated with LEF1 expression in LSGs, expanding the relationship between disease activity and expression of previously identified transcription factors. Overall, these data indicate a potential role for LEF1 in telomere-mediated dysfunction and the DNA-damage response within the salivary gland of pSS patients.

DEDICATION

To my parents and wife, who supported me every step of the way.

ACKNOWLEDGEMENTS

I would like to acknowledge the guidance and assistance of both Dr. Jean-Luc Mougeot and Dr. Farah Mougeot, who's wonderful mentorship made all this work possible. Thank you for the unrelenting encouragement, support, and opportunity in your laboratory. I would like to thank my committee: Dr. Valery Grdzelishvili, Dr. Ian Marriott, and Dr. Jerry Troutman for their feedback and assistance. Thank you to all the current and previous members of the Translational Research Laboratory in the Department of Oral Medicine at Carolinas Medical Center, Atrium Health. I would like to especially thank Dr. Nirav Shah for teaching me most of the fundamental techniques I utilized continually throughout my work. I am ever grateful to Dr. Jason Tucker and Dr. Anthony Blaeser for their technical expertise, advice, and for lending me reagents. Thank you to all the clinical and research staff in the Department of Oral Medicine at Carolinas Medical Center, Atrium Health, for their hard work and dedication to obtaining samples and components required for my research goals. I am grateful for Atrium Health in providing the facilities alongside the University of North Carolina at Charlotte Graduate School for Graduate Assistant Support Award (GASP) during the first three years of my degree.

TABLE OF CONTENTS

LIST OF TABLES

LIST OF FIGURES

LIST OF ABBREVIATIONS

AMY1A= Amylase Alpha 1A

AQP5= Aquaporin 5

AQP1= Aquaporin 1

ANO1= Anoctamin 1

AAV= Adeno-associated virus

ATM= ATM Serine/Threonine Kinase

ACTB= β-actin

α-SMA= Actin Alpha 2, Smooth Muscle

A253= submaxillary salivary gland carcinoma

ANA= Anti-nuclear antibody

BSA= bovine serum albumin

Ca^{2+}= Calcium

CDH1= Cadherin-1/ e-cadherin

CLDN1= Claudin 1

CST3= Cystatin C

Ct=Count

ChIP= Chromatin Immunoprecipitation

CXCL10= C-X-C motif chemokine ligand 10

CDKN2A= Cyclin Dependent Kinase Inhibitor 2A

DPBS= Dulbecco's phosphate-buffered saline

DNA= deoxyribonucleic acid

DAPI= 4′,6-diamidino-2-phenylindole

EDTA= Ethylenediaminetetraacetic acid

ELISA= Enzyme-linked immunosorbent assay.

ECM= Extracellular matrix

EGF= Epidermal growth factor

EpCAM= Epithelial Cell Adhesion Molecule

EMT= Epithelial-mesenchymal transition

ETS1= V-Ets Avian Erythroblastosis Virus E26 Oncogene Homolog 1

EMP= Epithelial-mesenchymal plasticity

Epi= epinephrine

FBS= Fetal bovine serum

FS= Focus score

GAPDH= Glyceraldehyde 3-phosphate dehydrogenase

HKGS= Human Keratinocyte Growth Supplement

HMC-3A= human mucoepidermoid carcinoma 3A

HC= Healthy control

HSG= human submandibular gland cell line

HSY= human parotid gland adenocarcinoma cell line

IFN-γ= Interferon-Gamma

iSGEC= immortalized salivary gland epithelial cell line

iSGEC-pSS1= immortalized salivary gland epithelial cell line primary Sjögren's Syndrome-1

iSGEC-nSS1= immortalized salivary gland epithelial cell line non-Sjögren's Syndrome-1

iSGEC-nSS2= immortalized salivary gland epithelial cell line non-Sjögren's Syndrome-2

Ki-67= Marker of Proliferation Ki-67

KRT5= Keratin 5 (also K5)

KRT8= Keratin 8 (also K8)

KRT18= Keratin 18 (also K18)

KRT19= Keratin 19 (also K19)

LSG= Labial salivary gland

LUC= Luciferase

LEF1= Lymphoid enhancer-binding factor 1

MET= Mesenchymal-epithelial transition

MALT= mucosa associated lymphoid tissue

MMP9= Matrix metallopeptidase 9

M-PER= Mammalian protein extraction buffer

MIST1= Basic Helix-Loop-Helix Family Member A15

mRNA= Messenger RNA

MF= multiplication factor (normalization)

NFAT= Nuclear Factor of Activated T cell

NA=Not Available

Non-pSS= non-primary Sjögren's syndrome

ORAI1= ORAI Calcium Release-Activated Calcium Modulator 1

pSS= Primary Sjögren's syndrome

POT1= Protection of Telomeres 1

p-14= passage 14 (early)

p-80= passage 80 (late)

P38-MAPK= Mitogen-Activated Protein Kinase 14

PBMC= Peripheral blood mononuclear cell

qRT-PCR=quantitative real-time polymerase chain reaction

RA= Rheumatoid arthritis

RF= Rheumatoid factor

ROS= reactive oxygen species

RAP1= RAP1A, Member of RAS Oncogene Family

RTL= Relative telomere length

SGEC= Salivary gland epithelial cell

SGCLs= salivary gland cancer cell lines

SLE= systemic lupus erythematosus

SSA= Sjögren's syndrome antigen A (Ro)

SSB= Sjögren’s syndrome antigen B (La)

SV40Lt= SV40 large T antigen

SDS-PAGE= sodium dodecyl sulfate–polyacrylamide gel electrophoresis

SEM= standard error of mean

SD= standard deviation

STIM1= Stromal Interaction Molecule 1

STIM2= Stromal Interaction Molecule 2

SLC12A2= Solute Carrier Family 12 Member 2

SRC= SRC Proto-Oncogene, Non-Receptor Tyrosine Kinase

STR= short tandem repeat

SG= Salivary gland

siRNA= Small interfering RNA

“S” = 36B4U and 36B4D primer set

“T” = Tel1 and Tel2 primer set

TGFβ1= Tumor growth Factor Beta-1

TERT= Telomerase Reverse Transcriptase

TIN2= TERF1 Interacting Nuclear Factor 2

TPP1= Tripeptidyl Peptidase 1

TRF1= Telomeric Repeat Binding Factor 1

TRF2= Telomeric Repeat Binding Factor 2

TRPC1= Transient Receptor Potential Cation Channel Subfamily C Member 1

TBS= Tris-buffered saline

TBST= Tris-buffered saline + Tween-20

TSS= Transcription Start Site

TNFα= Tumor necrosis factor α

VIM= Vimentin

ZO-1= Tight Junction Protein 1

2D= Two dimensional

3D=Three dimensional

CHAPTER 1: INTRODUCTION

1.1.1. Background: Primary Sjögren's syndrome (pSS)

Primary Sjögren's syndrome (pSS) affects approximately 1% of the general population, with a female to male ratio of 9:1 (Parisis et al., 2020). There is currently no cure for pSS, as therapies mainly target the management of symptoms (Min, H.K et al., 2021). Factors including gender, viral infection, genetic predisposition, abnormal innate and adaptive immune responses, and hormonal changes ultimately culminate when hypofunction and destruction of the salivary and lacrimal glands occurs (Parisis et al., 2020). Eventually, lymphocytic infiltration of glandular tissue exacerbates the disorganization and dysfunction of salivary acini structures (Molina et al., 2006). Although pSS is classified as an exocrinopathy, extra-glandular manifestations such as arthralgia, fatigue, myalgia, and Raynaud's phenomenon have been known to occur in as much as 75% of patients (Holdgate, N., & St Clair, E. W., 2016). One significant implication of pSS is the increased risk of developing non-Hodgkin B-cell lymphoma. The current estimates place pSS patients at a 16-fold higher chance of developing lymphoma as compared to the normal population and a cumulative risk of 9.8% after 15 years from pSS diagnosis (Solans-Laqué R et al., 2011). The most common tissue affected by non-Hodgkin B-cell lymphoma among pSS patients is the mucosa associated lymphoid tissue (MALT), where pSS is active (Alunno A, et al., 2018). Like many diseases with multifaceted etiologies, diagnosis can be tedious especially when multiple illnesses are present simultaneously. In the instance of Sjögren's syndrome, approximately 60% of the cases appear in concordance with other autoimmune diseases such as Systemic Lupus Erythematosus (SLE) and rheumatoid arthritis (RA) (*i.e.*, poly-autoimmunity) (Kassan SS, Moutsopoulos HM., 2004). When Sjögren's syndrome occurs in conjunction with another rheumatic disorder and is diagnosed subsequently, it is designated as secondary Sjögren's syndrome in lieu of pSS. In case of RA, roughly 20% of patients are subsequently diagnosed with secondary Sjögren's syndrome (Tim Both et al., 2017). Another complication

related to poly-autoimmunity stems from the high degree of symptom overlap. Up to 46% of systemic lupus erythematosus (SLE) patients and 21% of RA patients report reduced tear production, while 26% and 11% report xerophthalmia, respectively (Gilboe IM et al., 2001). In addition, patients with sarcoidosis, SLE, and viral hepatitis C infection were shown to be subject to lymphocytic infiltration in minor salivary glands (including LSGs) (Radfar, L et al., 2002). The degree of lymphocytic infiltration is based on the determination of the number foci (aggregates) of ≥ 50 lymphocytes (mainly T-cells and B-cells) within 4mm^2 area, corresponding to an ordinal scale of 0-12 focus score (FS), with 12 demonstrating the presence of merged foci (Shiboski CH et al., 2017) (Parisis et al., 2020). Depending on the nature of the autoimmune disease affecting salivary glands, focus scores ranging from 2-6 may be found in 15% of individuals with no clinical reports of keratoconjunctivitis sicca and/ or dry mouth (Radfar, L et al., 2002). With an evident problematic overlap of symptoms among diseases, diagnosis can be troublesome when determining whether a symptom is due to one disease or is a result of multiple diseases presenting simultaneously (Gilboe IM et al., 2001).

1.1.2. Non-pSS "sicca-complex"

Here, we define non-pSS as xerostomic patients who do not meet the diagnostic criteria following the 2017 ACR-EULAR guidelines (*e.g.*, subclinical) (Shiboski CH et al., 2017) (Aqrawi et al., 2019). These patients may suffer from "sicca complex" displaying objective xerostomia (dry mouth) / xeropthalmia (dry eyes) symptoms, however, their diagnostic salivary gland biopsy may not have reached reach the focus score (FS) ≥ 1 and/or do not present with serum Anti-SSA autoantibodies (Shiboski CH et al., 2017). Non-pSS patient's salivary glands may show both histopathological signs of inflammation and display marker(s) of pSS pathogenesis, *i.e.*, fibrosis (Aqrawi et al., 2019). In general, non-pSS sicca patients do not have Anti-SSA antibodies in serum, which carries the same diagnostic weight as a FS ≥ 1 (Shiboski CH et al., 2017) (Aqrawi et al., 2019). Indeed, the ACR-EULAR criteria define pSS based on a set of

inclusive questions (subjective) and objective criteria, which carries a max total point value of 9, where objective criteria scores ≥ 4 meet the threshold for pSS diagnosis (Shiboski CH et al., 2017). A total of five different objective measures are given, where both the presence of serum Anti-SSA and a labial salivary gland FS ≥ 1 each count for three diagnostic points. Patients with non-pSS sicca may demonstrate a positive (+) unstimulated whole saliva flow rate (≤ 0.1 ml per 5 min), (+) Schirmer's test (≤ 5 mm per 5 min, ≥ one eye), and (+) ocular staining score (≥ 5, ≥ one eye), however, may fail to meet the ≥ 4-point threshold. In conclusion, the diagnostic approach to pSS leans towards immune-involved patients, while such approach does not necessarily account for non-immune driven glandular dysfunction (*i.e.*, pSS patients FS≥1 and absence of Anti-SSA).

1.1.3. Limitations to current diagnostic approaches

Clinical manifestations of pSS have been demonstrated to fluctuate over time, such as during the "subclinical" phase's, sicca patients may not express anti-SSA, but eventually will later as the disease progresses (Lais Garreto et al., 2021). The presence of early anti-SSA may define subset(s) of pSS patients as highlighted by (Theander E et al., 2015). This implies that different disease etiologies and pathophysiological mechanisms are involved, converging to the same main outcome: the destruction of salivary glands (Theander E et al., 2015). The involvement of the immune system in pSS development and pathogenesis is accepted by both major institutions responsible for setting the current diagnostic guidelines (ACR-EULAR) (Shiboski CH et al., 2017). Unfortunately, the role and extent to which the immune system has a role in the development and progression of pSS is not well understood.

1.1.4. The need for salivary gland epithelium-specific (or surrogate oral) biomarkers

It is estimated up to 40% of xerostomic sicca patients may present with a negative diagnostic FS (FS<1) (Delli K et al., 2014) (Liao R et al., 2022) (Shiboski CH et al., 2017). Furthermore, as

a marker of disease progression and pathogenesis, FS is significantly associated with other immunologic features (anti-SSA/anti-SSB), while not with xerostomia or xeropthalmia symptoms, based on objective criteria (Berardicurti O, et al., 2021). On the contrary, increased FS could be a prognostic indicator of eventual non-Hodgkin lymphoma development in pSS patients (Berardicurti O, et al., 2021). Similar findings for anti-SSA pertaining to pSS progression have been found where its presence was indicative of systemic manifestations, earlier onset, and higher FS (Mavragani CP et al., 2000) (Fayyaz, A et al., 2016). Using focal scoring for pSS diagnosis provides a variable range of specificity and sensitivity, as outlined in the metanalysis conducted by Berardicurti et al. (Berardicurti O, et al., 2021). Although pSS is classified as a chronic syndrome, heterogeneity among symptomatic and diagnostic manifestations can shift, become more prevalent with age, or vary among individuals (Theander E et al., 2015) (Liao R et al., 2022). Populations of lymphocytic infiltrates shift from early- phase pSS as the syndrome progresses, going from a $CD4^+$ T-cell predominance to a B-cell majority later, therefore altering treatment focus (Christodoulou MI et al., 2010) (Singh, N., & Cohen, P. L.,2012). Patient stratification and disease progression of sicca patients without lymphocyte infiltration within salivary glands (*i.e.*, $0 \leq FS < 1$), may exhibit autoantibodies (ANA, RF, anti-Ro/SSA and anti-La/SSB) in serum years or decades prior to the onset of sicca symptoms (Theander E et al., 2015). Moreover, autoantibody profiles of pSS patients can change significantly over time, carry a large crossover with other rheumatic diseases, and occur in healthy individuals, emphasizing the need for different treatment strategies, biomarkers of progression, and classifications (Didier K. et al., 2018). Therefore, focusing on non-immunologic centered diagnostic approaches and biomarkers could be advantageous in circumventing many of the limitations and discrepancies of the current diagnostic procedures (*i.e.*, anti-SSA (+) and FS) for pSS as listed in Figure 1.8.1.

The time before symptom onset and diagnosis in pSS is estimated to be around 7.5 years (Sebastian, A et al., 2018). Owing to the gradual progression of the disease, treatment early on during the “sub-clinical” phases may prevent the eventual progression to diagnostic levels. In a case-control study by Pertovaara, M et al., roughly 36% of sub-clinical patients were later diagnosed with Sjögren’s syndrome, whereas 50% of subjects with subclinical levels of lymphocytic infiltrates demonstrated an increase in infiltration after an 11-year (median time) follow-up biopsy (Pertovaara, M et al., 1999). Additionally, Pertovaara, M et al., demonstrated an increase in the presence of anti-SSA (40%), anti-SSB (33%), and ANA (58%) from 5%, 4%, and 20%, respectively, after diagnosis of pSS compared to non-pSS sicca patients at a 11-year (median time, range of 8-17 years) follow-up visit (Pertovaara, M et al., 1999). These findings differ slightly from Theander E et al., 2015 who reported the presence of autoantibodies in pre-diagnostic pSS samples to range from 51%-29% for anti-SSA/ SSB and 68% for ANA, during a median time of 4.3-5.1 years (Theander E et al., 2015). Both studies indicated the prevalence of ANA in the post-diagnostic pSS population to be greater than either anti-SSA or anti-SSB, however, ANA was detected at relatively high levels in both control and case groups when compared to other antibodies (anti-SSA, anti-SSB) (Pertovaara, M et al., 1999) (Theander E et al., 2015). Overall, studies by Pertovaara, M et al., and Theander E et al., demonstrate similar etiological considerations regarding the development of pSS where pathogenic markers are present years prior diagnosis and/or symptom onset.

Furthermore, early treatment may aid in preserving salivary gland function rather than restore salivary gland structural integrity (Srivastava, A., & Makarenkova, H. P., 2020). The need for early treatment is supported by the high degrees of similarity between salivary gland expression profiles non-pSS sicca patients compared to pSS patients (Verstappen et al., 2021). Transcriptomic levels of LSG biopsies paired with parotid gland biopsies were relatively the same among pSS (FS>1) and non-pSS sicca patients (FS<1) (Verstappen et al., 2021).

Similarly, when comparing gene expression of cultured primary salivary gland epithelial cells (SGECs) of non-pSS (1<FS>0) to pSS (FS) ≥ 1 patients, we found a striking similarity regarding the overexpression of ETS1 and MMP9 in both groups (Noll et al., 2022).

1.2.1. Barriers to studying and treating pre-immune/ subclinical pSS

Progression and symptoms of pSS can vary depending on age of onset and the presence of autoantibodies (Theander E et al., 2015). Furthermore, re-biopsy of glandular tissue after disease progression among patients initially grouped into the non-pSS “sicca” category then later as pSS, is not recommended by the pSS treatment guidelines (Shiboski CH et al., 2017). Therefore, predicting disease development and progression through longitudinal studies is relatively unfounded and as such been eluded by researchers. To combat the lack of non-pSS sicca-to-clinical pSS transitional biopsy samples, most of the understanding of early-pSS has been elucidated through mouse models. Moreover, due to the late-phase diagnosis of pSS mainly beyond the glandular infiltration stage, treating non-pSS sicca/ pre-immune pSS would most likely involve mechanisms and targets that are not predominantly controlled by the immune system which is the target of many current pSS therapies. Due to the diagnostic weight of glandular focal infiltrates, diagnosis is usually made far into disease progression (Shiboski et al., 2017) (Sebastian, A et al., 2018) (Pertovaara, M et al., 1999). Therefore, focusing on early changes to the salivary epithelium, possibly replicated in the oral mucosal epithelium, including epigenetic, could provide surrogate biomarkers predictive of disease progression towards pSS stage.

1.2.2. The utility of mouse models to investigate early pSS pathogenesis

The use of mouse models for pSS has provided insights into the progression and development with key etiological features arising before immune infiltration into glandular tissue, since these models can at least partially recapitulate pre-immune pSS (Maria, N.I., et al., 2015). The pSS

non-obese diabetic (NOD)- severe combined immune deficiency (scid) mouse model mimics the changes in cell populations of pSS patient salivary glands where an increase in ductal cell populations with concomitant reduction of acinar cell populations in aging mice are observed (Robinson, C. P et al., 1997). NOD-scid pSS mice demonstrate a significant loss of acinar cells between 10-20 weeks of age, independent of lymphocytic infiltrates (Robinson, C. P et al., 1997). The use of NOD mouse models highlights the epithelial-specific dysfunction of the exocrine gland epithelium prior the immune onslaught. Xerostomia (subjective complaint of dry mouth) can result from not only a reduction in saliva secretion, but also from changes in the composition of saliva (Roescher, N et al., 2012). Within the salivary epithelium, ductal cells reabsorb the sodium from the acinar secreted isotonic saliva, thereby having an active role in saliva composition and xerostomia onset caused by pathological conditions, radiotherapy, or medications (Roescher, N et al., 2012). Indeed, pSS patients exhibit increased salivary sodium concentrations, indicating perturbations to the ductal cell compartment (Kalk WW et al., 2002) (Roescher, N et al., 2012). NOD mice demonstrate sialochemistry changes with increased sodium levels as young as age of 8 weeks, indicating early loss of homeostasis within the ductal cell compartment of the salivary epithelium (Roescher, N et al., 2012). In the same study by Roescher, N et al., most of the NOD mice did not exhibit focal lymphocytic infiltration at 8 weeks of age, whereas by 12 weeks all mice exhibited some infiltrates (Roescher, N et al., 2012). In addition, stimulated saliva and FS did not correlate among NOD mice, which is also the case in pSS (Roescher, N et al., 2012). These results further compound the need for better diagnostic approaches to subclinical-pSS and pSS by taking into account disease processes that are associated with autoimmunity and changes specific to the salivary epithelium. Combining disease characteristics and observations in both human pSS patients and mouse models support the notion that the salivary epithelium may be the main initiator/ driver in disease pathogenesis as outlined in Figure 1.8.2.

1.3.1. Challenges in the treatment and classifications of pSS

Revisions to pSS disease classification and treatment have indicated a more individual-targeted approach (Li N et al., 2021) (Bharaj et al., 2021). The use of factors outside of auto-antibody profiling and the determination of lymphocytic infiltration (salivary flow rate or composition) could provide a different strategy in classifying disease progression (Bharaj et al., 2021). Non-immunologic factors for diagnosis could include measures of glandular atrophy/ structure, extracellular matrix profiles/ constituents, inflammatory cytokines, and saliva composition (Bookman AA et al., 2011). The diagnostic determination of pSS relying on immune involvement has been the matter of debate since classification resulted from studies matching different symptoms and manifestations with clinical characteristics (Iris L A Bodewes et al., 2018). A study by Theander et al., concluded that the presence of anti-SSA/SSB was more heavily associated with systemic manifestations and earlier disease onset (Theander et al., 2015). These studies highlight the multifactorial and etiological nature of pSS, in which stratifying pSS patients into different subsets has been helpful in identifying treatments that were more effective therapies among patient subgroups.

1.3.2. Pathophysiology of pSS

Several etiological factors implicated in pSS pathogenesis, including hormonal changes, viral infection, genetic predisposition, immune system defects, and gender (X-chromosome) are responsible for the loss of homeostasis within the salivary epithelium (Parisis et al., 2020). Since the onset of symptoms can occur several years before progressing to clinical pSS, the perturbation of the salivary glands by many etiological factors, including those mentioned above (Figure 1.8.1.), could be interpreted as a low-grade, chronic disruption (Sebastian, A et al., 2018). The disruption may continue until an eventual “catalyst” is met, where these etiologic factors combine or meet with an external agent and deregulate the salivary epithelium. During the earlier phases of pSS, the activity and properties of the salivary gland epithelial cells

(SGECs) change, shifting towards a damaged-repair/ wound-healing phenotype as seen in Epithelial-Mesenchymal Transition (EMT) with a loss in epithelial defining characteristics (Barrera MJ, et al., 2013) (Lu, P et al., 2011) (Nisticò, P., Bissell, M. J., & Radisky, D. C., 2012). The shift in phenotype and expression profile is recapitulated during the de-differentiation of acinar cells after explant culture or when human parotid gland cells are exposed to various inflammatory cytokines (Arce-Franco, M) (Fujita-Yoshigaki J et al., 2008). The change in acinar function is described to be a product of explant culture stress through Src and p38-MAPK pathways, although the exact "stressor" remains unknown (Fujita-Yoshigaki J et al., 2008).

In pSS, the epithelial shape and function are lost alongside the breakdown of the surrounding extracellular matrix (ECM) by the increased expression of matrix metalloproteinases (MMPs), including MMP9 (Perez P et al., 2005) (Goicovich E et al., 2003). The pre-lymphocytic infiltration stage of pSS is associated with increases in acinar cell apoptosis and the destruction of the basal lamina, which corresponds to the ECM layer used for acinar cell attachment (Robinson CP et al., 1996) (Barrera et al., 2013). Destruction of the basal lamina in pSS is localized to the acinar cells and is not seen within the surrounding capillaries (Barrera et al., 2013). The reported destruction is thought to be due to specific proteolytic enzymes secreted by acinar and ductal cells, *i.e.*, MMP9. The overexpression of MMP9 is continued through the clinically diagnosed stages of pSS, where multiple factors (mainly inflammatory factors like nf-κβ) have been demonstrated to regulate its expression (Azuma M et al., 2000). However, the early expression of MMP9 and dysregulation of the salivary ECM occurs prior to infiltration, as seen in pSS mouse models, indicating other transcriptional pathways/ factors are responsible for the initial onset (Robinson CP et al., 1996) (Peck AB et al., 2011). Moreover, the mechanism driving MMP9 could shift during the early non-pSS sicca to clinical pSS phases seen with diagnostic focus score of more than 1 (FS>1). The ECM loss to MMP9 overexpression could prevent the necessary "feedback" loop for the re-epithelization of the damaged epithelia by stem/ progenitor

cells through mesenchymal-epithelial transition (MET) (You, S et al., 2012) (Scott LE et al., 2019). Restoration by resident stem/ progenitor cells remains futile, leaving the gland in its constant state of disrepair. Over time the stem/ progenitor cells are exhausted from perpetual repair - processes and enter a state of telomere-induced senescence which may be exacerbated by lifetime exposure to reactive oxygen species (ROS) involving environmental changes and epigenetics (Pringle S., et al 2019). Based on these previous findings, we sought to determine whether there was a significant correlation among telomere shortening and pSS in saliva-derived DNA (Noll BD, et al., 2020). We indeed demonstrated such correlation existed and also that LSG biopsies of pSS patients overexpressed ATM serine/threonine kinase (ATM), a gene involved in telomere DNA damage response. Dysregulation of the ECM could potentially be a significant, non-immunologic driving force behind salivary dysfunction through telomere-induced senescence. In the following sections, we provide evidence for the dysregulation of ECM and EMT mediated pathways impairing function within the pSS salivary epithelium, and their vast interconnectedness required for maintaining homeostasis.

1.4.1. Structure and function of the salivary gland epithelium: secretory defects in pSS

Salivary glands are primarily composed of acinar, ductal, and myoepithelial cells. Saliva may originate as a mucus based or watery solution produced by mucinous or serous acinar cells, respectively, present in varying proportions within major and minor salivary glands (Gábor Varga 2012) (Porcheri, C., & Mitsiadis, T. A. 2019). Saliva secretion is a complex process involving several different pathways, beginning with neurotransmitter signals (muscarinic (M_3), adrenergic (α_1)) stimulating the release of calcium into the cytoplasm through inositol triphosphate (IP_3) receptor signaling (Gábor Varga 2012) (Porcheri, C., & Mitsiadis, T. A. 2019). The influx of Ca^{2+} into the cytoplasmic space prompts activity of the store-operated calcium entry (SOCE) system. Multiple SOCE partners located within the plasma membrane potentiate Ca^{2+} into the cell, further triggering secondary channels releasing water through the acinar' s

apical pole (Gábor Varga 2012) (Porcheri, C., & Mitsiadis, T. A. 2019). In salivary acini, aquaporin 5 (AQP5) is the primary channel responsible for the release of water from acinar cells into the ductal-lined luminal space (Porcheri, C., & Mitsiadis, T. A. 2019). The saliva composition is further modified by the ductal cells until it is eventually secreted from the final excretory ducts (Porcheri, C., & Mitsiadis, T. A. 2019). Furthermore, myoepithelial cells aid in saliva excretion by contracting the acinus from/ during muscarinic acetylcholine receptor (mAChR) mediated cholinergic stimulation (Porcheri, C., & Mitsiadis, T. A. 2019).

Multiple studies have demonstrated defects in the SOCE pathway within salivary glands of pSS salivary glands (Ambudkar I., 2018). Alterations in Ca^{2+} signaling endoplasmic reticulum (ER) receptor, inositol 1, 4, 5 triphosphate (IP3R) are observed within area of little inflammation and without lymphocytic infiltrates of pSS patients (Teos, L Et al., 2015). Moreover, dysregulation of the osmotic gradient within Madin-Darby canine kidney (MDCK) cell spheroids can induce EMT through changes to E-cadherin mediated adherens junctions (Narayanan V et al., 2020). The observed defects illustrate changes occurring to salivary cell function, without a direct link to inflammatory status (Fox RI, Stern M., 2002) (Nikolov NP, Illei GG., 2009). Changes occurring to the SOCE or Ca^{2+} signaling pathways could be an important step in the dysregulation of the salivary epithelium in early non-pSS sicca disease stages. Downstream to SOCE signaling stands the aquaporin channel 5 (AQP5), which is responsible for apical-end secretion of H_20 by acinar cells (Porcheri, C., & Mitsiadis, T. A. 2019). Exposure of salivary acinar cells to a variety of chemokines alters the composition and presence of tight junctions, which in turn affects cell polarity allowing for diffusion of plasma membrane components to travel from the apical to basal ends (Ewert P, et al., 2010). Without proper secretory control, the ability to maintain internal osmotic levels is lost, leading to the eventual changes in salivary constituents and flow.

1.4.2. Function, development, and maintenance of the salivary gland ECM

Connective interactions between the various cell types and the structural framework within the acinus are dependent on the extracellular matrix (ECM). The ECM directs/mediates cell migration, function, and differentiation through a system of mainly protein-protein interactions (Cox TR, Erler JT., 2011). The chief constituents of the ECM are collagen (type I, IV), laminin, nidogen, proteoglycans, and fibronectin (Cox TR, Erler JT., 2011). Components of the ECM interact with the trans-membrane protein integrin (cell-ECM connection, i.e., hemidesmosomes), providing major signaling cues for establishing cell polarity and conversely cell-cell connections (Sequeira SJ, et al., 2010). The cell-cell connections important to salivary gland acinar function are primarily tight and *adherens* junctions (TJs) (AJs) (Barrera et al., 2013). The actions of the ECM and cell-cell connections mediate polarized secretion of acinar cells into the salivary lumen. Beyond cell polarity, the ECM directs epithelial cell differentiation and developmental signals (Scott LE et al., 2019) (Barrera et al., 2013). ECM components provide signaling cues to the epithelia in a feedback-loop, driving either further ECM degradation (epithelial to mesenchymal transition (EMT)) or epithelial development/ differentiation (mesenchymal to epithelial transition (MET)) (Scott LE et al., 2019). Products generated by ECM degradation inhibit epithelial cell differentiation (e.g., TGFβ1, collagen (IV)) and lead to the expression of EMT associated factors (i.e., Snail, ZEB1/2) (Lu, P et al., 2011). In the instance of pSS, extensive and chronic ECM degradation by MMPs (*i.e.*, MMP9) could be the perpetuating factor in maintaining the salivary epithelium in an undifferentiated and disorganized state. During ligation induced injury, ductal progenitor cells are capable of changing lineage states through dedifferentiation, and into acinar progenitor cells (Weng PL., et al 2018). However, an overabundance of progenitor-like ductal cells ($K5^{+}$) remaining in an undifferentiated state are observed in the salivary glands of the pSS NOD/ShiLtJ mouse model (Gervais, E.M., et al., 2015).

Overall, the ECM is a significant mediator of epithelial homeostasis, and its disruption following MMP9 overexpression could have overwhelming impacts on salivary gland acinar cell function as depicted in Figure 1.8.3. Epithelial cell-ECM interactions not only mediate epithelial homeostasis but are essential during salivary gland development (Sequeira SJ, et al., 2010). Integrin receptors mediate a variety of signaling pathways critical to cell function and are a major source of external cues for differentiation (Wu D., et al 2019). Integrins are commonly located in the plasma membrane, where they act as receptors for various external constituents primarily located with the innermost layer of the ECM, the basement membrane (*e.g.*, laminin) (Wu D., et al 2019). The basement membrane is responsible for signaling both orientation and survival to epithelium alongside several other functions (Wu D., et al 2019). Salivary gland development is mediated through ECM-cell interactions by integrin receptors (α6β1) during the branch formation stages (Porcheri, C., & Mitsiadis, T. A. 2019). Interactions of the epithelium with integrin receptors (α3 and β1) dictate cell polarity (apical-basal) by directing basement membrane formation, and therefore ultimately responsible for directional secretion (Scott LE et al., 2019).

ECM-cell interactions which are dysregulated in pSS, are not only critical for salivary gland homeostasis, but also for salivary gland development (Velozo J et al., 2009). In accordance with salivary gland development, during branching morphogenesis of mammary glands MMPs are expressed at protruding tips of the epithelium (Vu TH, Werb Z., 2000). MMP expression assists in remodeling the ECM, signaling for the migrating epithelium through the activation of latent ECM attached growth factors/ cytokines alongside degradation changes to the ECM constituents (Lu, P et al., 2011, Wiseman et al. 2003; Friedl and Gilmour 2009). ECM-cell interactions are critical for both epithelial function and development and are significantly affected in the pathogenesis of pSS.

The salivary epithelium relies on the ECM for homeostasis and progenitor cell maintenance/ replication (Zhang., et al 2019). Tight and *adherens* junctions (cell-cell) are essential for preserving the barrier function of epithelial (acinar) cells and maintaining their ability for polarized secretion alongside hemidesmosomes (ECM-cell) (M.j. Barrera et al., 2013). Finally, the depolarization of acinar cells alters tight-junctions and expression of e-cadherin (CDH1), causing acinar cells to detach and/or adapt a mesenchymal phenotype, as part of EMT seen in pSS salivary and lacrimal glands (Sisto et al., 2018) (You et al., 2012). Disruption of the ECM and cell-cell connections could be a driving factor in the excessive replication process of salivary progenitor cells in pSS, as determined by telomere length analysis (Pringle et al., 2019). Additionally, as mentioned earlier, salivary telomere DNA length of pSS patients is significantly shorter than healthy control subjects (Noll et al., 2020). Both phenomena can be explained by excessive degradation of extracellular structures, which impairs both epithelial cell function (polarity, secretion) and repair (progenitor cell duplication, re-epithelization, mesenchymal-epithelial transition (MET)).

1.5.1. EMT and Epithelial-Mesenchymal plasticity (EMP) in pSS pathogenesis

Glandular formation and repair are mediated through EMT and MET (You, S et al., 2012) (Nisticò, P et al., 2012). Reciprocal feedback cues from the ECM dictate epithelial migration, secretion (i.e., new basement membrane), and structure formation through multiple forms of EMT (Type I, II, III) (Kalluri R, Weinberg RA 2009). Type I EMT is associated with embryo formation such as during the transitional phase from blastula to gastrula (Kalluri R, Weinberg RA 2009). Type III EMT is the most common referred regarding EMTprocessing and is associated with the mesenchymal shift in epithelial cancer cells and metastatic potential (Kalluri R, Weinberg RA 2009). Type II EMT will be the most referred to EMT process pertaining to pSS pathology and is associated with all four phases of wound healing (Hemostasis, Inflammation, Proliferation, and Remodeling) (Guo S, Dipietro LA., 2010, Zhang J et al., 2019). Moreover,

Type II EMT occurs during tissue repair and fibrosis, of which the latter occurs during more progressed stages of pSS (Leehan, K. M, et al., 2018). Cells undergoing Type II EMT may appear morphologically epithelial and express several epithelial markers (i.e., cytokeratin, e-cadherin (CDH1)), while simultaneously expressing markers of a mesenchymal transition (*i.e.*, alpha-smooth muscle actin (α-SMA), and Vimentin (VIM)) (Kalluri R, Weinberg RA 2009) (Yang, J et al., 2020). In recent years, the rigid classifications of EMT and MET have become blurred, leading to new terminology and phrasing, such as Epithelial-Mesenchymal plasticity (EMP) (Yang, J et al., 2020). The addition of EMP has arisen due to the intermediary stages of EMT or MET where cells exhibit both epithelial and mesenchymal expression markers (Yang, J et al., 2020). Unfortunately, in the context of pSS, the dissection of EMP states has yet to be explored in-depth.

Using our novel immortalized-SGECs (iSGECs) derived from a pSS (iSGEC-pSS1, FS=1.8) and non-pSS sicca (iSGEC-nSS2, FS=0.3) patient, we investigated several epithelial (CDH1, K5, β-catenin) and mesenchymal (VIM) markers by ICC (Noll et al., 2022). iSGEC-pSS1 cells expressed both epithelial markers cytokeratin-5 (K5) and CDH1, while simultaneously expressing high levels of VIM, when compared to iSGEC-nSS2 (Noll et al., 2022). Furthermore, membranous epithelial marker (EpCAM) is aberrantly localized/ expressed in pSS LSGs and was found at very low levels in iSGEC-pSS1 nuclei, while not in the plasma membrane (Noll et al., 2022) (Zhang K et al., 2019). When assessed in primary tumors of Head and Neck Cancer, the reduction of EpCAM was connected to increased VIM expression, owing to a mesenchymal status (Baumeister, P et al., 2018). In addition, levels of cytokeratin 19 ($K19^{+}$) expression in iSGEC-pSS1 cells were much greater than iSGEC nSS2 (data not published). K19 is hypomethylated and overexpressed in pSS SGECs (Konsta OD et al., 2016). Although K19 is an epithelial marker, it has been found to be overexpressed with Vimentin in circulating tumor cells of HNSCC patients, owing to the EMP seen during tumorigenesis (Hiroe Tada et al., 2020).

Furthermore, K19 overexpression is observed in a variety of epithelial malignancies and its overexpression was demonstrated as a response to epithelial EMT transformation (Chin, V. L., & Lim, C. L. 2019). EMP can be both transitory or stable depending on the environment and tissue type and can be mediated through Wnt/β-catenin signaling (Chin, V. L., & Lim, C. L., 2019). In contrast, iSGEC-nSS2 cells displayed a greater epithelial phenotype with high uniform expression of membranous CDH1 and EpCAM (Noll et al., 2022). As previously discussed, the surrounding environment (including paracrine and autocrine signaling) plays a large role in dictating EMT, MET and EMP, therefore, these observed differences could be due to their change in environment (explant). This observation however does corroborate the Type-II EMT process occurring in pSS pathogenesis and highlights the intrinsic activation (even after environmental changes) of the pSS epithelium potentially driving the disease.

Chronic inflammation is commonly proposed to drive of Type 2 EMT (associated with wound healing and fibrosis). The observed “autoimmune-epithelitis” (i.e., chronic inflammation) within pSS salivary glands has been/ could be hypothesized as the source for initiating the observed/ similar Type 2-EMT glandular response. However, fibrosis is more associated with lymphocytic infiltrates, whereas the correlation of glandular function/ main pSS symptoms and infiltrates is not as clear (Verstappen, G.M. et al., 2021) (Fox RI, Stern M., 2002) (Nikolov NP, Illei GG., 2009). Overall, these events suggest a greater role of the salivary epithelium in pSS initiation and pathogenesis, whereas immune involvement compounds many of the pathologic features noted early in the disease. Such as the initial onset of a wound healing response in the salivary glands (Type 2-EMT) promotes the downstream eventual fibrotic changes. Moreover, no association of fibrosis and focus score has been found (Bookman AA et al., 2011). In pSS salivary glands, it appears lymphocytic infiltrates exacerbate the epithelial dysfunction, but are not the initial drivers. Therefore, interruptions in salivary gland form/ function occurring to the ECM or the altered expression of EMT-associated factors disrupting glandular homeostasis are

potential drivers of early salivary hypofunction and future pSS progression, pSS patients frequently have reduced amounts of saliva alongside changes in its composition (Pedersen, A.M.L et al., 2005). In the instance of ligation-induced damage to rat submandibular glands led to functional changes to both acinar and ductal cell populations (Okumura K et al., 2003). After de-ligation, acinar cell populations appeared normal after 8-weeks (Okumura K et al., 2003). In contrast, ductal cell function was still inhibited after 24 weeks measured by sodium and chloride levels within secreted saliva (Okumura K et al., 2003). These changes reflect potential alterations in saliva osmolarity observed within pSS, of which could be initiating and perpetuating the homeostatic disturbance within the salivary epithelium and inducing EMT associated changes (Pedersen, A.M.L et al., 2005).

1.5.2. Dysregulation of EMT associated genes in pSS

Extracellular matrix remodeling is a significant intermediary process during EMT-driven changes to the epithelium (Kalluri R, Weinberg RA 2009). Factors associated with EMT-changes (Increases in Mesenchymal: ETS1, LEF1, MMP9, Vimentin, TGF-β1, SMAD4, collagen type I, Snail, claudin-1,), (Decreases in Epithelial: CDH1, occludin, ZO-1, α6β4 integrin) are found to be differentially expressed or localized in the salivary epithelium of pSS patients (Jordan NV, et al., 2011) (Schenke-Layland K et al., 2008) (Perez P et al., 2005) (Velozo J et al., 2009) (Chen, M et al., 2009) (Sisto M, et al., 2018) (Tandon M et al., 2017) (Suh Y et al., 2013) (Barrera MJ, et al., 2013). Adding to the evidence of a dysregulated or chronic EMT/ EMP response in the salivary epithelium, we uncovered the overexpression of two EMT-associated transcription factors (ETS1, LEF1) in the pSS patients (Shah et al., 2019) (Jordan NV, et al., 2011). Both ETS1 and LEF1 are overexpressed in the labial salivary gland (LSG) biopsies of pSS patients alongside MMP9, without proximity to infiltrating CD4+ lymphocytes (Shah et al., 2019). ETS1 and LEF1 were previously demonstrated to directly regulate MMP9 transcription/expression in multiple epithelial cancer cell models (Nakamura Y et al., 2004) (Nazir SU et al., 2019)

(Santiago L, et al., 2017). All three factors have been shown to independently induce or regulate EMT and are frequently associated with cancer metastasis (Wakako Kobayashi, Masayuki Ozawa., 2018) (Santiago L, et al., 2017) (Li Y et al., 2020) (Taki M et al., 2006).

1.5.3. MMP9

The foundation of the basal lamina consists of type IV collagen and laminins, where MMP9 directly targets and breaks down the type IV collagen fraction (Barrera et al., 2013 review). Salivary acinar cells secrete higher amounts of MMPs (MMP9) and detach from the ECM in pSS, leading to anoikis (M.j. Barrera et al., 2013) (Margherita Sisto et al., 2009). Changes to basal lamina components of the ECM (collagen IV and laminin) are observed within the salivary gland epithelia acini and not surrounding capillaries, demonstrating the significance of pre-inflammatory expression of MMP9 and its gradual effects on the salivary ECM (M.j. Barrera et al., 2013).

MMP9 can activate multiple chemokines and cytokines, alongside enhancing lymphocyte adhesion and attraction (Van Lint, Libert., 2007). Reducing MMP9 in salivary glands could serve a dual function in reducing the activation of several inflammatory factors while limiting infiltration, as seen in the lacrimal glands of the two pSS mouse models (Aluri et al., 2015). In turn, a reduction of infiltrating immune cells might also reduce the risk of lymphoma development in pSS patients, which occurs in the foci of the affected salivary tissues (Theander E, et al., 2011). Moreover, proteolytic cleavage of ECM components through the overexpression of MMP9 releases sequestered growth factors (e.g., VEGF, FGF2) and activates latent chemokines, which reciprocally stimulate lymphocyte chemotaxis and paracrine mediated EMT-induced fibrosis (J Taipale et al., 1997) (Yabluchanskiy et al., 2013) (DeLeon-Pennell et al., 2015). MMP9 is overexpressed by the salivary epithelium with limited or no presence of infiltrating lymphocytes (Seunghee Cha et al., 2000). Reducing acinar cell expression of MMP9 could

potentially limit immune cell infiltration and consequently foci development. Therefore, targeting pSS during the pre-infiltration phase or early stages of infiltration might provide an optimal therapeutic strategy to reduce the progressive glandular destruction and further downstream immune cell infiltration. Overall, early MMP9 overexpression and degradation of salivary gland structures, generally occurring over several years, sets the stage for eventual lymphocytic infiltration and fibrosis (Marja Pertovaara et al., 1999).

1.5.4. ETS1 (ETS Proto-Oncogene 1)

ETS1 is part of the large ETS family of transcription factors which bind to a conserved (GGAA/T) DNA sequence (Dittmer J, 2003). Pathways involving glandular morphogenesis, tissue remodeling, EMT, leukocyte migration, differentiation, and cytokine/ chemokine expression have been linked to ETS1 expression (Kalluri R, Weinberg RA. 2010) (Dittmer J, 2003) (Teng, Y et al., 2020) (Yang, Ling-Xiaa et al., 2021). One important relationship previously demonstrated in multiple epithelial cancer cell models is the significance of ETS1 in MMP9 expression and cancer metastasis (Nakamura Y et al., 2004) (Nazir SU et al., 2019). ETS1 upregulates MMP9 through transcription control by directly binding the MMP9 promoter (Nakamura Y et al., 2004). During glandular morphogenesis and cancer metastasis, two EMT-driven processes, ETS1 participates by modulating ECM-cell interactions (i.e., adhesion, integrins, MMPs, collagen) and EMT transcription factor expression (Fafeur V et al., 1997) (Delannoy-Courdent A et al., 1996) (Alessandro Furlan and Albin Pourtier 2015).

In the context of autoimmune diseases, ETS1 is associated with defects in B-cell maturation of SLE and alters epithelial responses to chemokine/cytokine exposure (Sullivan KE et al., 2000) (Wang D et al., 2005). However, the involvement of ETS1 in pSS and salivary gland homeostasis has yet to be determined. We previously demonstrated a strong relationship the transcription factors ETS1/LEF1 and MMP9 expression within the epithelium of pSS patients

(Shah et al., 2019). The relationship was present within the epithelial cells without proximity to $CD4^+$ infiltrates (Shah et al., 2019). Further investigating the connection of ETS1, LEF1, and MMP9, we uncovered the direct regulation of MMP9 by ETS1 using immortalized salivary gland epithelial cell lines (iSGECs) derived from a non-pSS "sicca" patient (iSGEC-nSS2, FS=0.3) and pSS patient (iSGEC-pSS1, FS=1.8). iSGEC-pSS1 cells exhibited a reduced MMP9 response compared to iSGEC-nSS2 cells when ETS1 expression was knocked down using ETS1 target siRNA (Noll et al., 2022). Although the response was reduced, we did highlight the significant correlation in SGECs of ETS1 and MMP9 mRNA expression. Furthermore, ETS1 and MMP9 were overexpressed in the pSS (FS≥1), and non-pSS sicca (1<FS>0) group compared to non-pSS "sicca" FS=0. ETS1 activity is modulated by a variety of factors through post-translational modification (acetylation, phosphorylation) and cooperative binding (Dittmer et al., 2003) (Garrett-Sinha, 2013). ETS1 activity is further modulated by regulating its intracellular localization (Dittmer et al., 2003) (Garrett-Sinha, 2013). Many of the ETS1 partners, such as androgen receptor (AR), TPX2, CBP/p300, potentiate the accumulation of active ETS1 within the nucleus (Dittmer et al., 2003) (Garrett-Sinha, 2013). Due to the relatively convoluted regulation of ETS1 and differential regulation of MMP9 within iSGECs, the activity of ETS1 on the MMP9 promoter is most likely influenced by a cooperative binding partner.

1.5.5. LEF1 (Lymphoid Enhancing Binding Factor-1)

LEF1 is a member of the TCF transcription factor family with DNA-bending properties and regulates transcription of a variety of genes both through direct transcriptional activity and indirectly by regulating promotor accessibility (Werner MH, Burley SK., 1997) (Wakako Kobayashi, Masayuki Ozawa., 2018). LEF1 is frequently observed bound to β-catenin, enabling its transport into the nucleus where it exerts its transcription activities (Santiago L et al., 2017). The association of β-catenin and LEF1 is associated with a loss in epithelial characteristics, such as detachment from the ECM (Santiago L et al., 2017). During cell detachment, internally

bound β-catenin is freed from the disassociated E-cadherin cell-cell junction complexes, where its able to associate with different functional binding partners (*e.g.*, LEF1) in the nucleus (Santiago L et al., 2017). Thus, LEF1 expression and activity is frequently associated with mesenchymal gene expression and metastatic transformation of epithelial cells (Santiago L et al., 2017). LEF1 is an important facilitator of Wnt signaling, which controls a variety of significant pathways including stem cell differentiation/plasticity, inflammatory responses, cell adhesion and polarization, and salivary gland development (Bo Hai et al., 2010) (Nusse, et al., 2008) (Jridi et al., 2020) (Amin et al., 2012). Induced injury by ductal ligation of mouse submandibular glands resulted in an increase of Wnt signaling and is similarly upregulated in the tear-fluid of pSS patients by proteomic analysis (Hai B. et al., 2010) (Lara A. Aqrawi et al., 2019). Salivary gland organoid cultures containing $EpCAM^{high}$ progenitor cells were capable of self-renewal and produced well-differentiated cell types under Wnt stimulation (Martti Maimets et al., 2016). Moreover, Wnt-antagonized salivary gland stem cells transplanted into mice led to enhanced saliva secretion and acini formation (Martti Maimets et al., 2016). Lastly, LEF1 and Wnt signaling controls FGF4 expression in mouse models of tooth organogenesis, which has been found to be under-expressed in pSS saliva compared to non-SS controls (Klaus Kratochwil et al., 2002) (Nicolas Delaleu et al., 2015). Overall, the significance of LEF1 expression in relation to the salivary environment and regeneration is an area in need of further investigation.

1.6.1. Consequences of MMP9 overexpression

In healthy epithelial tissue, damage to the ECM stimulates the EMT signaling cascade, which begins with the proteolysis of ECM structures by MMPs to facilitate lymphocyte infiltration and ECM restructuring for eventual reepithelization by stem/ progenitor cells (Mohan et al., 2002) (Caley, et al., 2015) (Niklason, 2018). The newly restructured ECM in-turn dictates the differentiation of the re-epithelizing progenitor cells into the functional epithelium (You et al., 2012). However, in non-diseased tissue models, MMP9 is transiently upregulated by the

epithelium after injury to facilitate lymphocyte infiltration and ECM restructuring for reepithelization by stem/ progenitor cells (Mohan et al., 2002) (Caley, et al., 2015) (Niklason, 2018). This process is mediated through EMT and is integral to the regeneration of damaged lacrimal gland tissue (You et al., 2012). In pSS, MMP9 is chronically overexpressed within the salivary and lacrimal gland epithelium, leading to constant ECM restructuring disrupting repair progression, thus maintaining the degradation/disorganization of the ECM with reduced glandular function (Perez at al., 2005) (Konttinen et al., 1998) (Perez et al., 2000) (Goicovich et al., 2003).

1.6.2. The complicated roles of MMP9 during wound healing

MMPs and their natural inhibitors have a diverse number of functions falling under the general process of wound repair including tissue remodeling, fibrosis, and scar formation among others (Giannandrea M, et al 2014). MMP9 has several complex roles depending on the tissue MMP9 source and other local factors including the presence of various cytokines (Giannandrea M, et al 2014). In idiopathic pulmonary fibrosis models, high MMP9 expression was correlated with increased fibrosis within the alveolar tissue (Giannandrea M, et al 2014). Nevertheless, in different studies lower MMP9 levels were found to correlate with lower degrees of lung fibrosis later on (Giannandrea M, et al 2014). MMP9 may serve a dual role where its expression is beneficial only transiently during tissue remodeling and sustained MMP9 expression may further exacerbate chronic local inflammatory conditions (Giannandrea M, et al 2014 review). In all, knockdown of MMP9 within the salivary glands for sustained periods may negatively impact salivary gland regeneration and increase fibrosis within the tissue. Using a transient method, such as for example small inhibitory ribonucleic acids (siRNA), could better protect against the potential complications with long term reduced MMP9 expression. Moreover, targeting the upstream transcription factors responsible for MMP9 overexpression could provide an effective approach needed to reduce MMP9 to non-pathogenic levels.

1.6.3. Therapeutic strategies targeting MMP9

The role of MMP9 overexpression has been previously studied in multiple diseases, including atherosclerosis and idiopathic lung fibrosis, leading to the development of novel therapeutic approaches (Zervoudaki A et al., 2004) (Zervoudaki A et al., 2003) (Martinez M et al., 2006) (Tanner RM et al., 2011) (Giannandrea M, et al 2014). Of these studies, multiple systemic agents have been shown to nonspecifically reduce expression or activity of MMPs (Zervoudaki A et al., 2004) (Zervoudaki A et al., 2003) (Martinez M et al., 2006) (Tanner RM et al., 2011) (Frucht-Pery J et al., 1993). Reduction of MMP9 activity on the ocular surface has been exhibited using oral doxycycline, where doxycycline acts by chelating the catalytic zinc ion from the MMP9 active site (Frucht-Pery J et al., 1993). However, daily oral administration of doxycycline was associated with 12.5% of patients suffering gastrointestinal complications (Frucht-Pery J et al., 1993). In addition, pSS patients have a greater propensity for dental caries formation due to chronic dry mouth and introduction of antibiotics may further drive this microbiome dysbiosis (Taco A van der Meulen et al., 2018). Moreover, the orally administered doxycycline pill dosage needed to reach sufficient MMP9 inhibition within the salivary gland could extend beyond its optimal therapeutic range, leading to more complications. Outside antibiotics, two other agents have been shown to reduce MMP9 expression and activity in plasma samples, which includes the calcium channel blockers amlodipine and lercanidipine (Zervoudaki A et al., 2004) (Zervoudaki A et al., 2003) (Martinez M et al., 2006) (Tanner RM et al., 2011)).

Overall, local delivery of siRNAs targeting MMP9 regulators using an appropriate viral vector with a tropism for salivary glands or engineered nanoparticles might be desirable for the fine tuning of cell-specific down regulation of MMP9. We previously demonstrated the overexpression of ETS1 and MMP9 in both non-pSS sicca (1>FS>0) and pSS patients (Noll et al., 2022). Targeting dysregulated genes (e.g., ETS1) within the non-pSS sicca (1>FS>0) and

pSS patient populations could provide a better therapeutic strategy towards slowing the progression of pSS. Therefore, ETS1 siRNAs could represent a novel therapeutic approach in treating both non-pSS sicca and clinical pSS patients, without the drawbacks of directly targeting MMP9 (Taco A van der Meulen et al., 2018) (Frucht-Pery J et al., 1993).

1.7 Concluding Remarks

Current diagnostic markers for pSS are essentially focused on immune involvement, with significant limitations to associate disease activity with rate of progression. Biomarker's indicative of the pathogenesis involving the salivary epithelium (e.g., ETS1 and LEF1) could help in assessing pSS progression or to follow response to treatment. The salivary glands of pSS patients display a disorganized EMT process, contributing to the hypofunction of the salivary gland epithelia. Indicators of EMT are expressed prior to immune cell infiltration into glandular tissue and could serve as a therapeutic target early enough to prevent unaffected salivary gland tissue to be damaged by a possible increase of lymphocytic infiltration in non-pSS sicca patients. Factors susceptible to affect ETS1/LEF1 expression prior to the manifestation of symptoms may be monitored along with the presence of serum autoantibodies. Targeting the initial production of MMP9 through ETS1 and LEF1, using local delivery systems, would thus provide a viable therapeutic strategy for combating the glandular deterioration and salivary hypofunction in pSS. Overall, reducing early overexpression of MMP9 could preserve glandular architecture, thereby limiting lymphocytic infiltrates and loss of structural integrity of the acinar structure.

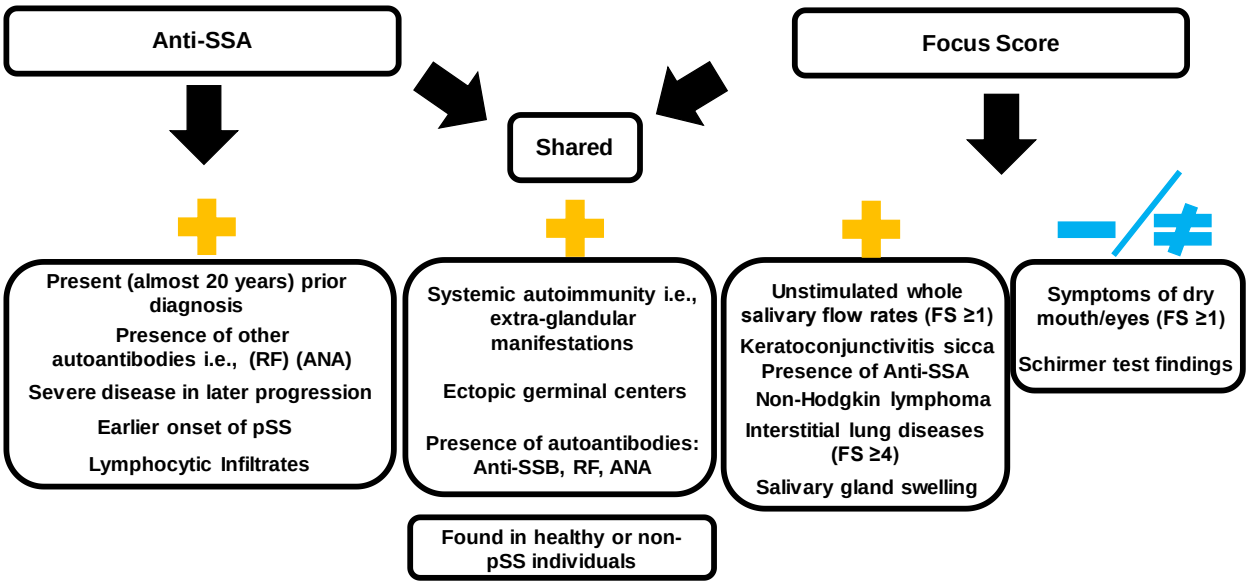

Figure 1.8.1: Associations among diagnostic markers Anti-SSA and/or Focus Score (FS): Poor indicators of epithelial disease progression and activity in pSS. Associations and findings regarding the presence of Anti-SSA and/or Focus Score (FS) with symptoms and manifestations of pSS. Positively associated symptoms/manifestations represented under the plus sign (+) in yellow are listed under their respective diagnostic feature (anti-SSA or FS). Features positively associated with both anti-SSA or FS diagnostic markers are listed under the shared header. Although not a positive association, both anti-SSA and FS ≥ 1 can be found in both healthy (asymptomatic) or non-pSS individuals. Symptoms/manifestations found to be negatively or not associated with FS are listed under the blue (-/≠) symbol. Overall, diagnostic markers (anti-SSA and FS) overlap or represent patients sharing a large degree of clinical manifestations. However, neither criterium provides an adequate measure or association with glandular function and atrophy. New diagnostic approaches originating from the salivary epithelium should be investigated to better represent and track pathogenesis, since current guidelines have limitations in the determination of disease activity within the salivary glands which are primarily affected in pSS.

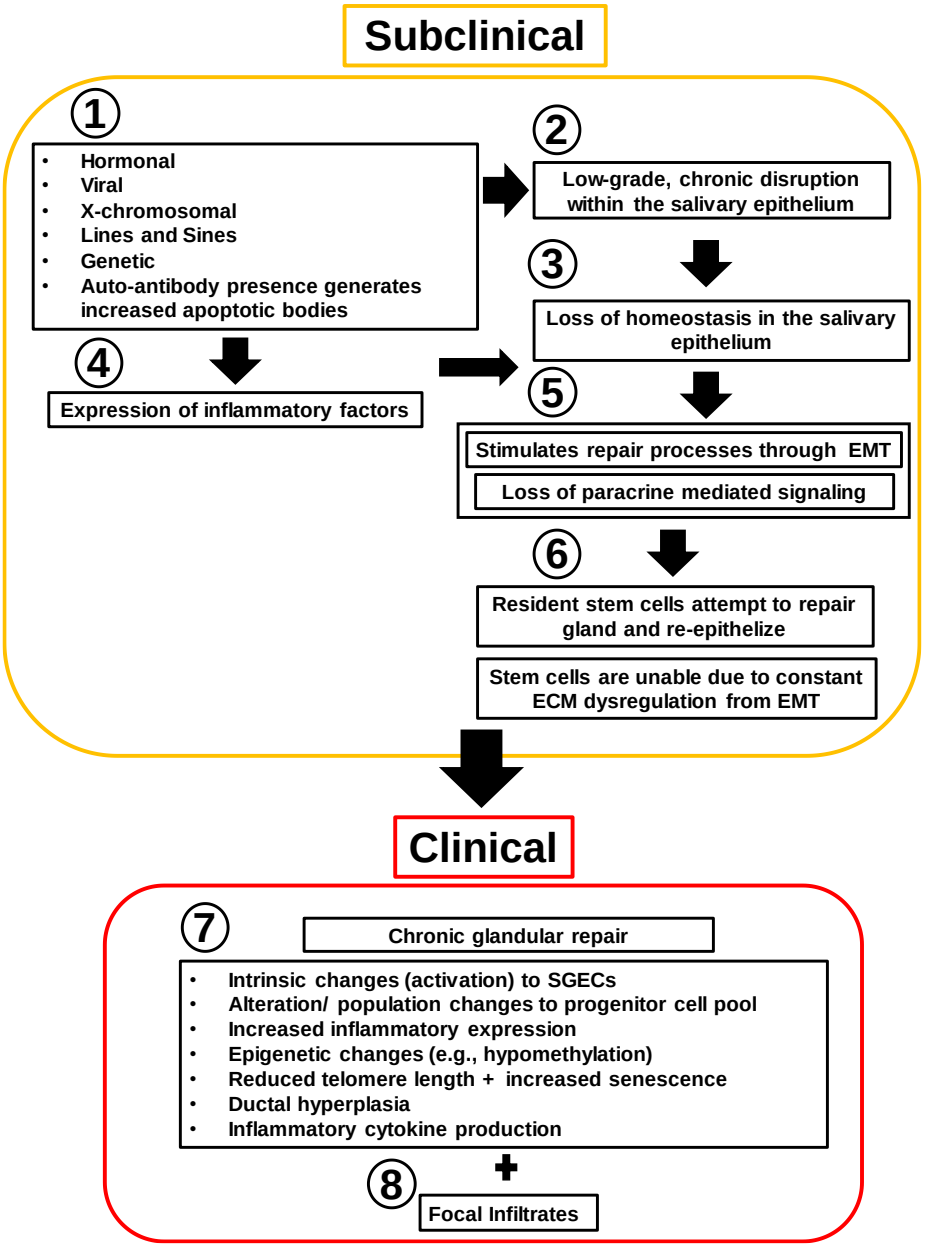

Figure 1.8.2: Salivary epithelium driven pathogenesis of pSS. 1) The pathogenesis of pSS arises from a complex etiology where several predisposing factors have been linked to its development. 2) Combinations of genetic and environmental perturbations culminate in the eventual disruption of the salivary epithelium, and hence, acini structures. 3) Homeostatic disruption brought on by etiological factors induces or is exacerbated by 4) local inflammatory processes, which are often associated with varying etiological agents or induced as a product of repair-signaling pathways. 5) Repair of the glandular epithelium is mediated through epithelial-mesenchymal transition (EMT), where acinar and ductal cells lose their epithelial characteristics and take on a mesenchymal-like phenotype. Damaged extracellular matrix (ECM) is removed through enhanced expression of proteases, including Matrix metalloproteinase-9 (MMP9), 6) to provide an adequate foundation for the re-epithelization by resident stem/ progenitor cells, which relies on cues from the ECM. However, due to the chronic disorganization and repair processes of the salivary epithelium, resident stem/ progenitor cells are unable re-epithelize the damaged area. 7) Eventually, mechanisms dictating the chronic state of repair within the salivary epithelium lead to many of the changes observed in the pathogenesis of pSS, which is ultimately characterized by 8) lymphocytic infiltration into the glandular tissue.

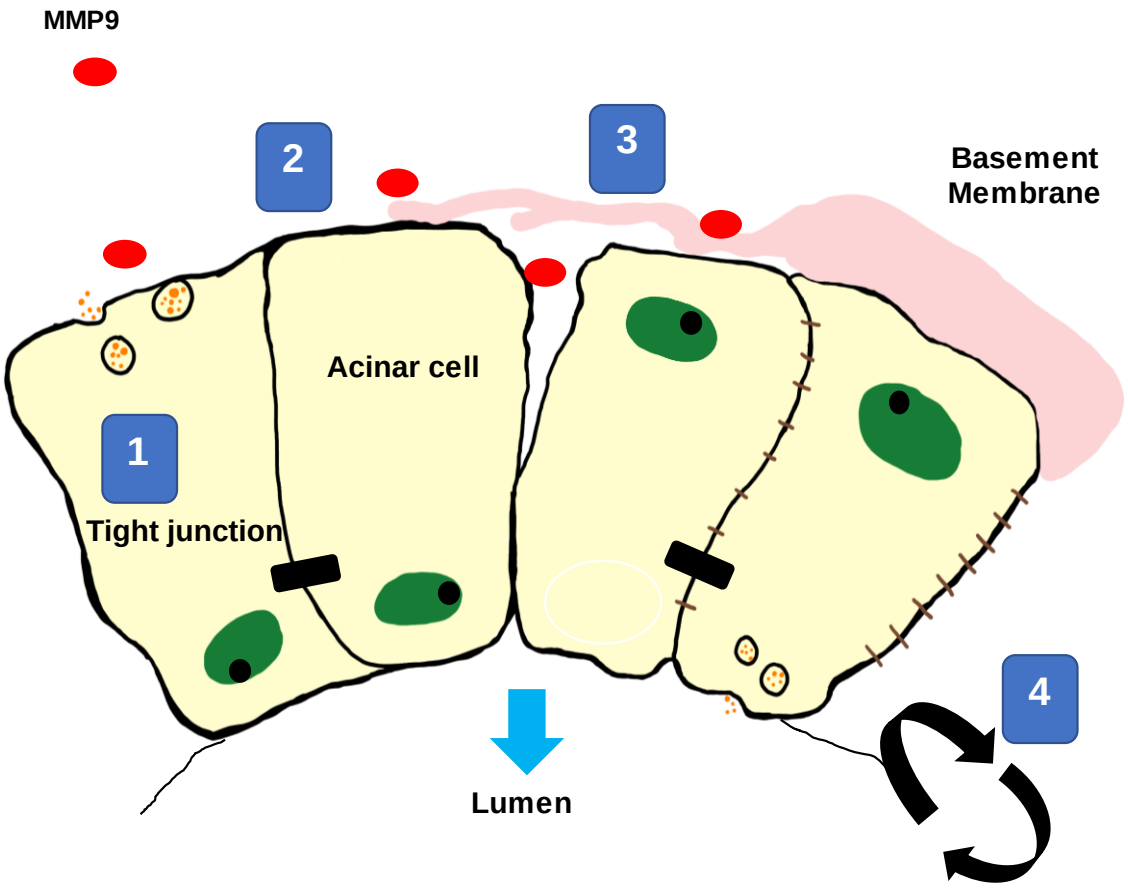

Figure 1.8.3: Potential disruptions in acinar cell function and homeostasis by MMP9. Epithelial function and integrity depend on both internal and external factors to support glandular epithelial homeostasis. External factors may include the integrity of cell-cell connections (tight junctions) and cell connections with the extra cellular matrix (ECM). Changes or loss of these external factors can disrupt epithelial homeostasis and initiate pathologic changes, which have been observed in the glandular epithelium of pSS patients. Disruption of both tight junctions and cell-ECM connections have been attributed to the overexpression of Matrix Metalloproteinase-9 (MMP9), which is overexpressed in both non-pSS (1>FS<0) sicca and pSS (FS≥1) salivary epithelium. MMP9 can degrade multiple components within cell-cell junctions and the surrounding ECM. 1) Degradation of tight junctions by MMP9 can alter directional secretory abilities of epithelial cells. 2) Loss of tight junctions causes cellular components located within apical/ basolateral sections to diffuse among the plasma membrane, inhibiting directional (polarized) secretion. 3) Breakdown of the ECM and tight junctions increases the permeability of the epithelium, in turn facilitating lymphocytic infiltration into tissues. 4) After subsequent damage to tissues, re-epithelization of the damaged region by resident stem/ progenitor cells relies on external cues from the surrounding ECM. However, MMP9 overexpression and excessive breakdown of ECM structures could impair healing and repair of the glandular epithelium in pSS patients.

CHAPTER 2: IMMORTALIZATION OF SALIVARY GLAND EPITHELIAL CELLS OF XEROSTOMIC PATIENTS: ESTABLISHMENT AND CHARACTERIZATION OF NOVEL CELL LINE

Abstract

Primary Sjögren's Syndrome (pSS) is an autoimmune disease mainly affecting salivary and lacrimal glands. Previous pSS studies have relied on primary cell culture models or cancer cell lines with limited relevance to the disease. Our objective was to generate and characterize immortalized salivary gland epithelial cells (iSGECs) derived from labial salivary gland (LSG) biopsies of pSS patients (focus score > 1) and non-Sjögren's Syndrome (nSS) xerostomic (i.e., sicca) female patients. To characterize iSGECs (n = 3), mRNA expression of specific epithelial and acinar cell markers was quantified by qRT-PCR. Protein expression of characterization markers was determined by immunocytochemistry and Western blot. Secretion of α-amylase by iSGECs was confirmed through colorimetric activity assay. Spheroid formation and associated alterations in expression markers were determined using matrigel-coated cell culture plates. Consistent mRNA and protein expressions of both epithelial and pro-acinar cell markers were observed in all three iSGEC lines. When cultured on matrigel medium, iSGECs formed spheroids, secreted α-amylase after β-adrenergic stimulation, and expressed multiple acinar cell markers at late passages. One iSGEC line retained adequate cell morphology without a loss of SV40Lt expression and proliferation potential after over 100 passages. In conclusion, our established iSGEC lines represent a viable model for salivary research due to their passaging capacity and maintenance of pro-acinar cell characteristics.

2.1 Rational

Development of restorative therapies for salivary gland dysfunction has been significantly hampered by a lack of accessible and pertinent cell culture models. Salivary glands are made of several cell types, including the saliva producing acinar cells, ductal cells modifying the saliva as it travels through the lumen, and myoepithelial cells mediating acinus contraction. Acinar cells commonly fail to regenerate following high dose radiation therapy, aging, or from autoimmune exocrinopathy such as primary Sjögren's syndrome (pSS) (Baum, Ship et al. 1992, Guchelaar, Vermes et al. 1997, Pringle, Wang et al. 2019). pSS is a chronic autoimmune disease characterized by a loss of salivary acinar cell function and a decline in acinar progenitor cell populations exacerbated by lymphocytic glandular infiltration.

Dysfunction of the salivary glands can lead to a reduction in salivary flow, thereby altering saliva composition, pH, and buffering capacity causing the sensation of dry mouth (xerostomia) (Baum, Ship et al. 1992). Cell culture models for pSS and xerostomia have been limited, leading researchers to rely on cancer cell lines or short-term cultures of primary salivary gland epithelial cells (SGECs) (Jang, Ong et al. 2015, Lin, Elkashty et al. 2018). Moreover, the cell lines extensively used in salivary research (e.g., HSG, A253, NS-SV-AC) are of male origin (Giard, Aaronson et al. 1973, Shirasuna, Sato et al. 1981, Azuma, Tamatani et al. 1993, Lin, Elkashty et al. 2018). These cell lines may not recapitulate the pathological processes occurring in pSS, a disease with a higher incidence in female patients (Patel and Shahane 2014).

Isolated SGECs have been shown to share ductal and pro-acinar characteristics and exhibit a moderate cell division capacity when grown in serum-free low calcium media (Dimitriou, Kapsogeorgou et al. 2002, Ittah, Miceli-Richard et al. 2006, Kawanami, Sawaki et al. 2012, Jang, Ong et al. 2015, Nam, Kim et al. 2018). As with any primary cell culture model, their limited growth potential can impede reproducibility and applications including, but not limited to, high throughput

drug screening assays. In addition, pSS patient derived SGECs show a markedly reduced proliferation capacity in vitro (Pringle, Wang et al. 2019). The reduced growth capacity of pSS SGECs is mirrored in affected patient's salivary glands where narrowed pools of progenitor cells are found with markedly shortened telomeres (Pringle, Wang et al. 2019). Overall, suboptimal cell culture models combined with the reduced growth ability of pSS SGECs have proven to be major obstacles in salivary research.

Diagnosis of pSS may require a labial salivary gland (LSG) biopsy for histologic analysis of lymphocytic aggregates within the tissue (Shiboski et al. 2017). LSG biopsy tissue is a common explant source for culturing SGECs, but due to limited availability based on clinical access, their potential as a universal model is restricted. Culture of SGECs is typically performed using a dual media approach, where the initial explant medium contains 2.5% fetal bovine serum and is replaced with a second serum free media to sustain passaging and growth (Dimitriou, Kapsogeorgou et al. 2002, Jang, Ong et al. 2015). Minor differences in culture conditions, including FBS concentration and time spent in explant medium can have a profound effect on salisphere (i.e., 3D spheroid) formation and passage number, as previously shown for parotid gland progenitor cells isolated from mice (Nguyen, Dawson et al. 2018).

Primary SGEC cultures are comprised of cells with pro-acinar and/or ductal cell-like features depending on the growth substrate, presence of serum in medium, and the specificity of characterization markers used (Dimitriou, Kapsogeorgou et al. 2002, Ittah, Miceli-Richard et al. 2006, Kawanami, Sawaki et al. 2012, Jang, Ong et al. 2015, Nam, Kim et al. 2018). The previous work of Fujita-Yoshigaki et al., demonstrated the dedifferentiation of primary parotid acinar cells occurs in culture, which could explain the variety of ductal and acinar cell features expressed (Fujita-Yoshigaki, Matsuki-Fukushima et al. 2008, Fujita-Yoshigaki 2010). In addition, Jang et al., revealed that primary SGECs (known as phmSG) of ductal origin exhibited trans-epithelial resistance, expressed several acinar and epithelial cell markers (i.e., AQP5, SLC12A2, AMY1A),

and secreted α-amylase upon β-adrenergic stimulation (Jang, Ong et al. 2015). Overall, SGECs represent a suitable cell culture model to investigate salivary gland dysfunction in vitro but lack the unlimited growth potential needed for widespread use.

To our knowledge no reliable immortalized human primary SGEC lines derived from female patients' LSG biopsies have been developed or made readily available to researchers. To address this gap, the objective of our study was to generate an in vitro cell culture model for the investigation of the pathophysiology of salivary gland disorders. Using a SV40 Large-T (SV40Lt) lentiviral vector, we generated and characterized immortalized SGECs isolated from LSG biopsies of pSS and xerostomic (sicca) patients. SV40Lt antigen subunit inhibits both cell cycle regulators, pRB and p53, and prevents telomere shortening-induced cell senescence in some cell types (Satyanarayana, Greenberg et al. 2004, Ahuja, Sáenz-Robles et al. 2005). We characterized immortalized SGECs (iSGEC) lines from two non-Sjögren's syndrome (nSS) female patients (referred to as iSGEC-nSS1 and iSGEC-nSS2) and one pSS (referred to as iSGEC-pSS1) female patient, based on the expression of pro-acinar and epithelial cell markers using various molecular methods. iSGECs were grown on matrigel coated plates to determine three-dimensional (3D) spheroid forming ability, along with the extent to which spheroids recapitulated acinus characteristics, such as differentiated myoepithelial and acinar cells.

2.2 Materials and Methods

Culture of Salivary Gland Cell Lines (SGCLs) and HeLa Cells

Salivary gland cell lines, HSG and HSY, and HeLa cells were cultured in DMEM supplemented with 10% FBS (VWR, Radnor, PA, USA) (37°C; 5% CO2). A253 cells were cultured according to the provider's (ATCC, Manassas, VA, USA) recommendations (ATCC 2020). HMC-3A cells were cultured according to the providers' recommendations (Warner, Adams et al. 2013). SGCLs (HSG, HSY, A253, and HMC-3A) and HeLa cells were grown in T-75 tissue culture

treated flask (Corning Life Sciences, Tewksbury, MA, USA) until 80-90% confluency. For experiments, SGCLs and HeLa cells were re-plated using 0.25% trypsin+0.053mM EDTA (Corning Life Sciences, Tewksbury, MA, USA).

LSG Biopsies and Culture of Salivary Gland Epithelial Cells (SGECs)

Atrium Health institutional review board (Charlotte, NC, USA) approval was granted for this study and all patients gave informed consent. Anti-Ro (SSA) serum negative (-) xerostomic patients undergoing a LSG biopsy for the assessment of pSS according to the 2016 ACR/EULAR classification criteria were asked to participate in this study (Shiboski et al., 2017). Xerostomic nSS and pSS patient clinical characteristics are listed in Table 1. Remaining LSG biopsy tissue was transported to the research laboratory in complete SGEC explant medium supplemented with 5x antibiotic/antimycotic solution (Gibco, Thermo Fisher Scientific, Waltham, MA, USA).

SGEC cultures were established according to the methods outlined by Jang et. al., and are briefly explained as follows. LSG tissue was minced into 0.5-1mm2 fragments and placed in T-75 flask with 3.5mL of complete SGEC explant medium supplemented with 1x antibiotic/antimycotic solution (Gibco, Thermo Fisher Scientific, Waltham, MA, USA) and grown (37°C, 5% CO2). Complete SGEC explant medium consisted of 1:3 Ham's F12 and DMEM supplemented with 2.5% FBS (VWR, Radnor, PA, USA), 10 ng/mL EGF (Gibco, Thermo Fisher Scientific, Waltham, MA, USA), 500 ng/mL insulin (MP Biomedicals, Santa Ana, CA, USA), 400 ng/mL hydrocortisone (Sigma-Aldrich, Saint Louis, MO, USA), and 1x antibiotic/antimycotic solution (Gibco, Thermo Fisher Scientific, Waltham, MA, USA). After 72 hours, 5mL of SGEC explant media was added. Cells at 80-90% confluency were split 1:3 into T-75 flask with 0.05% trypsin + 0.045mM EDTA. Trypsin was neutralized by soybean trypsin inhibitor (Gibco, Thermo Fisher Scientific, Waltham, MA, USA) at a 1:1 ratio (v/v). For remaining

passages, SGEC sub-culturing medium was used. SGEC sub-culturing medium consisted of Epi-life Basal medium (0.06mM Ca^{2+}) (Gibco, Thermo Fisher Scientific, Waltham, MA, USA, Catalog# MEPI500CA) supplemented with 1x human keratinocyte growth supplement (HKGS) (Gibco, Thermo Fisher Scientific, Waltham, MA, USA, Catalog# S0015). Fibroblast were gradually removed from culture using a combination of 0.02% EDTA or 0.01% trypsin.

Transduction of SGECs by Lentiviral SV40Lt Particles

During passage number 2 (p-2), SGECs were spit into 6-well (VWR, Radnor, PA, USA) tissue culture-treated plates at a confluency of 60–70% and allowed to adhere for 24 h. Cell medium was removed and replaced with 1 mL SV40Lt lentiviral supernatant (ABMgood, Richmond, Canada, Catalog# G258) diluted with 1 mL of SGEC sub-culturing medium (2 mL total) and polybrene (Sigma-Aldrich, Saint Louis, MO, USA) at a final concentration of 4 µg/mL. After 48 h, SV40Lt lentiviral cell medium was replaced with SGEC sub-culturing medium and grown for 24 h. Medium was removed and cells were supplied with 1 mL SV40Lt lentiviral supernatant diluted with 1 mL of SGEC sub-culturing media (2 mL total) and polybrene at a final concentration of 4 µg/mL, for 48 h.

SV40Lt lentiviral cell medium was removed and replaced with SGEC sub-culturing medium and cells were grown to 80–90% confluency before being split into 6-well tissue culture-treated plates at a ratio of 1:6. For cell passages after SV40Lt lentiviral transfection, cells were split 1:6 up to passage 10. The remaining passages were split at 1:3 using T-75 (Corning Life Sciences, Tewksbury, MA, USA) tissue culture-treated flasks. To determine increased expression of pro-acinar markers in high Ca^{2+} supplemented medium, all iSGECs at early passage 14 (p-14) and only iSGEC-nSS2 at passage 80 (p-80) were subjected to 1.2 mM Ca^{2+} in SGEC medium for 72 hrs prior to experimentation.

RNA Extraction and cDNA Synthesis

RNA was extracted from iSGECs, SGCLs, and Hela cells in 6-well plates using the RNAeasy kit (Qiagen, Valencia, CA, USA) according to the manufacturer's protocol. RNA was quantified using a Nanodrop 1000 (Thermo Fisher Scientific, Waltham, MA, USA). A total of 500ng RNA from each sample was used per cDNA synthesis reaction. cDNA synthesis was carried out using the SmartScribe reverse transcription kit (Takara Bio, Mountain View, CA, USA) with random hexamers (20µg) (Promega, Madison, WI, USA) and dNTP's (10mM final) (Promega, Madison, WI, USA) according to the manufacturer's protocol. After synthesis, the cDNA was diluted to a final volume of 200 µL.

Matrigel Induced 3D Spheroid Cultures

Matrigel (Corning Life Sciences, Tewksbury, MA, USA) diluted in 1.2mM Ca2+ SGEC sub-culturing medium (2mg/mL final concentration) was solidified in 8-well Nunc™ Lab-Tek™ II Chamber Slides™ (Thermo Fisher Scientific, Waltham, MA, USA) or 12-well tissue culture treated plates (VWR, Radnor, PA, USA) and incubated for 1hr at 37°C. Cells were seeded at $3x10^5$ or $1x10^6$ per well, respectively. Cell cultures on matrigel coated plates were grown at 37°C and 5% CO_2 for up to 7 days.

Real-Time Quantitative and Semi-Quantitative Polymerase Chain Reaction

All qRT-PCR and semi-qRT-PCR reactions were performed using a BioRad C1000 Touch Thermal Cycler (Biorad, Hercules, CA, USA) in 96-well qPCR plates. All qRT-PCR reactions were carried out in triplicate wells per plate using three separate plates and average cycle threshold (Ct) values were used for quantification. Relative expression was calculated applying the ΔCt method for iSGECs, SGCLs, and Hela cells normalized to expression of GAPDH. Per well, 10µL of RT2 SYBR Green Fast Master Mix (Qiagen, Valencia, CA, USA) was added to 2µL of cDNA, 1µL of forward and reverse primers (10mM) (IDT, Newark, NJ, USA) and 7µL of

nuclease-free water. Primers are listed in Table 2.6.2. along with their respective target for cell expression characterization purposes.

Semi-qRT-PCR was employed to detect expression of the SV40Lt transcript at multiple passage numbers (Figure 2.5.9.). Products from semi-qRT-PCR reactions were run on a 1% agarose TAE gel alongside a 1kb DNA ladder (New England Biolabs, Ipswich, MA, USA) for 35 min and visualized using a gel-doc system (GE Healthcare Life Sciences, Chicago, IL, USA).

Expression of ZO-1, AQP5, and α-Amylase by Western Blot

iSGECs and SGCLs were plated at 80% confluency in 6-well tissue culture treated plates and allowed to adhere for 48 hours prior to experimentation. To generate whole cell lysates, medium was removed from cells and the wells washed 3x with DPBS. Protein was harvested from cells using M-PER buffer (Pierce, Thermo Fisher Scientific, Waltham, MA, USA) and briefly sonicated before centrifugation at 15,000xg for 10 min. The resulting insoluble pellet was discarded, and the supernatant was used for western blotting of ZO-1, AQP5, and vinculin.

For the determination of α-amylase secretion, iSGECs were grown in SGEC sub-culturing media without HKGS for 24hrs and then replaced with complete SGEC sub-culturing media supplemented with 10μM epinephrine (MP Biomedicals, Santa Ana, CA, USA). After 45 minutes the cell culture media was harvested and centrifuged (4°C, 1000xg) for 10 min to remove whole cells. The media was then spun in Millipore concentrator tubes with a 10 kDa size exclusion limit (Millipore, Burlington, MA, USA) for 30minutes and an appropriate amount of 6x reducing Lameli buffer (Roche, Basel, Switzerland) added to the resulting concentrated supernatant. iSGECs adhered to the tissue culture plate were lysed and harvested using M-PER buffer. Protein samples in M-PER were briefly sonicated and centrifuged at 15,000g for 10 minutes and the pellet discarded.

Samples were measured by Bradford assay (Pierce, Thermo Fisher Scientific, Waltham, MA, USA) and equal amounts of protein were loaded into each lane and subjected to electrophoresis on a 7-14% gradient pre-cast SDS-PAGE gel (Biorad, Hercules, CA, USA). Proteins were transferred onto nitrocellulose membranes (GE Healthcare Life Sciences, Chicago, IL, USA) and blotted (12 hrs, 4°C) with selected antibodies at listed concentrations (Table 2.6.4.) followed by incubation (room temperature, 1 hour) with HRP-conjugated anti-mouse secondary (Cell signaling Technology, Danvers, MA, USA).

Membranes were washed (3x, 5 min) and developed using Super Signal West pico Chemiluminescent substrate kit (Pierce, Thermo Fisher Scientific, Waltham, MA, USA). Western blots were photographed using an ImageQuant LAS4000 (GE Healthcare Life Sciences, Chicago, IL, USA) system. Densitometry was performed using Image Studio V.5.2 software (LI-COR, Lincoln, NE, USA) and protein levels were normalized to vinculin in their corresponding whole cell lysate.

β-adrenergic Stimulation and Measurement of α-Amylase Activity in Supernatant

iSGECs were plated at a density of $4x10^5$ cells in either uncoated (2D) or coated (matrigel) tissue culture plates. Cells were grown in SGEC sub-culturing medium supplemented with 1.2mM Ca^{2+} for 72 hours or 5 days prior to experimentation. At the times indicated, medium supplemented with 10μM epinephrine (MP Biomedicals, Santa Ana, CA, USA) was added. After 45 min, cell culture medium was collected and subjected to the colorimetric amylase activity assay (Biovision, Milpitas, CA, USA) per manufacturer's protocol.

Immunocytochemistry (ICC)

iSGECs and SGCLs were plated onto Coating Matrix (2D) (Gibco, Thermo Fisher Scientific, Waltham, MA, USA,) covered 8-well Nunc™ Lab-Tek™ II Chamber Slides™ (Thermo Fisher Scientific, Waltham, MA, USA). Antibodies and concentrations are listed in Table 2.6.4. Cells were grown for 48-72 hours, then fixed with ice-cold methanol (-20°C, 10 min) and incubated with the following antibodies directed against: KRT8, KRT18, KRT19, AQP5, ZO-1, α-SMA, Vimentin, and E-cadherin proteins. Cells were also fixed with 4% paraformaldehyde (room temperature, 15 min) to stain Ki-67 and α-amylase. Fixed cells were permeabilized with 0.25% Triton X-100 in TBS (room temperature, 10 min).

Cells were fixed then washed (3x) in TBS and incubated (room temperature, 5 min) in 3% H202 (v/v) TBS to block endogenous peroxidases. Next, cells were incubated in blocking buffer consisting of 1% BSA (w/v), 2% skim-milk (w/v), and 0.1% Tween-20 in TBS (room temperature, 1 hour). Primary antibodies were diluted in TBS with 0.1% Tween-20 and 1% BSA. The fixed cells were incubated with the primary antibody (4°C, 12 hrs) (Table 2.6.4). Cells were washed with TBS (3x, 5 min each) and incubated with anti-mouse secondary at different concentrations (Table 2.6.4.) diluted in TBS with 0.1% Tween-20 (room temperature, 1-2 hrs). After incubation, cells were washed with TBS (3X).

Monolayer culture fixed cells were incubated in diaminobenzidine (DAB) (Pierce, Thermo Fisher Scientific, Waltham, MA, USA) 1x solution (2-7 min). DAB was washed away using TBS to stop the reaction and the cells were counterstained with Gills II hematoxylin (Richard-Allan Scientific, Kalamazoo, MI, USA) (diluted 1:5 v/v DPBS) for 30 seconds to highlight nuclei. Slides without primary antibody served as negative controls.

For ICC-immunofluorescence (IF) visualization of 3D spheroid cultures grown on Matrigel, cells were fixed using 4% paraformaldehyde (room temperature, 25 min) and permeabilized with 0.25% triton X-100 in TBS (room temperature, 10 min). The same blocking and incubation procedure previously outlined was followed except 4′,6-diamidino-2-phenylindole (DAPI) (Abcam, Cambridge, UK) was used to highlight DNA. Slides without primary antibody served as negative controls.

Slides were observed using an Olympus BX51 fluorescence microscope (Shinjuku City, Tokyo, Japan) and photographed with an Olympus DP70 (Shinjuku City, Tokyo, Japan) mounted camera. Cells in culture plates were viewed by phase contrast on an Olympus IX-71 inverted fluorescence microscope and photographed using an Olympus DP70 mounted camera. Proliferation scores were determined based on Ki-67 protein detection, a nuclear protein expressed during several cell cycle phases (G1/S/G2/M) and is frequently employed as an indicator of actively proliferating cells (Bruno and Darzynkiewicz 1992). Proliferation scores (%) were generated by selection of three random images for nuclei counting using Fiji-ImageJ software (Schindelin, Arganda-Carreras et al. 2012). Total number of cell nuclei was divided by the total number of Ki-67 (+) nuclei and averaged among three images.

Data Analysis and Statistics

Data are presented as mean +/- standard error of means (SEM) from a minimum of three separate experiments. Significant results were calculated using the Student's t-test on GraphPad Prism 8 (San Diego, CA, USA). P-values were determined to be significant using the Holm–Šidák post hoc test for multiple comparisons with $\alpha=0.05$.

2.3. Results

2.3.1. Primary Isolation, Culture, and Growth of iSGECs

LSG biopsy fragments remained in SGEC explant medium for approximately 7-14 days to ensure sufficient cell outgrowth. Once the cells reached approximately 70-80% confluency, the culture medium was replaced with SGEC sub-culturing medium. Transitioning to the serum-free low calcium (0.06mM) medium for 3-5 days prior to trypsinization reduced fibroblast contamination in following passages. Before SV40Lt transduction in all three cell lines, two separate populations of cells were observed and consisted of either larger cells with complex cytoplasm or smaller cells with reduced cytoplasm. The smaller cells were predominant during later passages in all three iSGEC lines. At late passages iSGEC-pSS1 gave rise to colonies appearing mixed in size of polygonal or cobblestone-like cells with differing rates of cytoplasmic complexity (Figure 2.5.1). iSGEC-nSS1 late passages demonstrated a mix of small polygonal and filiform-appearing cells (Figure 2.5.1). Mixed morphology of iSGECs most likely indicates an inhomogeneous population (Table 2.6.2) (Figure 2.5.3). Therefore, we selected iSGEC-nSS2 for late-passage outgrowth and in-depth characterization over iSGEC-pSS1 and -nSS1. Long term passaged iSGEC-nSS2 exhibited a stable, small cobblestone morphology and did not give rise to filiform-appearing cells (Figure 2.5.1). iSGEC-nSS2 cultured in 1.2mM Ca^{2+} acquired more complex appearing cytoplasm with granulations and formed tight clusters at both early and late passages (Figure 2.5.1).

During later passages (iSGEC-nSS2, p-80), colony formations different in overall shape arose from single cell clonal outgrowths (Figure 2.5.8.). However, these single cell outgrowth populations quickly became incorporated into other colonies and were unremarkable at lower confluency.

Proliferation rates of iSGEC-nSS2 did not substantially waver across early (p-14) and late (p-80) passages indicated by Ki-67 staining percentage (Figure 2.5.1). No decrease in the % of Ki-67 (+) cells was observed at later passages. Spheroid formation on matrigel was observed after 24 hours in all three cell lines (Figure 2.5.2, Figure 2.5.8). iSGEC-nSS2 retained spheroid formation ability into late passages (>p-80), which could be observed after 24 hours of plating. At three-days in matrigel, spheroids measured roughly ~75-200µm in all iSGECs.

2.3.2. Characterization of iSGECs by qRT-PCR

mRNA expression of epithelial and acinar markers was determined by qRT-PCR in iSGECs, SGCLs, and Hela cells. Expression of epithelial and acinar cell markers showed slight deviation among all three iSGECs when grown as a monolayer culture (Figure 2.5.3). Compared to SGCLs and Hela, A253 and HMC-3A showed the greatest similarity to iSGEC cultures. Mucoepidermoid carcinomas have been shown to exhibit increased expression of AQP5 and among all cell lines analyzed, HMC-3A expressed AQP5 highest (Figure 2.5.3) (D'Agostino, Elkashty et al. 2020).

The two consistently over-expressed pro-acinar genes by iSGEC-nSS2 were ANO1 and SLC12A2, compared to both iSGEC-pSS1 and -nSS1 (Figure 2.5.3). We did not observe a difference in pro-acinar expression of AMY1A, AQP5, STIM1, and STIM2 when comparing iSGEC-nSS2 to both iSGEC-pSS1 and -nSS1.

iSGEC-nSS1 exhibited the highest expression of both VIM and CST3, and the lowest expression of KRT19 (a ductal/epithelial cell maker of salivary glands) among iSGECs, indicating a heterologous mesenchymal phenotype (Figure 2.5.3) (Jang, Ong et al. 2015, Sisto, Tamma et al. 2020). KRT5 is a marker for progenitor and basal ductal cells of the salivary gland (Kwak, Ninche et al. 2018, May, Cruz-Pacheco et al. 2018). In agreement with the work by Jang

et al., on primary SGECs, KRT5 was the gene with highest expression in iSGECs by qRT-PCR among the characterization markers, which did not differ significantly among all three iSGEC lines (Jang, Ong et al. 2015). HSG, HSY, and HeLa cells expressed most transcripts consistently at the same level and exhibited a mesenchymal expression pattern reflected by iSGEC-nSS1 with low CDH1 and high VIM expression (Sisto, Tamma et al. 2020).

2.3.3. Changes in mRNA Expression Among Early and Late Passage iSGECs by qRT-PCR

Expression of acinar and other characterization markers was assessed over early and late passages. iSGEC-pSS1 was the most stable cell line where only AMY1A and CST3 expression increased in later passages. Both iSGEC-nSS1 and -nSS2 exhibited pro-acinar changes in expression profiles at later passages where most markers increased (Figure 2.5.4). In iSGEC-nSS1 p-45, pro-acinar markers (AMY1A, AQP5, ANO1, SLC12A2, CST3, and TRPC1) increased in expression compared to early (p-14) cultures (Figure 2.5.4). iSGEC-nSS2 at p-80 expressed AMY1A, ORAI1, STIM1, SLC12A2, CST3, and TRPC1 higher, and only one marker lower (ANO1) compared to p-14. Both AQP5 and STIM2 were stably expressed during extended passaging in iSGEC-nSS2. Overall, AMY1A and CST3 increased during late passages of all three iSGECs lines, which could be important for maintaining pro-acinar characteristics.

Characterization markers were the most differentially expressed and exhibited the greatest changes in late passaged iSGECs. Epithelial marker CDH1 was the only stably expressed gene among all characterization markers, whereas ZO-1 increased in late passages of all three iSGECs (Figure 2.5.4). iSGEC-nSS2 maintained an epithelial expression pattern, including a decrease in the mesenchymal marker VIM and a significant increase in CLDN1 expression. Over passages, both KRT5 and KRT19 decreased in expression and the progenitor cell marker

NANOG increased and could indicate a shift towards a less-differentiated cell population in iSGEC-nSS2

2.3.4. Effects of Ca^{2+} on iSGECs mRNA Expression

Calcium concentration in media affects SGEC expression of pro-acinar genes, including AQP5, ORAI1, STIM1 and STIM2 (Jang, Ong et al. 2015, Jang, Ong et al. 2016). Jang et al., demonstrated an increase in activity of the store-operated Ca^{2+} entry (SOCE) system upregulates AQP5 expression through nuclear factor of activated T-cells 1 (NFAT1) (Jang, Ong et al. 2016). To evaluate changes produced by an increase in Ca^{2+}, we cultured iSGECs in 1.2mM Ca^{2+} for three days and then assessed mRNA expression by qRT-PCR. Early iSGEC-nSS2 cultures (p-14) did not exhibit any alterations in expression of acinar markers when cultured in 1.2mM Ca^{2+} (Figure 2.5.5). Late iSGEC-nSS2 (p-80) cells supplemented with 1.2mM Ca^{2+} demonstrated an increase in AQP5 and ANO1 mRNA expression and decreases in other acinar markers (AMY1A, ORAI1, STIM1, SLC12A2, TRPC1) (Figure 2.5.5). Moreover, a change in ductal characterization marker KRT19 was decreased in p-14 iSGEC-nSS2 cells cultured in 1.2mM Ca^{2+} (Figure 2.5.5). Late (p-80) iSGEC-nSS2 responded differently by increased expression of tight junction component ZO-1 and myoepithelial marker α-SMA. The lack of response to 1.2mM Ca^{2+} in iSGC-nSS2 p14 cells reiterates the possibility of a de-differentiated cell population seen in Figure 2.5.4, where p-80 demonstrated a response to increased Ca^{2+} more similar to other SGEC publications (Jang, Ong et al. 2015, Jang, Ong et al. 2016).

2.3.5 Characterization of iSGECs by ICC and Western Blot

The cytokeratins, KRT8, KRT18, and KRT19 are cytoplasmic proteins expressed in the salivary gland epithelium and are characterization markers for ductal and acinar cells (Draeger, Nathrath et al. 1991, Pringle, Wang et al. 2019). We first characterized iSGECs by KRT8/18/19 protein expression and found iSGEC-nSS1 expressed all three epithelial markers more intensely and

uniformly than iSGEC-pSS1 and -nSS2 (Table 2.6.2, Figure 2.5.11). KRT19 protein localized within cells containing a larger cytoplasm and were dispersed throughout iSGEC-nSS2 cultures, whereas smaller cells demonstrated a low or lack of expression (Figure 2.5.11). KRT18 was the most uniform and ubiquitously expressed cytokeratin among iSGECs, whereas KRT8 exhibited focal protein expression in iSGEC-nSS2 (Figure 2.5.11). Heterogenous expression of KRT19 and KRT8 could indicate multiple stages of differentiation among cells (May, Cruz-Pacheco et al. 2018). Overall, the expression of KRT8, KRT18, and KRT19 indicates these cell lines to be of ductal origin and reflects other long-term cultures of SGECs in both mice and humans (Draeger, Nathrath et al. 1991, Jang, Ong et al. 2015, Ikeura, Kawakita et al. 2016).

Acinar cell markers, AQP5 and AMY1A, were expressed in all three iSGECs, and highest in both iSGEC-pSS1 and -nSS2. Within these cultures, cells in close contact expressed the highest levels of AQP5, unlike AMY1A where intercellular contact or proximity to other cells did not appear to have an influence. We observed an increase of AQP5 protein expression in both p-14 and p-80 iSGEC-nSS2 cultures when supplemented with 1.2mM Ca^{2+}. Increased AQP5 protein was determined by ICC and replicated by western blot of whole cell lysates (Figure 2.5.11, Figure 2.5.6). ZO-1 expression was low in all iSGECs when accessed by ICC and confirmed by western blot in whole cell lysate. iSGEC-nSS1 exhibited the lowest expression of ZO-1 and CDH-1 and higher expression of VIM in monolayer culture, which reiterates the observed mesenchymal phenotype (Sisto, Tamma et al. 2020).

In case of iSGEC-nSS2, α-SMA was not detected in either p-14 or p-80 monolayer cultures as compared to iSGEC-pSS1 and -nSS1, where it was expressed at very low levels (Figure 2.5.11). Pringle et al., demonstrated low α-SMA expression in cultured salivary gland stem cells (SGSCs) likely originating from intercalated and striated ductal cells and could explain these results (Pringle, Wang et al. 2019). Vimentin is a marker for mesenchymal cells within the

salivary glands (You, Avidan et al. 2012, Hosseini, Nelson et al. 2018). Vimentin was expressed sporadically in iSGEC-nSS2 monolayer culture and could indicate a small population of mesenchymal cells or epithelial cells reverting to a mesenchymal-like state within cultures (Figure 2.5.11).

In all three iSGEC lines, α-amylase was secreted into the cell culture medium after β-adrenergic stimulation by epinephrine (Figure 2.5.6). Additionally, iSGEC-nSS2 early (p-14) and late passages (p-80) secreted α-amylase into cell culture media with and without β-adrenergic stimulation (Figure 2.5.6). iSGECs-nSS2 p-80 secrete α-amylase, demonstrating retention of pro-acinar cell characteristics after significant cellular expansion. Moreover, iSGEC-nSS2 cells cultured on matrigel formed spheroid structures and secreted α-amylase in response to 10mM epinephrine stimulation (Figure 2.5.6). An overall increase in α-amylase secretion when compared to unstimulated cells was observed in iSGEC-nSS2 and could indicate a stricter regulation of secretion within the differentiated cells

2.3.6. 3D-Matrigel Spheroid Culture

Matrigel contains a mixture of basement membrane and extracellular matrix proteins which have been shown to promote SGEC and salivary gland stem cell (SGSC) differentiation (Dimitriou, Kapsogeorgou et al. 2002, Maria, Zeitouni et al. 2011, Shin, Hong et al. 2018, Pringle, Wang et al. 2019). SGECs plated on matrigel form spheroids resembling basic acinus structure composed of differentiated acinar and ductal cells (Maria, Zeitouni et al. 2011, Shin, Hong et al. 2018, Pringle, Wang et al. 2019). iSGECs began to form spheroids within 24 hours of plating on matrigel (2mg/mL) and were cultured for a total seven days. ICC-IF protein expression analysis of iSGEC-nSS2 spheroid cultures showed high localization of acinar and epithelial cell markers ZO-1, AQP5, and AMY1A within acinus-like spheroid structures (Figure 2.5.7). Cytokeratins KRT8, KRT18, and KRT19 were all expressed in iSGEC-nSS2 cultured on matrigel (Figure 7).

We observed greater levels of KRT8 expression within interior cells of spheroids similar to previously described high expression in luminal cells (Su, Morgan et al. 1993). At a matrigel concentration of 2mg/mL, some cells formed monolayer sheets across the matrigel that expressed KRT18 and KRT19 at high levels (Figure 2.5.7). α-SMA protein expression was localized to myoepithelial-like cells located on the spheroid exteriors.

mRNA expression analysis by qRT-PCR of iSGEC-nSS2 matrigel cultures demonstrated an increase in pro-acinar cell expression of AQP5 compared to monolayer cultures (Figure 2.5.8). Spheroids from late passaged iSGEC-nSS2 expressed AMY1A and AQP5 at levels higher than early (p-14) cultures while expressing ANO1 at significantly lower (Figure 2.5.8). Most characterization markers in iSGEC-nSS2 (p-14 and p-80) cultured on matrigel were differentially expressed (Figure 2.5.8). Two consistent differentially expressed genes were VIM and KRT19, where VIM increased in matrigel cultures and KRT19 decreased. Similar to monolayer cultures on plastic, p-80 expressed NANOG at higher and KRT19 at lower levels, indicating a potential dedifferentiation when cultured for extended periods. However, p-80 exhibited the same increase in AQP5 mRNA expression as p-14 iSGEC-nSS2 cells on matrigel, retaining their ability to differentiate.

2.4. Discussion

This is the first study to establish immortalized primary cultures of xerostomic female patients using LSG biopsy tissue. We generated three novel composite iSGEC lines, with one capable of growing over 100 passages and maintaining expression of characterization markers.

Characterization of iSGEC-nSS2 indicates these cells to be of an undifferentiated ductal cell origin due to their high mRNA expression of KRT5 and relatively spotty distribution of KRT19 protein by ICC during monolayer culture on plastic (Knox, Lombaert et al. 2010, Knox, Lombaert

et al. 2013). When grown on matrigel, expression of KRT19 protein appeared more uniform over cells spread across the dish as a monolayer and is a marker expressed in both acinar and ductal cells (Emmerson, May et al. 2017, Pringle, Wang et al. 2019). Although a low concentration of 2mg/mL was used for the entirety of this study, we tested whether higher at concentrations of matrigel, those monolayer cells would remain. At a concentration of (4.5mg/mL) those monolayer cells fully incorporated into spheroid structures (data not shown).

Isolated acinar cells undergo dedifferentiation into ductal-like cells when explanted into cell culture plates (Fujita-Yoshigaki, Matsuki-Fukushima et al. 2008). Dedifferentiation of rat acinar cells can be halted by the inhibition of Src and p38 pathways, allowing the cells to retain high cytoplasm complexity and size in culture (Fujita-Yoshigaki, Matsuki-Fukushima et al. 2008). Understanding the interactions between ductal and acinar cells within the salivary gland epithelium could provide more insight into acinar cell regeneration and population maintenance. Additionally, SGECs have demonstrated the ability to trans-differentiate into acinar-like cells in matrigel cultures (Min, Song et al. 2018, Nam, Kim et al. 2018). Pathways regulating trans-differentiation would likely provide viable therapeutic targets, for example with small-molecule inhibitors, bypassing the need for stem-cell implantation (Lombaert, Brunsting et al. 2008). iSGEC-nSS2 spheroids resembled acinus-like structures with cells high in AQP5 expression and exterior surrounding myoepithelial-like cells expressing α-SMA (Figure 2.5.7). Changes in protein expression exemplified by a lack of α-SMA in iSGEC-nSS2 monolayer cultures and high expression in matrigel indicate cell differentiation during spheroid formation.

KRT5 transcript was found highly expressed in our iSGEC cultures similar to non-transformed SGECs, which is in agreement with reported protein expression by progenitor and ductal basal cells within the salivary gland epithelium (Jang, Ong et al. 2015). Under normal homeostatic conditions KRT5 positive cells give rise to intercalated and striated ductal populations (Weng,

Aure et al. 2018). However, during radiation induced salivary gland injury KRT5 expressing ductal cells are capable of differentiation into acinar cells (Weng, Aure et al. 2018). KRT5 positive ductal cells demonstrate higher robustness than acinar cells to radiation induced salivary gland damage and represent a favorable target in restoring acinar cell populations within damaged salivary glands (Knox, Lombaert et al. 2013). Importantly, SV40Lt immortalization has been shown to not affect the differentiation potential of immortalized progenitor cells (Wang, Chen et al. 2019). iSGEC-nSS2 could be a suitable model for understanding the cellular factors associated with trans-differentiation potential due to their high KRT5 mRNA expression.

Early (p-14) and late (p80) passaged iSGEC-nSS2 cells expressed AQP5 at higher levels in spheroid cultures (Figure 2.5.8), possibly indicating a greater extent of differentiation and therefore, displaying increased heterogeneity. However, expression of characterization marker, KRT19, decreased while VIM expression increased in iSGEC-nSS2 cells cultured on matrigel. Higher VIM expression may indicate an increase in stemness properties by dedifferentiation, along with reduced KRT19 expression (differentiated ductal cell marker), which could also further indicate an increase in stemness (Costa, Altemani et al. 2011). Similarly, changes in VIM and KRT19 expression were observed in long term 2D cultured (p-80) cells (Figure 2.5.4). Overall, dedifferentiation of iSGEC-nSS2 cells in both 2D and 3D cultures is likely associated with their high growth and differentiation potentials when cultured on matrigel. Last, iSGEC-nSS2 could offer an in-vitro alternative for salivary gland developmental research due to its dedifferentiation properties.

Direct introduction of an AQP1 expressing AAV vector into salivary glands demonstrated favorable clinical trial results where participants experienced a subjective decrease in xerostomia symptoms (Baum, Alevizos et al. 2012). Although the original rationale behind AQP1

AAV therapy was to increase water permeability in ductal cells, it was later found that acinar cells were responsible for the expression of AQP1 and saliva secretion (Alevizos, Zheng et al. 2017). As previously stated, KRT5 protein expressing ductal progenitor cells are more abundant and can differentiate into acinar cells after injury (Knox, Lombaert et al. 2013). Spheroid cultures obtained via iSGEC-nSS2 differentiation could serve as a suitable model to investigate how KRT5 positive progenitor cells possibly contribute to the generation of AQP1 expressing acinar after salivary gland damage and AQP1 AAV therapy.

2.4.1. Limitations

SGECs express AQP5 mRNA and protein under established culturing conditions, although being commonly identified of ductal origin (Kawanami, Sawaki et al. 2012, Jang, Ong et al. 2015). Moreover, a spontaneously immortalized mouse cell line expressing mixed ductal and myoepithelial protein markers when cultured as a monolayer showed mRNA expression of acinar markers in monolayer and 3D culture (Min, Song et al. 2018). Markers of differentiated ductal cells include KRT8 and KRT19 among others (May, Cruz-Pacheco et al. 2018). The lack of uniform expression by either KRT8 and KRT19 in monolayer cultures of iSGEC-nSS2 indicates a potential progenitor cell population, which is capable of differentiation into acinar-like and ductal-like cells when cultured on matrigel. Following culture on matrigel, iSGEC-nSS2 cells could be replated onto plastic tissue culture plates and further grown, thereby potentially expanding the differentiated cell populations for further analysis. To determine the extent of differentiation among acinar-like cells, immunocytochemistry targeting the terminally differentiated acinar cell marker, MIST1, should be employed. Moreover, dual staining of acinar and differentiated ductal cell markers to better identify and characterize the iSGEC-nSS2 cell line could be required to determine the extent of heterogeneity within the monolayer cultured cells.

Further research is needed to analyze the presence of tight junctions and their location throughout the apical portion of the plasma membrane, an important feature for polarized secretion by acinar cells (Baker 2010). Previous studies have demonstrated trans-epithelial resistance and polarized secretion of α-amylase within monolayer SGEC cultures (Jang, Ong et al. 2015). Among the several cell mechanisms dictating epithelial polarization and directional secretion, tight junction formation is a critical factor (Baker 2010). Techniques better visualizing the location of tight junctions within iSGEC-nSS2 spheroids should be employed to better determine the extent of polarization and direction secretion of the high AQP5 expressing acinar cells. Furthermore, ZO-1 was expressed at low levels in monolayer iSGEC cultures indicated by immunocytochemistry and its presence confirmed by Western Blot. Spheroids were un-cut during immunocytochemistry procedure, which could have impacted interior binding of the ZO-1 antibody or visualization of 3D architecture.

When salivary glands are damaged, acinar cells revert to a ductal-like state in mouse models (Shubin, Sharipol et al. 2020). Similar to the phenomenon observed in mice, rat acinar cells when extracted and cultured on plastic revert to a ductal like state, which can be reversed by inhibition of p38 and/or Src pathways (Fujita-Yoshigaki, Matsuki-Fukushima et al. 2008, Fujita-Yoshigaki 2010). Due to the outlined characteristics of iSGEC-nSS2, populations of differentiated acinar-ductal cells and ductal-progenitor cells could be present. Overall expression of AQP5 protein within iSGEC-nSS2 monolayer cultures localized within the plasma membrane and cytoplasm. Confirmation of AQP5 protein was further demonstrated by Western blot and exhibited a level of protein expression comparable to HMC-3A, which expressed AQP5 mRNA highest among all cell lines tested. When transitioned to culture on matrigel, AQP5 protein expression appeared to increase substantially within spheroid formations by ICC-IF. The increase in AQP5 expression among cells in matrigel culture could be a result of either de-differentiated acinar cell populations or progenitor-like cell populations (KRT5-positive) further

differentiating into acinar cells. Before iSGEC-nSS2 use in developing therapies for increasing AQP5 expressing cells within the salivary gland, further cell sorting would need to be employed to ensure a homogenous cell population to the extent possible for reproducibility in drug assays.

In addition, age, gender, and associated hormonal changes account for possible factors affecting expression profiles of iSGECs, impacting their biological properties. Also, acinar cells of lacrimal glands, acinar progenitor cells of salivary glands, and saliva DNA of pSS patients may have shortened telomeres, which could be more prominent with older age (Pringle, Wang et al. 2019, Noll, Bahrani Mougeot et al. 2020). Extensive cell passaging due to age combined with chronically shortened telomeres could lead to chromosomal instability and changes in DNA expression. Short Tandem Repeat (STR) profiling would be useful in the future to determine the extent of chromosome stability when passaged for extended periods and to establish a unique identifier for iSGEC-nSS2.

Although spheroids were formed by iSGEC-nSS2 in both early and late cultured cells, lumen formation needs to be further visualized, which could be useful in determining the extent of differentiation and cell types present. Also, a panel of cell lines derived from different types of xerostomic patients (i.e., nSS “sicca” or radiation-induced) may be needed to develop effective treatments.

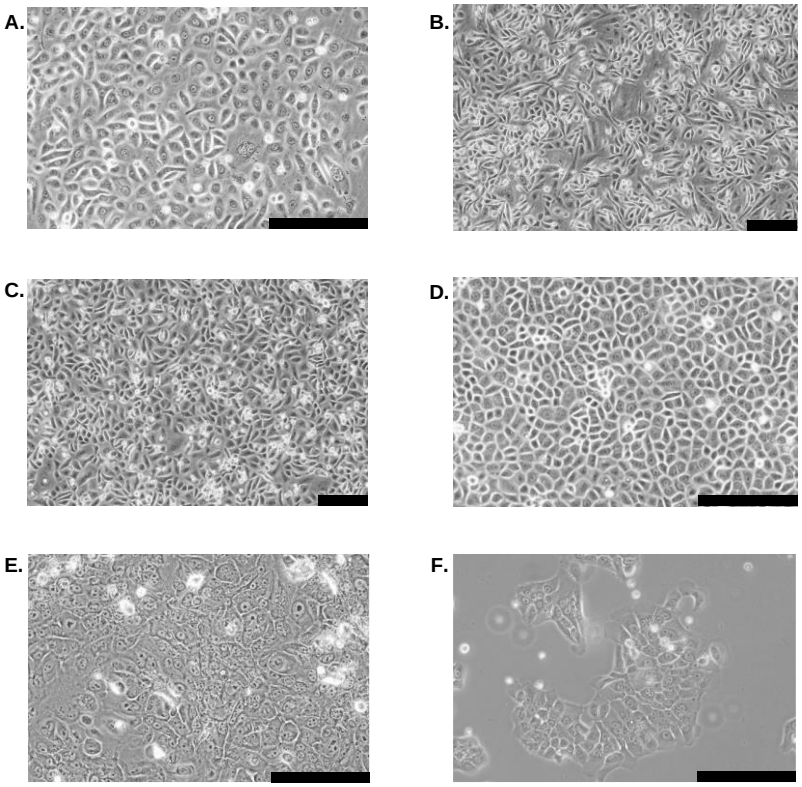

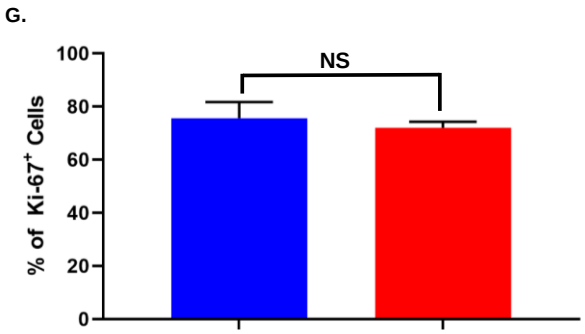

Figure 2.5.1: Morphology and proliferation of iSGECs. Representative images of early passage (p-14) monolayer culture (A) iSGEC-pSS1 (B) iSGEC-nSS1 (C) iSGEC-nSS2 and (D) late (p-80) iSGEC-nSS2. iSGEC-nSS2 "cobblestone" morphology was maintained across multiple passages when grown in SGEC sub-culturing media with low (0.06mM) Ca^{2+}. Cell morphology changes in (E) iSGEC-nSS2 p-14 and (F) iSGEC-nSS2 p-80 when supplemented with 1.2mM Ca^{2+} (final concentration) for 72 hours. (G) Proliferation of iSGEC-nSS2 was assessed by the percentage (%) of Ki-67^{+} cells using immunocytochemistry. No significant difference in the percentage of Ki-67^{+} cells was detected between early (p-14) and late (p-80) iSGEC-nSS2 cultures. Student's *t-test* (*p<.05, NS = not significant). Data are means +/- SEM. Magnification x20, scale bar = 200µm.

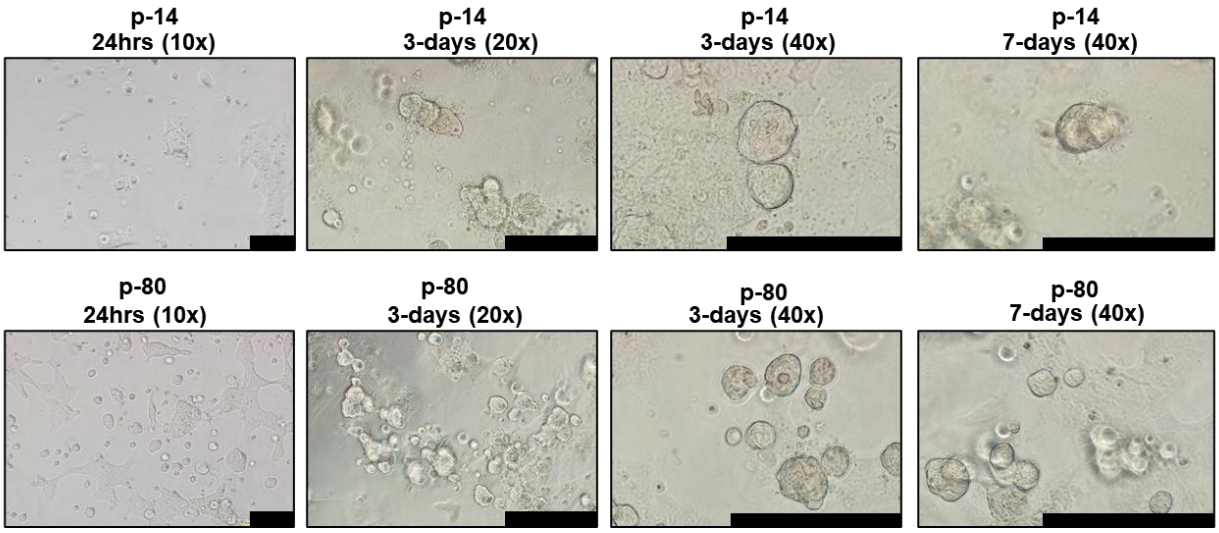

Figure 2.5.2: iSGEC-nSS2 early (p-14) and late (p-80) spheroid formation on Matrigel. Cells were initially seeded at 4x104 per well. Cultures began to form spheroids at 24 hours on matrigel (2mg/mL). Early passages (e.g., p-14) formed larger, but overall fewer spheroids when assessed after 3 days. Spheroids appeared to reach their final size after 3-4 days. Scale bars represent 200µm.

A) Acinar expression markers

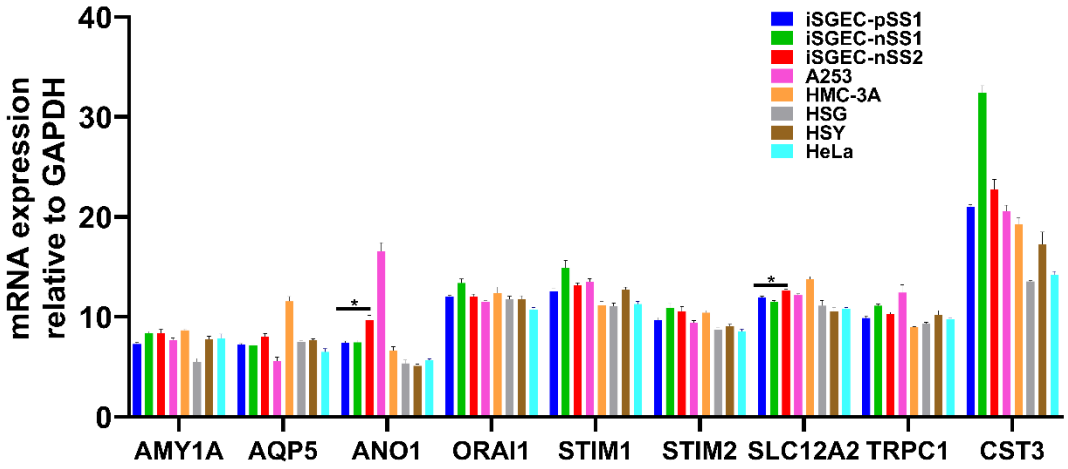

B) Characterization markers

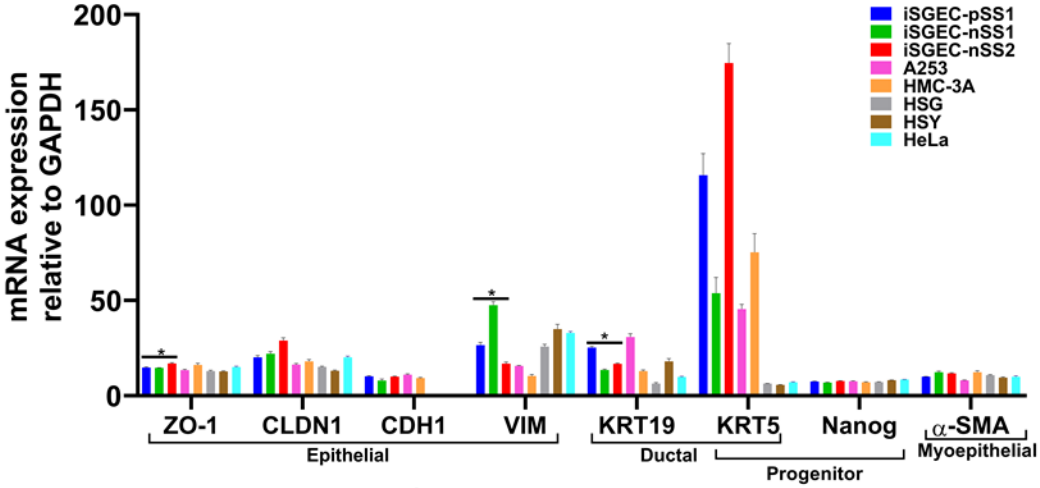

Figure 2.5.3: mRNA expression of acinar and characterization markers in monolayer cultured iSGECs, SGCLs, and HeLa cells by qRT-PCR. A) Pro-acinar markers were highly expressed in all iSGECs. ANO1 and SLC12A2 were expressed highest in iSGEC-nSS2 compared to other iSGECs. B) Characterization markers for epithelial, ductal, progenitor, and myoepithelial expression in all cell lines examined. The epithelial marker ZO-1 is an integral component of tight junctions and was overexpressed, whereas VIM (Vimentin) was under-expressed in iSGEC-nSS2. KRT-19, a ductal cell marker, was differentially expressed in iSGECs. *Indicates significant difference in expression determined by Student's *t-test* (alpha=0.05) and corrected using the Holm–Šidák method. Error bars represent mean +/- SEM.

A) Acinar marker expression

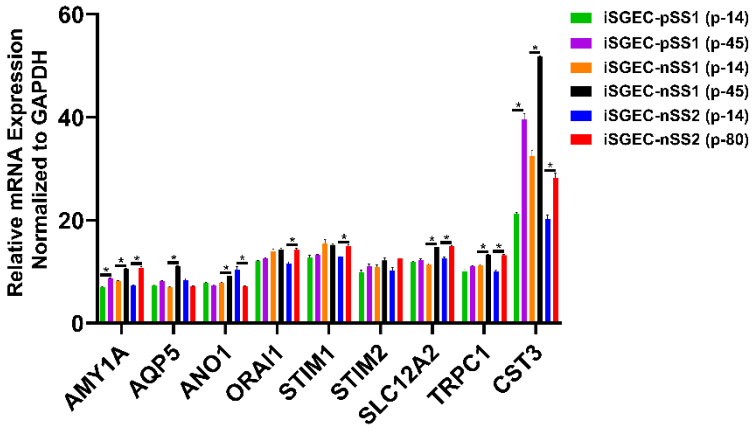

B) Changes in acinar marker expression

C) Characterization marker expression

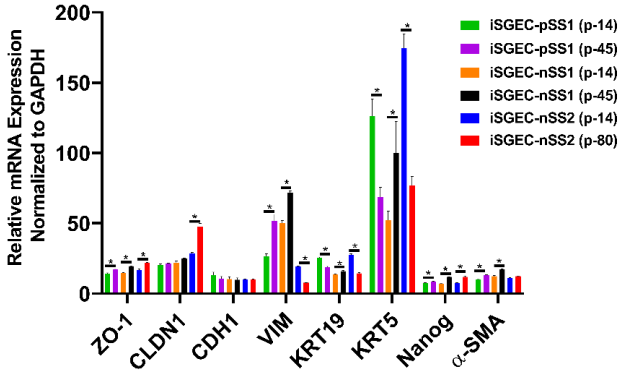

D) Changes in characterization marker expression

Figure 2.5.4: Changes in mRNA expression of early and late passaged iSGECs by qRT-PCR. mRNA expression of acinar (A) and characterization markers (C) in monolayer cultures of early and late passaged iSGECs by qRT-PCR (ΔCT). iSGECs increased in AMY1A (A), ZO-1 (C), and Nanog (C) in later passages. Changes in gene expression of iSGEC-nSS2 early (p-14) and late (p-80) are indicated with arrows: increased (red), decreased (green), and no change (yellow). (B, D) iSGEC-nSS2 differentially expressed several acinar and characterization markers in later passages. Significance of differences between the means was determined by Student's *t-test* and *p*-values corrected using the Holm–Šidák multiple comparisons *post hoc* test (alpha=0.05). Error bars represent mean +/- SEM. *p<0.05

A) Acinar marker expression

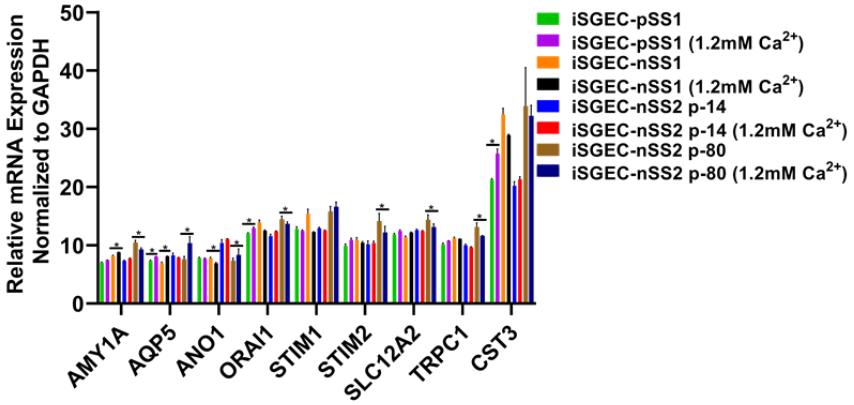

B) Changes in acinar marker expression of iSGEC-nSS2 p-14

C) Changes in acinar marker expression of iSGEC-nSS2 p-80

D) Characterization marker expression

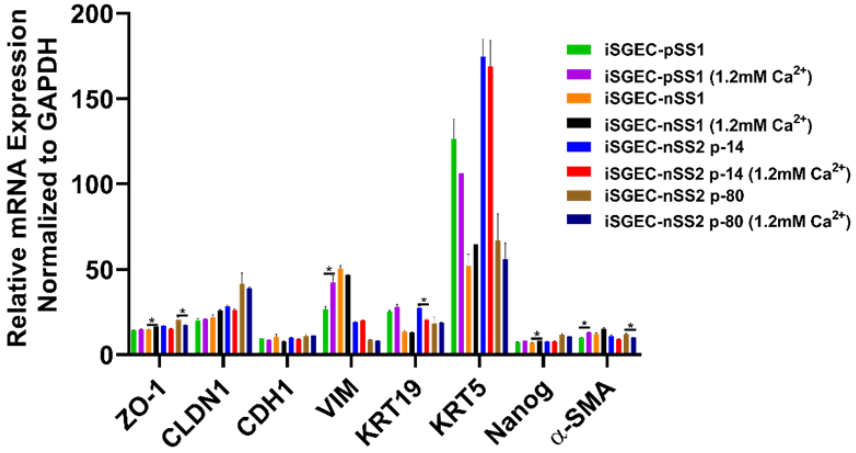

(E) Changes in characterization marker expression of iSGEC-nSS2 p-14

(F) Changes in characterization marker expression of iSGEC-nSS2 p-80

Figure 2.5.5: Changes in mRNA expression mediated by 1.2mM Ca^{2+}. Changes in acinar (A-C) and characterization markers (D-F) gene expression in iSGECs when cultured in 1.2mM Ca^{2+} for 72 hours. Changes in gene expression of iSGEC-nSS2 are indicated with arrows: increased (red), decreased (green), and no change (yellow). B) iSGEC-nSS2 p-14 did not display changes in expression whereas late passaged (p-80) exhibited increases in acinar markers AQP5 and ANO1. AMY1A, ORAI1, STIM2, SLC12A2, and TRPC1 expression decreased in 1.2mM Ca^{2+} p-80 cells. C) Overall, characterization markers exhibited little change in 1.2mM Ca^{2+} supplemented medium. D) Ductal cell marker (KRT19) decreased in early passage (p-14) iSGEC-nSS2 to levels similar in late (p-80) cells. Conversely, ZO-1 and α-SMA expression decreased in later passaged (p-80) iSGECs with 1.2mM Ca^{2+} and did not change in early (p-14) cells. Results calculated by Student's *t-test* and *p*-values corrected by the Holm-Šídák multiple comparisons *post hoc* test (*$p<0.05$). Error bars represent mean +/- SEM.

A.

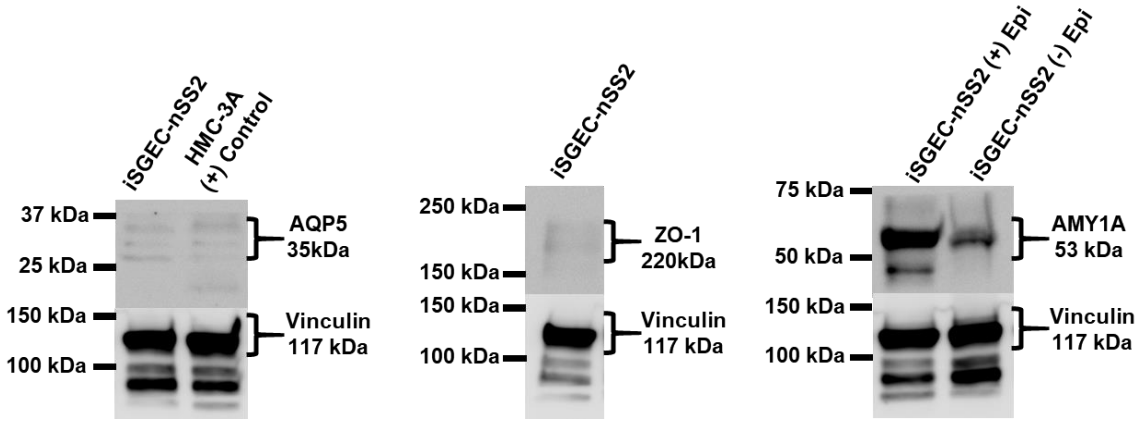

B.

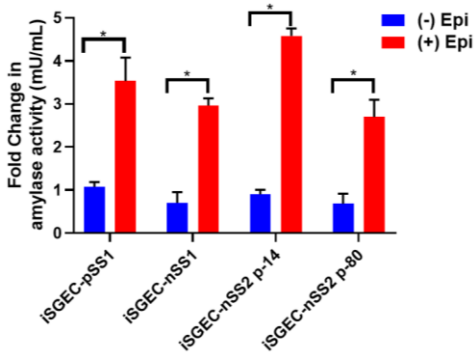

C.

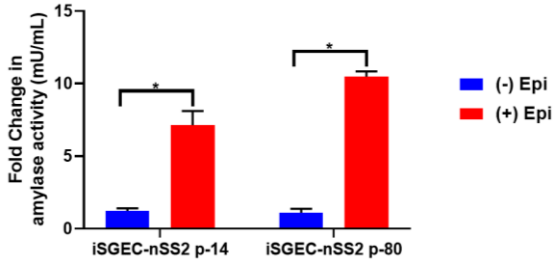

Figure 2.5.6: Protein expression of acinar and epithelial cell markers by western blot in iSGEC-nSS2. A) Protein expression of acinar (AQP5) (left) and epithelial (ZO-1) (middle) markers in whole cell lysate of monolayer cultured iSGEC-nSS2. (left) Expression of AQP5 in iSGEC-nSS2 whole cell lysate compared to HMC-3A, which was used as a (+) control for AQP5 in western blots. (right) After stimulation with 10μM epinephrine for 45 minutes ((+) Epi) cell culture supernatant was replaced, and cells were grown for 72 hours before media was collected and concentrated. Cells without stimulation by media supplementation with 10μM epinephrine ((-) Epi) served as the control. Secreted α-amylase was detected in both stimulated ((+) Epi) and unstimulated ((-) Epi) cultures. 10μM epinephrine stimulated ((+) Epi) iSGEC-nSS2 cultures exhibited higher levels of α-amylase in cell culture supernatant than unstimulated cultures after 72 hours. Western blots were normalized to vinculin expression in whole cell lysate of their respective sample. B-C) Media was harvested after stimulation with 10μM epinephrine for 45 minutes and amylase activity measured by colorimetric assay. B) Supernatant of monolayer cultured iSGECs treated with 10μM ((+) Epi) had significantly higher α-amylase activity compared to untreated cells ((-) Epi). C) Comparison of early (p-14) and late (p-80) passaged iSGEC-nSS2 secretion of α-amylase into media when cultured on matrigel. Results are listed as fold-change over the untreated control. Significance of differences between means was determined by Student's *t-test* and *p*-values corrected using the Holm–Šidák multiple comparisons test (alpha=0.05). Error bars represent mean +/- SEM. *p<0.05

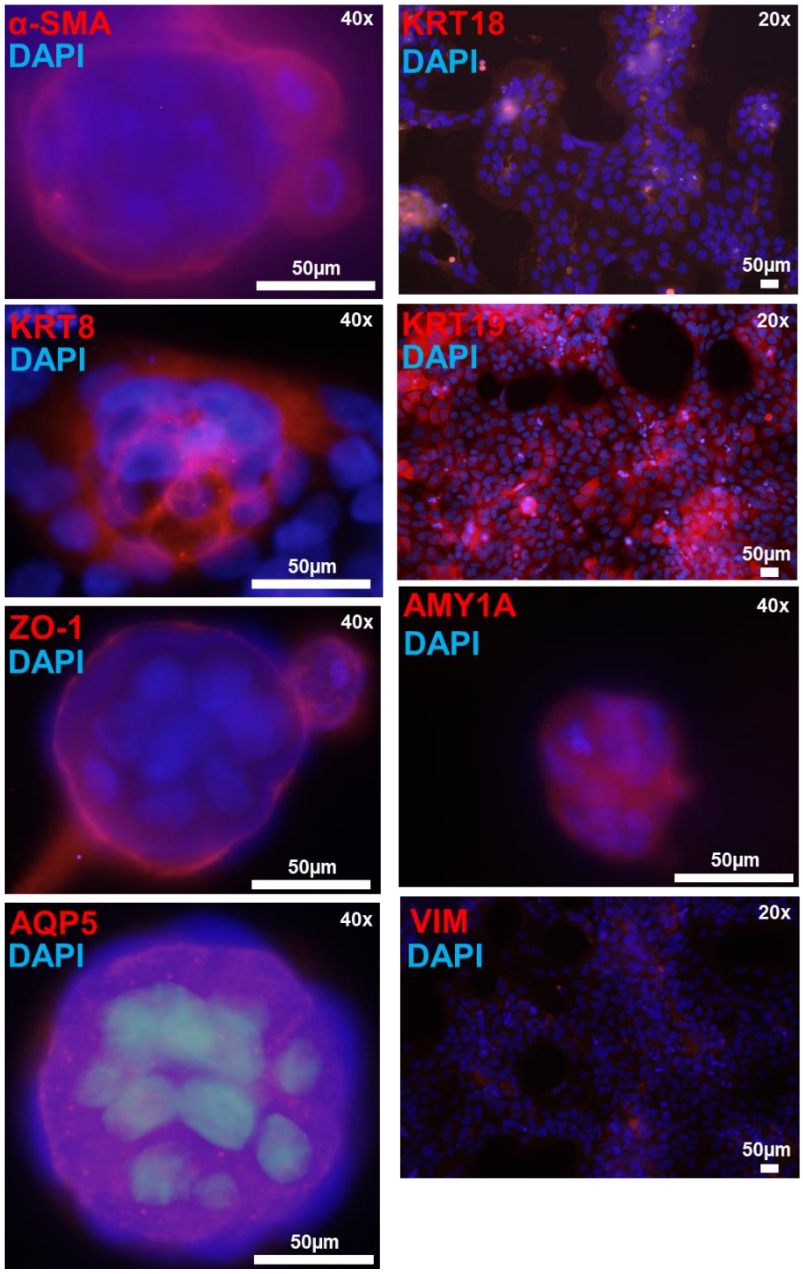

Figure 2.5.7: Immunofluorescence detection of salivary epithelium markers in matrigel cultured iSGEC-nSS2 cells. Detection of salivary epithelium markers (red) by immunofluorescence in matrigel cultures of iSGEC-nSS2 p-80 after 7 days. Spheroids expressed acinar cell markers (AQP5, AMY1A), tight-junction protein (ZO-1), and had clearly defined myoepithelial cells (α-SMA). Cells growing on the surface of the matrigel, and spheroids expressed salivary epithelial markers KRT8, KRT18, and KRT19 proteins. Vimentin was expressed low and sparsely among cells and did not indicate regular staining patters. Scale bar represents 50µm. DNA (blue) is highlighted with DAPI.

A.

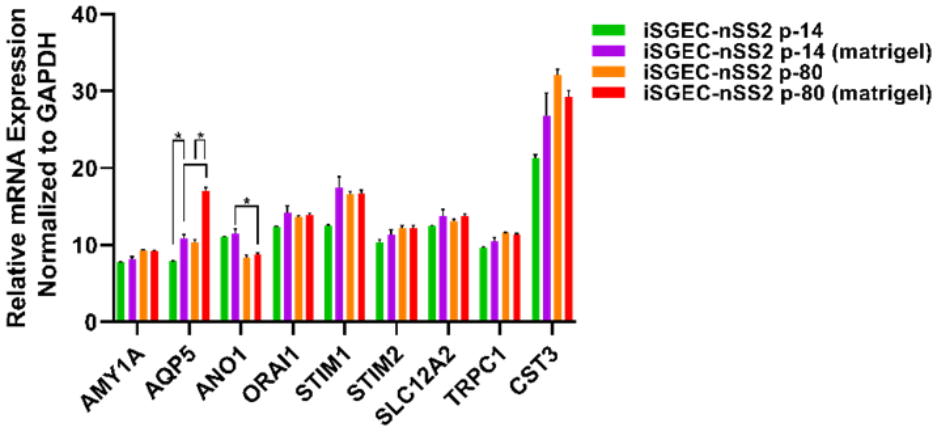
Relative mRNA Expression
Normalized to GAPDH
40
30
20
10
0
iSGEC-nSS2 p-14
iSGEC-nSS2 p-14 (matrigel)
iSGEC-nSS2 p-80
iSGEC-nSS2 p-80 (matrigel)
AMY1A
AQP5
ANO1
ORAI1
STIM1
STIM2
SLC12A2
TRPC1
CST3

B and C.


AMY1A
AQP5
ANO1
ORAI1
STIM1
STIM2
SLC12A2
TRPC1
CST3

D.


AMY1A
AQP5
ANO1
ORAI1
STIM1
STIM2
SLC12A2
TRPC1
CST3

E.

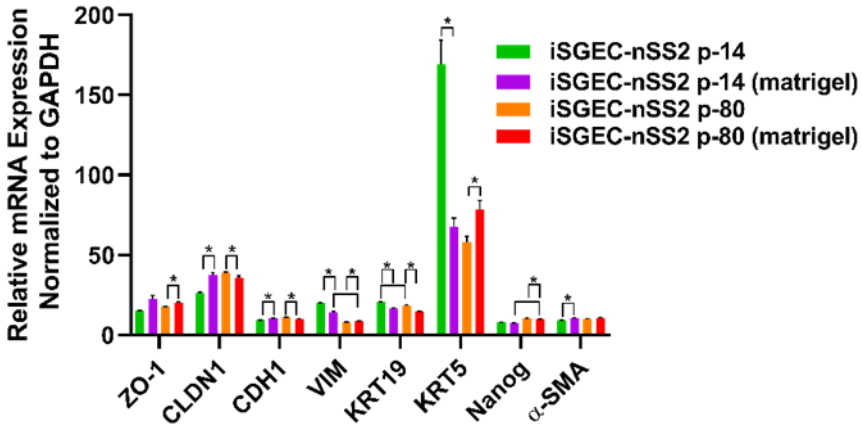
Relative mRNA Expression
Normalized to GAPDH
200
150
100
50
0
iSGEC-nSS2 p-14
iSGEC-nSS2 p-14 (matrigel)
iSGEC-nSS2 p-80
iSGEC-nSS2 p-80 (matrigel)
ZO-1
CLDN1
CDH1
VIM
KRT19
KRT5
Nanog
α-SMA

F.

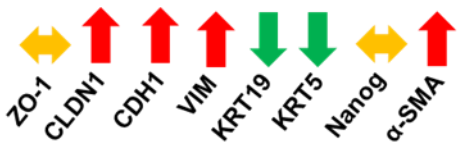

G.

H.

Figure 2.5.8: Changes in mRNA expression of early (p-14) and late (p-80) iSGEC-nSS2 cultures grown on matrigel. mRNA expression of early (p-14) and late (p-80) passaged iSGEC-nSS2 grown on either uncoated (monolayer) or matrigel coated plates by qRT-PCR (ΔCT). Changes in gene expression are indicated with arrows: increased (red), decreased (green), and no change (yellow). A, B-C) AQP5 expression was the only acinar cell marker to increase in both p-14 (B) and p-80 (C) when cultured on matrigel (final: 2mg/mL) coated plates. In p-80 cells, matrigel had a greater effect on AQP5 expression compared to p-14. D) Over extended passages, iSGEC-nSS2 expressed both AQP5 and AMY1A higher, whereas ANO1 decreased in expression over time. E-H) The mRNAs of characterization markers CLDN1, CDH1, VIM, and KRT19 were differentially expressed in both p-14 and p-80 cultures, respectively, when grown as a monolayer or matrigel coated plates. F-G) Only the ductal cell marker, KRT19, was consistently downregulated by matrigel. F-G) Vimentin (VIM) can be an indicator of dedifferentiation in SGECs and was increased (red) in both p-14 and p-80 matrigel cultures. Results calculated by Student's *t-test* and *p*-values corrected by the Holm-Šídák multiple comparisons test (*$p<0.05$). Error bars represent mean +/- SEM.

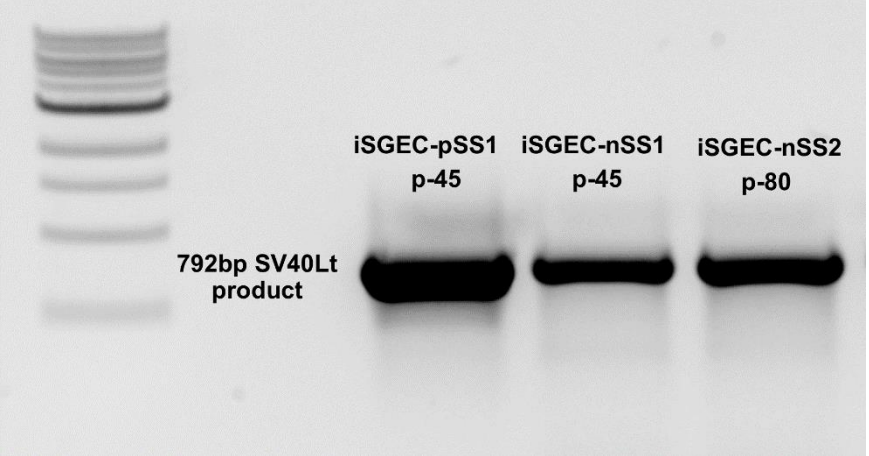

Figure 2.5.9: Semi-qRT-PCR analysis of SV40Lt expression in late passaged iSGECs. SV40Lt expression in the three iSGEC lines (pSS1, nSS1, and nSS2) at late passages p-45 and p-80.

A. p-80 single cell colonies

B-G. iSGEC-pSS1 and iSGEC-nSS1 spheroids

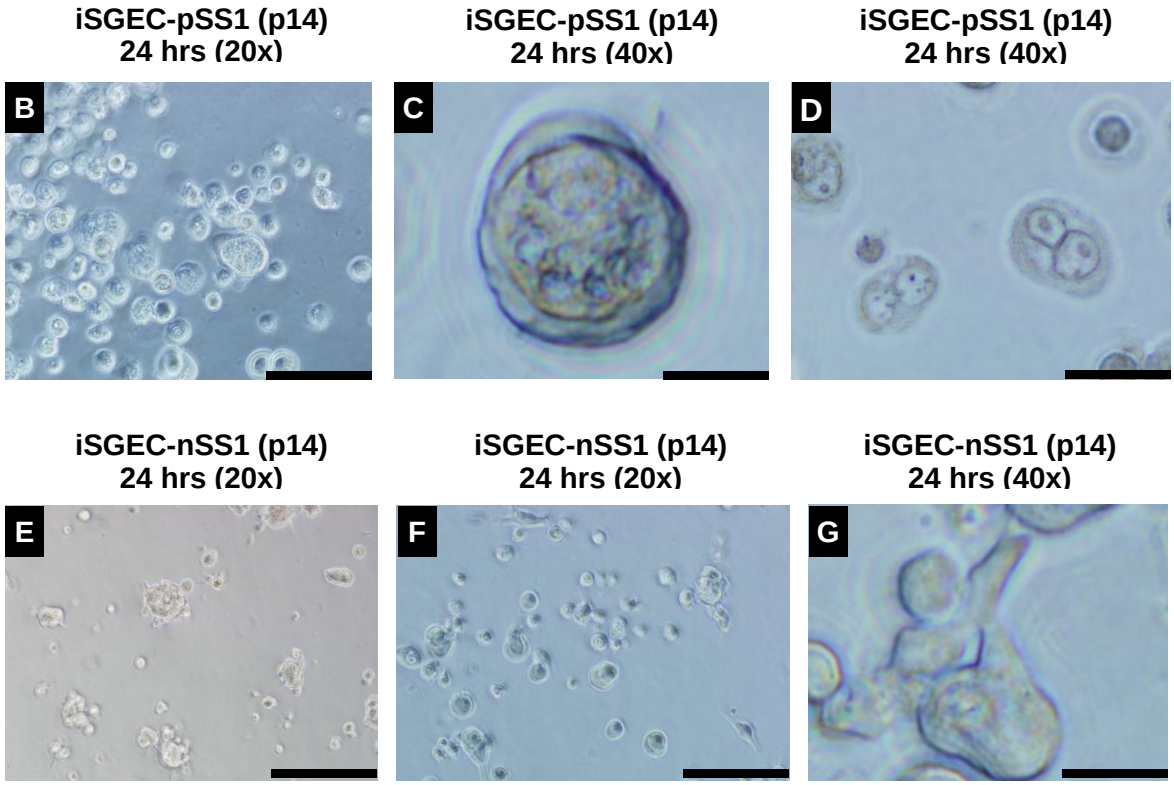

Figure 2.5.10: A. Phase contrast microscopy images of generated iSGEC lines. A) Single cell suspensions of iSGEC-nSS2 p-80 were plated on tissue culture treated plastic 12-well plates and grown for a minimum of 5-days before photographing. Linear shaped colonies formed from either filiform-appearing or cuboidal appearing cells. Circular shaped colonies would mainly arise from polygonal/ cuboidal appearing cells. Scale bar represents 200µm (20x). B-G) iSGEC-pSS1 and iSGEC-nSS1 were cultured on matrigel for 24 hours before photographing. iSGEC-pSS1 (B-D) formed spheroids with apparent differentiation into acinar-like structures (C) and myoepithelial-like structures (D). iSGEC-nSS1 formed spheroids (E-F) like other iSGECs, however, some spheroids exhibited tubular-like protrusions (G) resembling ductal formation. Scale bar represents 200µm (B, E, F) (20x) and 50µm (C, D, G) (40x).

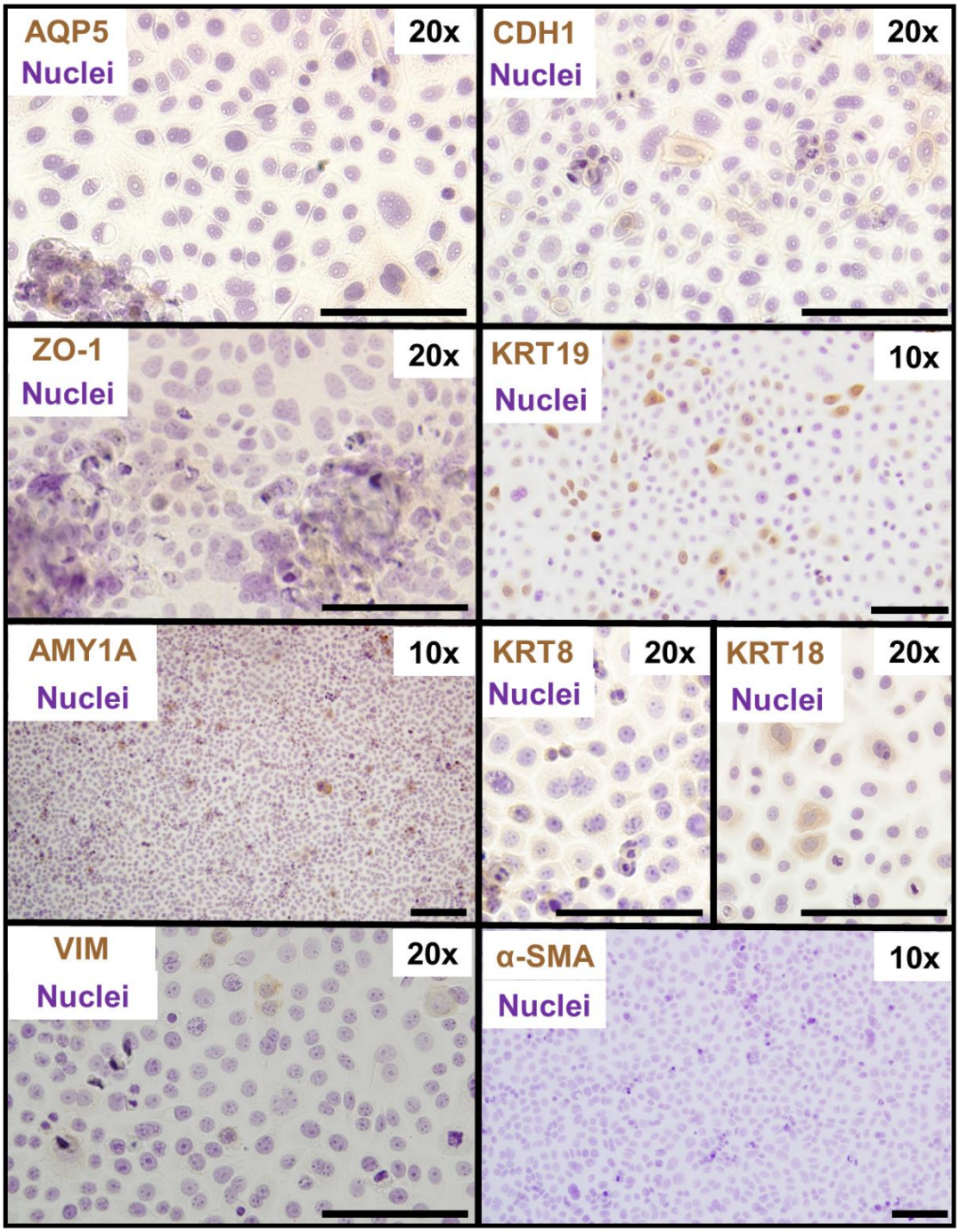

Figure 2.5.11: Expression of characterization markers in iSGEC-nSS2 cells by ICC. iSGEC-nSS2 cultures at p-14 were cultured on type-1 collagen coated glass coverslips and incubated with the antibodies . Protein targets (brown) are listed per each respective section. Nuclei (purple) were counterstained using Hematoxylin. Among proteins indicated, α-SMA was not detected in culture. The scale bar represents 200µm.

Table 2.6.1: Patient demographics and clinical features. Labial salivary gland biopsies used in this study were collected from one pSS and two sicca patients. All patients were negative (-) for serum Anti-Ro (SSA) and were not taking disease-modifying anti-rheumatic drugs (DMARDs). *The patient with the lowest focus score had the lowest salivary flow rates (unstimulated/ stimulated). NA: Schirmer's test was not performed due to patient objection or information not listed in electronic medical records.

Demographics	iSGEC-pSS1	iSGEC-nSS1	iSGEC-nSS2
Age	70	57	47
Gender	Female	Female	Female
Race	C	C	C
Clinical Features	pSS	nSS	nSS
Focus Score	1.8	0.3	0.16
Anti-Ro (SSA)	(-)	(-)	(-)
Unstim. Salivary Flow (<1.5mL/15min)	0.66	0.66	0.06*
Stimulated Salivary Flow (mL/min)	11.7	8.91	1.02*
Schirmer's (+/-)	NA	NA	(-)
DMARDs	(-)	(-)	(-)

Table 2.6.2: iSGECs, SGCLs, and HeLa protein expression of characterization markers by ICC. Results of protein expression of characterization markers in iSGECs, SGCLs, and HeLa cells by ICC are shown. Cells were grown on type-1 collagen coated coverslips for up to 72 hours prior fixation. iSGECs were additionally plated on coverslips and grow in SGEC sub-culturing media supplemented with 1.2mM Ca^{2+} to access changes in acinar cell marker expression. (+) indicates positive expression of protein. (+/-) indicates low or diffuse expression of protein. (-) indicates no protein expression was detected by methods outlined.

Protein Target	K8	K18	K19	ZO-1		E-Cadherin		AQP5		Vimentin		α-Amylase		α-SMA
				0.06 mM Ca^{2+}	1.2mM Ca^{2+}	0.06 mM Ca^{2+}	1.2 mM Ca^{2+}	.06 mM Ca^{2+}	1.2 mM Ca^{2+}	.06 mM Ca^{2+}	1.2 mM Ca^{2+}	0.06mM Ca^{2+}	1.2mM Ca^{2+}	
Cell Line														
iSGEC-pSS1	+	+	+	+	+	+	+	+	+	+	+	+	+	(-/+)
iSGEC-nSS1	+	+	+	(-/+)	(-/+)	+	+	+	+	+	+	+	+	(-/+)
iSGEC-nSS2	+	+	+	+	+	+	+	+	+	+	+	+	+	(-)
A253	+	+	+	(-/+)		+		(-/+)		+		+		+
HMC-3A	+	+	+	(-/+)		+		+		+		+		+
HSY	+	+	+	(-/+)		+		(-/+)		+		+		+
HSG	+	+	+	(-/+)		+		(-/+)		+		+		+
HeLa	+	+	+	(-/+)		(-)		(-/+)		+		(-/+)		+

Table 2.6.3: RT-PCR Primers

Target	Primer-F	Primer-R
Acinar cell markers		
AMY1A	CCTTCTGGGATGCTAGGCTG	ATCTTGGCCAACGGTAGCTT
AQP5	GCTCACTGGGTTTTCTGGGTA	CCTCGTCAGGCTCATACGTG
ANO1	CTGTCTTCATGGCCCTCTGG	TGACAGCCTCCTCTTCCTCT
ORAI1	GATGAGCCTCAACGAGCACT	ATTGCCACCATGGCGAAGC
STIM1	GGGATCTCAGAGGGATTTGACC	TCATGGCATTGAGAGCCTCG
STIM2	CAGTGACCGGAGTCACAGAC	CAGTTATGAGGTGGGCGTGT
SLC12A2	TTGGGCCCGATTTTCGAGAG	GGCTGACTGAGGATCTGCAAG
TRPC1	GTGATGGCGCTGAAGGATGT	ATAGTCACCCTTGTCGCACG
CST3	AGCCACATCTGAAAAGGAAAGC	GGGTGGGAGGTGTGCATAAG
Epithelial		
ZO-1	CGGTCCTCTGAGCCTGTAAG	GGATCTACATGCGACGACAA
CLDN1	CCCAGTCAATGCCAGGTACG	CAAAGTAGGGCACCTCCCAG
CDH1	CGCATTGCCACATACACTCT	TTGGCTGAGGATGGTGTAAG
KRT19	CCTCCCGAGATTACAACCACT	GGCGAGCATTGTCAATCTGT
Myoepithelial		
α-SMA	CTATGCCTCTGGACGCACAACT	CAGATCCAGACGCATGATGGCA
Mesenchymal		
VIM	CGGGAGAAATTGCAGGAGGA	AAGGTCAAGACGTGCCAGAG
Progenitor		
KRT5	TTGGACCAGTCAACATCTCTGT	CACTGCTACCTCCGGCAAGA
Nanog	AGTCCCAAAGGCAAACAACCCACTTC	TGCTGGAGGCTGAGGTATTTCTGTCTC
Housekeeping		
GAPDH	AGGGCTGCTTTTAACTCTGGT	CCCCACTTGATTTTGGAGGGA
Immortalization		
SV-40	AGCCTGTAGAACCAAACATT	CTGCTGACTCTCAACATTCT

Table 2.6.4: Antibodies and concentrations used for western blots and immunocytochemistry (ICC) experiments using horseradish peroxidase (HRP) and immunofluorescence (IF) based detection. Primers sets used for qRT-PCR and Semi-qRT-PCR analysis of epithelial and acinar cell characterization markers.

Gene Symbol	Protein Target	Dilution		Company	Cat#
		ICC	Western		
KRT8	Cytokeratin-8	1:250		SCBT	sc-8020
KRT18	Cytokeratin-18	1:250		SCBT	sc-6259
ACTA2	α smooth muscle actin (α-SMA)	1:250		SCBT	sc-53015
AQP5	Aquaporin 5 (AQP5)	1:100	1:300	SCBT	sc-514022
AMY1A	α-amylase	1:250	1:400	SCBT	sc-46657
TJP1	Zona-Occudin- 1 (ZO-1)	1:100	1:300	SCBT	sc-33725
KRT19	Cytokeratin-19	1:250		SCBT	sc-6278
MKI67	Ki-67	1:250		SCBT	sc-23900
VIM	Vimentin	1:250		SCBT	sc-6260
CDH1	E-Cadherin	1:200		SCBT	sc-8426
VCL	Vinculin		1:1000	SCBT	sc-73614
	(Secondary) anti-mouse IgG-HRP	1:50-1:250		SCBT	sc-516102
	(Secondary) anti-mouse IgG-HRP		1:1000-3000	Cell Signaling Tech.	#7076
	(Secondary) Goat anti-Mouse IgG-Alexa Fluor 594	1:250-500		Invitrogen	A11005

CHAPTER 3: REGULATION OF MMP9 TRANSCRIPTION BY ETS1 IN IMMORTALIZED SALIVARY GLAND EPITHELIAL CELLS OF XEROSTOMIC AND PRIMARY SJÖGREN'S SYNDROME PATIENTS

Abstract

Objectives

Primary Sjögren's syndrome (pSS) patients exhibit enhanced degradation of the salivary epithelium initially through MMP9 overexpression. We assessed the expression of MMP9 and associated transcription factors ETS1 and LEF1 in primary salivary gland epithelial cells (SGECs) and investigated potential regulatory mechanism(s) in immortalized SGECs.

Methods

SGECs and iSGECs were derived from pSS and/or xerostomic "sicca" patients. siRNA knockdown of ETS1 and/or LEF1 in iSGECs was performed to determine MMP9 mRNA (qRT-PCR) and protein expression (ELISA). ETS1 binding to MMP9 promoter was assessed by luciferase activity and binding confirmed by mutagenesis and ChIP. Effects of ETS1 and LEF1 overexpression on progenitor and Epithelial-Mesenchymal transition (EMT) associated markers (were determined by Western blot.

Results

ETS1 and MMP9 were overexpressed in SGECs of pSS and non-pSS sicca patients with salivary gland lymphocytic infiltration compared to non-pSS "sicca" patients without infiltration. ETS1 siRNA knockdown reduced MMP9 mRNA and protein levels. LEF1 knockdown had limited effects. ETS1 and LEF1 overexpression affected the expression of both EMT, and progenitor cell markers. ETS1 bound MMP9 promoter within DNA region -296bp to -339bp.

Conclusion

ETS1 may impair salivary function through direct transcriptional control of MMP9 promoter. ETS1 upregulation may also affect factors involved in repair of the dysfunctional pSS salivary epithelium.

3.1 Rationale

pSS clinical manifestation and management

Primary Sjögren's syndrome (pSS) affects approximately 1% of the general population with a 9:1 female to male predominance (Mavragani and Moutsopoulos 2014). Although the disease presents largely within the salivary and lacrimal glands, major systemic complications can occur which include nephritis, vasculitis, and lymphoma (Mavragani and Moutsopoulos 2014). Patients with pSS have a roughly 40 times higher risk of developing lymphoma than the general population (Mavragani and Moutsopoulos 2014). The classification of pSS based on disease-defining characteristics is still a matter of debate (Shiboski, Shiboski et al. 2017). Xerostomia patients with limited or no lymphocytic infiltration or characterized by the absence of anti-SSA auto-antibodies in the salivary and lacrimal glands are designated as "sicca" patients (Tashbayev, Garen et al. 2020). Xerostomia patients with significant lymphocytic infiltration and/or serum anti-SSA (Anti-Ro52/60/SSA Sjögren's syndrome antigen A) autoantibodies are designated as pSS. The cut-off for lymphocytic infiltration defining pSS is a focus score (FS) of 1 corresponding to the presence of at least one focus (focal accumulation of cells) with at least 50 lymphocytes per $4mm^2$ tissue area (Shiboski, Shiboski et al. 2017). pSS usually presents in mid-life (40-50 years of age) and generally evolves over several years (Mignogna, Fedele et al. 2005, Mavragani and Moutsopoulos 2014).

Currently, pSS is treated mainly symptomatically through the administration of immunosuppressants in conjunction with compounds used to stimulate fluid secretion (Chowdhury, Tappuni et al. 2021). Even with the advent of antibody targeted therapies, none have yet to be adopted into mainstream practice (Chowdhury, Tappuni et al. 2021). In 2016, the American College of Rheumatology-European League Against Rheumatism (ACR-EULAR) joint organization re-defined the symptoms and clinical criteria for pSS, increasing the emphasis of anti-SSA positive serology (Shiboski, Shiboski et al. 2017). Roughly 24% of pSS patients

remain autoantibody negative (Theander, Jonsson et al. 2015). The relative ineffectiveness of biological therapies such as rituximab for pSS combined with a lack of ubiquitous autoantibody expression, highlights other non-immunologic aspects contributing to disease onset and pathogenesis (Mignogna, Fedele et al. 2005, Theander, Jonsson et al. 2015, Chowdhury, Tappuni et al. 2021).

Non-immunologic early onset and pathogenesis of pSS

pSS pathology has been described as an “autoimmune epithelitis,” mainly affecting epithelial cells within the salivary and lacrimal glands (Mitsias, Kapsogeorgou et al. 2006). A loss of salivary epithelial homeostasis is demonstrated in pSS pathogenesis where disruptions to epithelial architecture are commonly observed (Barrera, Bahamondes et al. 2013). Changes to salivary and lacrimal functions were shown to occur during the “pre-immune” phase of pSS mouse models prior to autoimmune development and lymphocytic infiltration (Robinson, Yamamoto et al. 1996, Cha, Brayer et al. 2004, Peck, Saylor et al. 2011).

The extracellular matrix (ECM) is the primary structure essential to epithelial homeostasis and maintaining salivary gland epithelial cell function (Sequeira, Larsen et al. 2010, Cox and Erler 2011). Degradation of ECM structures by proteolysis and breakdown of topological epithelial integrity are prominent traits early in pSS pathophysiology (Schenke-Layland, Xie et al. 2008). Interruptions in ECM-cell connections trigger various processes, such as anoikis-mediated cell death or an Epithelial-Mesenchymal Transition (EMT) response in the salivary epithelium (Sisto, D'Amore et al. 2009, Scott, Weinberg et al. 2019). Detachment of acinar cells from the ECM disrupts homeostatic communication, hampering development and survival signaling among neighboring cells (Barrera, Bahamondes et al. 2013).

Role of MMP9 in pSS pathobiology

In pSS patients' salivary glands, the ECM is under perpetual degradation and remodeling by matrix metalloproteinases (MMPs), including MMP9 (Perez, Kwon et al. 2005). MMP9, also known as Gelatinase B, is a zinc-dependent endopeptidase, capable of degrading tight junction proteins and protein components located in multiple layers of the ECM (i.e., collagen IV, V, XI; laminin; elastin; aggrecan) (Vermeer, Denker et al. 2009, Laronha, Carpinteiro et al. 2020). MMP9 is overexpressed by the salivary epithelium in pSS without proximity to immune cell infiltration in glandular tissue (Perez, Goicovich et al. 2000, Goicovich, Molina et al. 2003, Tandon, Perez et al. 2017). In pSS patients, acinar and ductal cells have been shown to be responsible for local MMP9 secretion (Perez, Goicovich et al. 2000, Goicovich, Molina et al. 2003, Tandon, Perez et al. 2017). Additionally, MMP9 glandular expression and activity are highly correlated with the degree and severity of salivary gland damage and functional changes (Perez, Goicovich et al. 2000, Perez, Kwon et al. 2005). The mechanisms triggering and governing the overexpression of MMP9 in pSS are poorly understood

ETS1 and LEF1 as regulators of MMP9 expression

We have previously shown the overexpression of two transcription factors, namely V-Ets Avian Erythroblastosis Virus E26 Oncogene Homolog 1 (ETS1) and Lymphoid Enhancer-Binding Factor 1 (LEF1) in labial salivary glands (LSGs) of pSS patients (Shah, Noll et al. 2017, Shah, Noll et al. 2019). In pSS patients, ETS1 and LEF1 were co-overexpressed with MMP9 in glandular epithelium without proximity to lymphocytic ($CD4^+$) infiltrates (Shah, Noll et al. 2019). ETS1 has functions in multiple critical pathways implicated in pSS pathogenesis (*i.e.*, ERK/MAPK, Ras-MAPK, p-38, RAR, and Ca^{2+} signaling), impacting cell differentiation/development, cytokine production, hematopoiesis, and EMT (Yordy and Muise-Helmericks 2000, Dittmer 2003, Jordan, Johnson et al. 2011). ETS1 activity is primarily attributed to its hallmark ETS binding site (EBS) 5'-GGA(A/T)-3' motif, although cooperative

actions with other factors (*e.g.*, AP-1, RUNX, PAX3/5) enables binding to sites deviating from its core recognition sequence (Dittmer 2003, Garrett-Sinha 2013). LEF1 is involved in the Wnt signaling mediated by CTNNB1 (β-catenin) pathway (Jordan, Johnson et al. 2011, Santiago, Daniels et al. 2017). LEF1 also acts as a transcriptional activator that targets genes involved in EMT, cell migration, stem cell maintenance, and differentiation (Jordan, Johnson et al. 2011, Santiago, Daniels et al. 2017). LEF1 is an architectural transcription factor, which facilitates bending and loop formation of DNA into higher order structures with distant transcription factors (*e.g.*, ETS1), thereby regulating T-cell receptor expression through a remote enhancer site (Werner and Burley 1997). Overall, ETS1 and LEF1 are critical drivers of EMT, regulating MMP9 in a variety of epithelial cell types (Nakamura, Esnault et al. 2004, Santiago, Daniels et al. 2017, Nazir, Kumar et al. 2019). However, their role in regulating MMP9 expression in pSS salivary gland epithelia has not been determined (Nakamura, Esnault et al. 2004, Santiago, Daniels et al. 2017, Nazir, Kumar et al. 2019).

Here, we establish the correlation of ETS1 with MMP9 mRNA expression in our cultured primary salivary gland epithelial cells (SGECs) from labial salivary gland biopsies of sicca and pSS patients. Further, using immortalized SGEC (iSGEC) lines derived from one pSS and one sicca patient (Noll, Grdzelishvili et al. 2020), and two salivary gland cell line (SGCL) models of oral cancer origin, we demonstrate the regulation of MMP9 by ETS1 through direct promoter binding. We also determined the downstream effects of ETS1 and/or LEF1 on both pSS and non-pSS iSGECs regarding the expression of progenitor cell and EMT protein markers.

3.2 Materials and Methods

Salivary gland cell lines: A253, HMC-3A, iSGEC-nSS2, and iSGEC-pSS1

A253 cells (ATCC) were cultured per ATCC's recommended protocol. HMC-3A cells were a generous gift from Dr. Jacques E. Nor, DDS and Kristy Warner (University of Michigan School of Dentistry, Ann Arbor, MI, USA) and cultured as outlined by Warner *et al*. (Warner, Adams et al. 2013). Immortalized salivary gland epithelial cell lines (iSGEC-nSS2 and iSGEC-pSS1) were previously generated in our laboratory (Noll, Grdzelishvili et al. 2020). iSGEC-nSS2 and iSGEC-pSS1 immortalized cell lines were derived from a non-pSS "sicca" female patient with a focus score (FS) of 0.16 and a female pSS patient with FS=1.8, respectively. iSGEC cultures were grown in serum-free Epi-life Basal media (Gibco) without HKGS for 24hrs prior to experimentation. Detailed procedures are described in Appendix B.

Primary culture of salivary gland epithelial cells

LSG biopsies were collected from xerostomic patients undergoing routine diagnostic evaluation for glandular lymphocytic infiltrates (Shiboski, Shiboski et al. 2017). Clinical information for patient groups (*i.e.*, non-pSS (FS=0), non-pSS (0<FS<1), and pSS (FS≥1)) is presented in Table 3.6.1. Salivary gland tissue and derived primary cultures were approved by Atrium Health Institutional Review Board (Charlotte, NC, USA) and performed as previously described (Dimitriou, Kapsogeorgou et al. 2002, Jang, Ong et al. 2015). SGEC cultures were maintained in serum-free Epi-life Basal media (Gibco) with HKGS (1x) (Gibco) at 37°C and 5% CO_2. Media were replenished every three days and cells passaged 3-5x were used for mRNA extraction. Detailed SGEC culture protocols are in Appendix B

Generation of stable clones

HMC-3A cells ($3x10^5$ cell/well) were seeded in 6-well plates and allowed to adhere for 24hrs prior to transfection. pCMV3-Empty or pCMV3-ETS1 from SinoBiological (500ng) were used for

transfection (1.5µl of Lipofectamine 3000/well) (ThermoFisher). After 72hrs, cells were treated with 2xLD_{50} concentration of hygromycin (Enzo Life Sciences) for initial selection process and then reduced to 1xLD_{50} for remaining clonal selection.

MMP9 promoter plasmid constructs

The online NCBI primer-blast tool was used to design primers for MMP9 promoter luciferase-reporter plasmids (NCBI Entrez Gene: 4318) (Table 3.6.2). The -923bp to +18bp of the MMP9 proximal promoter was amplified by PCR using Phusion Polymerase (ThermoFisher). Restriction sites were incorporated into the forward (*mluI*) and reverse (*xhoI*) primers of the initial -923bp to +18bp promoter section for insertion into a pGL3-basic *renilla* luciferase reporter plasmid (Promega) upstream of the luc+ gene. Remaining 5'-deletion fragments (-439bp MMP9), (-366bp MMP9), (-216bp MMP9) were generated by PCR and cloned into the pGL3-basic luciferase reporter plasmid.

MMP9 promoter luciferase assay

SGCLs were seeded at approximately 70-80% confluency in 12-well plates 24hrs prior to transfection. Lipofectamine 3000 (ThermoFisher) was used for transfection following the manufacturer's recommended protocol. In each experiment, 300ng of either the control vector (pGL3-basic) or MMP9 proximal promotor pGL3 vector was co-transfected with 30ng pRL-TK (*renilla* luciferase plasmid) under the control of a thymidine kinase promoter using Dual Luciferase Assay system (Promega). Relative luciferase units (RLU) were calculated by the normalization of pGL3 luciferase activity to the co-transfected control plasmid (pRL-TK (Promega).

Promoter truncates and site-directed mutagenesis

Preliminary putative ETS1 transcription factor binding sites on MMP9 proximal promoter region were determined using online tool ALGEN-PROMO (Messeguer, Escudero et al. 2002, Farré, Roset et al. 2003). Mutations of the five consensus ETS1 (5'-GGA/T-3') binding sites (EBS) between -216 to -366 were generated by site-directed mutagenesis using primers described in Table 3.6.2. Detailed methods are in Appendix B.

siRNA knockdown and transient transfection

Native expression of ETS1 and/or LEF1 was knocked down using SMARTpool siRNA (Dharmacon) and Lipofectamine 3000 (ThermoFisher). siRNAs (Dharmacon) were obtained alongside the non-targeting siRNA #2 serving as negative control. Relative expression knockdown was calculated using average ∆CT of three independent experiments including non-targeting siRNA as control, from which relative ∆CT values were generated. Cells were harvested after 48hrs for mRNA isolation or 72hrs for protein isolation. Transient transfection of iSGECs with overexpression plasmids was performed similarly with the addition of 500ng of plasmid DNA added per well.

Quantitative real-time PCR

Total RNA was isolated from cells using the RNeasy mini kit (Qiagen) following the manufacturer's protocol. RNA (500ng) from each sample was reverse transcribed using TAKARA MMLv reverse transcriptase kit following the provider's instruction. Random Hexamers were purchased from IDT. dNTPs were purchased from Promega. Levels of ETS1, LEF1, and MMP9 were expressed as relative to GAPDH based on ΔCt method. qRT-PCR primers are listed in Table 3.6.2.

Western blot

Levels of target proteins in whole cell lysates of iSGECs, A253, and HMC-3A post-transfection were assessed by Western blot. Detailed methods are presented in APPENDIX B. Antibodies and concentrations are listed in Table 3.6.3.

ELISA

MMP9 secretion into media was measured by QuickZYME MMP9 (Quicktime Biosciences). MMP9 (active and inactive) quantification was normalized to total cellular protein. Experimental relative fold changes were determined by comparison to the non-targeting siRNA control. Detailed ELISA methods are described in Appendix B.

Chromatin immunoprecipitation (CHIP) assays

ChIP assays were performed using the EpiQuick Tissue Chromatin Immunoprecipitation Kit per manufacturers' instructions. Nuclear extracts were immunoprecipitated with antibodies targeting ETS1 (SCBT) or normal mouse IgG and subjected to qPCR with primers targeting the MMP9 promoter region from -197bp to -421bp (Table 3.6.2). Experimental samples and controls (mouse IgG) were normalized to 5% of the initial input of non-immunoprecipitated DNA. Detailed ChIP protocol is described in Appendix B.

Detection of iSGECs protein markers by immunofluorescence (IF)

Untreated iSGECs were cultured on 8-well chambered slides (ThermoFisher) coated with gelatin (0.2%) for 24-48hrs prior to fixation with 4% PFA. Dilutions for primary and secondary antibodies are listed in Table 3.6.3. Detailed IF methods are described in Appendix B.

Statistical analysis

Correlation of mRNA expression among SGECs was determined using Spearman's rank correlation ($\alpha = 0.05$). Comparisons were performed using Mann-Whitney U-test to determine significant differences between groups ($\alpha = 0.05$). Data are presented as mean +/- standard deviation (SD). Experiments were performed with a minimum of three biological replicates per condition. Statistical analyses were conducted using Graphpad Prism 9.2.

3.3 Results

The experimental approach and design for characterizing the ETS1 mediated regulation of MMP9 are outlined in Figure 3.6.6.

3.3.1 Differential expression of ETS1, LEF1 and MMP9 in pSS SGECs

To determine the relationship between MMP9, ETS1, and LEF1, we cultured primary SGECs of non-pSS (n=14; FS=0, 0<FS<1) and pSS (n=9; FS≥1) patients. ETS1 and MMP9 were significantly overexpressed in pSS SGECs compared to the non-pSS FS=0 group (Figure 3.5.1). Non-pSS patients (n=9; 0<FS<1) also showed increased ETS1 expression compared to non-pSS FS=0 (n=5) patients, although with marginal statistical significance (p=0.06) (Figure 3.5.1). ETS1 and MMP9 displayed a significant correlation in cultured SGECs (p=0.0125, r=0.5120), whereas LEF1 expression correlated with ETS1, not MMP9 (p=0.0085, r=0.5350) (Figure 3.5.1). LEF1 was not expressed at higher levels in either non-pSS (0<FS<1) and pSS FS≥1 groups (p>0.05) compared to non-pSS (FS=0), which differs from the *in vivo* context (Shah, Noll et al. 2019).

To further examine MMP9 regulation by ETS1 and LEF1, siRNA targeting ETS1 and/or LEF1 was transfected in iSGECs, HMC-3A, and A253 (Figure 3.5.1). In all cell lines tested, MMP9 mRNA expression was significantly decreased when ETS1 expression was reduced. LEF1

siRNA knockdown reduced MMP9 expression in iSGEC-nSS2 cells but not in HMC-3A, A253, and iSGEC-pSS1 cells. Overall, ETS1 and LEF1 did not appear to exhibit a combined effect on MMP9 downregulation, suggesting that ETS1 contributes a larger direct regulatory role for MMP9 expression in pSS pathogenesis. This result is consistent with LEF1's role as an architectural transcription factor (Werner and Burley 1997). The observed correlation between ETS1 and LEF1 (Figure 3.5.1) mRNA expression of pSS and non-pSS cultured SGECs was explained in part by siRNA treatment showing that ETS1 and LEF1 were reciprocally affected by each other's expression. LEF1 knockdown increased ETS1 expression in iSGEC-nSS2 ($p<0.05$) but not in iSGEC-pSS1. The same effect was not observed in either A253 or HMC-3A, where A253 cells demonstrated an increase in LEF1 expression with ETS1 knockdown. These results suggest a relationship among all three genes (ETS1, LEF1, MMP9), however, not to the extent demonstrated by the regulatory effect of ETS1 on MMP9 expression alone. Accordingly, we focused on the regulation of MMP9 by ETS1.

3.3.2. Reduction of intracellular MMP9 expression and secreted MMP9 by siRNA knockdown of ETS1

To further investigate regulation of MMP9 by ETS1, we evaluated the effects of ETS1 and/or LEF1 siRNA after 72hrs on MMP9 protein levels in whole cell lysate of HMC-3A and A253 cells (Figure 3.5.2). Western blot analysis showed MMP9 protein was decreased in both HMC-3A and A253 cells by ETS1 and/or LEF1 siRNA. Expanding on the previously uncovered regulation of LEF1 by ETS1 at the mRNA level (Figure 3.5.1), total LEF1 protein increased with ETS1 siRNA knockdown in A253 cells (Figure 3.5.2). Secreted MMP9 protein levels were assessed by ELISA (Figure 3.5.2). ETS1 inhibition led to a significant decrease in secreted total MMP9 of all four cell lines ($p<0.05$). In contrast to unchanged MMP9 mRNA expression after siRNA knockdown of LEF1 in HMC-3A, MMP9 protein levels were significantly reduced in cell culture supernatants (Figure 3.5.2).

3.3.3. Identification of the ETS1 responsive region(s) within MMP9 promoter

We determined DNA regions containing putative ETS-1 binding sites (EBS) that were most responsive by transient transfection into HMC-3A ETS1 overexpressing clone (HMC-3A-E6). The most responsive region span -216bp to -366bp upstream of MMP9 transcription start site (TSS) (Figure 3.5.3). The largest increase in luciferase activity was observed for this region with ~2-fold higher activity than the -216bp and ~2.5-fold over the -439bp truncates. Two putative EBSs within this promoter region (-216bp to -366bp) were uncovered using online ALGGEN-PROMO tool. Based on consensus ETS1 binding sequence 5"-GGAA/(T)-3", we selected additional three potential EBS within this region (Figure 3.5.3). Site-directed mutagenesis revealed three separate sites responsible for ETS1 binding on MMP9 promoter **(**Figure 3.5.3). EBS-MUT1 contains the sequence 5'-AAGGGAT-3' with consensus sequence underlined. EBS-MUT2 contains the sequence 5'-GGATCC-3' sites, conferring two potential binding sites in palindrome orientation. Mutations disrupting MUT1 or MUT2 regions reduced promoter activity by (57%) -2.32-fold and (59%) -2.44-fold, respectively. To confirm whether the presence of one or both sites was required for ETS1 activity, we constructed the -366bp-MMP9 pGL3 EBS-MUT1+2 plasmid containing both EBS-MUT1 and EBS-MUT2 site mutations.

Changes in both sites showed either site is required for ETS1 activity, whereas tandem mutations did not further decrease MMP9 promoter activity (66%) (-2.93-fold) ($p>0.05$) compared to either EBS-MUT1 or EBS-MUT2 individually. The final EBS (MUT5) represents a consensus EBS previously described as a significant motif in ETS1-responsive promoter regions of both ETS/AP-1 responsive RAS/ERK mediated epithelial gene expression and B-cell maturation (Dittmer 2003, Garrett-Sinha 2013). Here, EBS-MUT5 (5'-CAGGAAA-3") reduced promoter activity by 70%, *i.e.*, ~3.3-fold, compared to the full length -366bp-MMP9 pGL3 plasmid ($p<0.01$). Serial deletion and site-directed mutagenesis of the -216bp to -366bp MMP9 promoter region revealed three potential EBSs which were further analyzed in A253, iSGEC-

pSS1, and iSGEC-nSS2 cells (Figure 3.5.3). iSGEC-nSS2 and A253 responded similarly to HMC-3A (E6) using EBS-MUT2 and MUT5 with significant reductions in luciferase activity, *i.e.*, 47%/62% and 49%/58%, respectively. Among iSGEC-nSS2, A253 was the only one showing a decrease in promoter activity of EBS-MUT1 -2.5-fold (60%) ($p<0.05$) reduction in luciferase expression. Overall, iSGEC-pSS1 showed a modest decrease in MMP9 expression for all EBS-MUTS (1, 2, 1+2, and 5) with the largest decrease observed in EBS-MUT1 (-1.3-fold) (24%) ($p>0.05$).

To confirm ETS1 was responsible for binding to the MMP9 promoter region within -216bp to -366bp of the transcription start site, ChIP was performed using an ETS1 antibody with qPCR primers targeting the 224bp surrounding region from -421bp to -197bp of the MMP9 TSS (Figure 3.5.3). All four cell lines displayed a significant increase in the percentage of input bound over the control (normal mouse IgG). Together, these results demonstrated the regulation of ETS1 at either the EBS-MUT 1, 2, 1+2, and/or 5 site(s) was responsible for MMP9 promoter activation in the salivary gland epithelial cell lines tested.

3.3.4. Epithelial and mesenchymal marker expression and ETS1 nuclear localization in iSGECs

The regulatory role of ETS1 in MMP9 expression was markedly different in non-pSS sicca *vs.* pSS derived iSGEC. To further characterize the mechanism(s) contributing to the regulatory disparities of ETS1 and possible relationship to pSS pathogenesis, we analyzed the basal expression of epithelial (CDH1), mesenchymal (VIM), and salivary progenitor cell (K5, EpCAM) markers by immunofluorescence assay (IF). iSGEC-nSS2 produced a uniform expression of CDH1 and EpCAM in the plasma membrane, whereas iSGEC-pSS1 demonstrated intermittent CDH1 without membranous EpCAM (Figure 3.5.4). The most apparent difference observed was expression of VIM, where iSGEC-pSS1 expressed VIM to a greater extent over iSGEC-nSS2.

Additionally, dual IF using a specific Phos(T38)-ETS1 antibody revealed a distinct relationship among nuclear Phos(T38)-ETS1 and MMP9 expression (Figure 3.5.4) in iSGEC-pSS1 cells.

3.3.5. Effects of ETS1 and/or LEF1 overexpression in iSGECs on epithelial and EMT-associated markers

We assessed whether ETS1 and/or LEF1 overexpression altered the expression of salivary progenitor cell (EpCAM, K5), epithelial (CDH1, AQP5, B-catenin), mesenchymal (VIM), and MMP9 markers in whole cell lysates of iSGECs by transfection with ETS1 and/or LEF1 expression vectors. MMP9 protein expression increased after ETS1 overexpression in both iSGEC lines (Figure 3.5.5). An inverse trend was observed for CDH1 and VIM after overexpression of ETS1 and/or LEF1 in iSGEC-nSS2 cells where CDH1 expression decreased as VIM increased (Figure 3.5.5). Conversely, iSGEC-pSS1 levels of CDH1 remained relatively unchanged while VIM expression increased after ETS1 and/or LEF1 overexpression. AQP5 expression increased in iSGEC-nSS2 cells after transfection with either ETS1 and/or LEF1, following the same trend as both EpCAM and K5.

3.4. Discussion

We demonstrated for the first time the overexpression of ETS1 and MMP9 in cultured SGECs of pSS patients and confirmed a significant relationship between ETS1 and MMP9 expression. We also utilized siRNA targeted against ETS1 in two SGCLs (A253 and HMC-3A) and two iSGEC lines (iSGEC-pSS1 and iSGEC-nSS2), showing reduced MMP9 mRNA and protein expression. To uncover the regulatory nature of this connection, we generated an ETS1 overexpressing clone of the SGCL HMC-3A to investigate ETS-mediated regulation of MMP9. Luciferase activity assays implied significant ETS1 regulatory features within -216bp to -366bp upstream of the MMP9 TSS. Site-directed mutagenesis of three binding sites demonstrated that ETS1

regulated MMP9 transcription in all four cell lines tested, which was further confirmed by ChIP assay.

3.4.1. Consequences of pathologic MMP9 overexpression in the salivary epithelium

The functional role of MMP9 in the pre-immune phase of pSS has so far to be fully elucidated. Figure 3.5.7 presents a model outlining the downstream effects of MMP9 overexpression and possible consequences of ECM breakdown, consistent with pathological observations demonstrated in pSS salivary glands. It was previously shown that pSS mouse models demonstrate breakdown of glandular structures by MMP9 in the epithelium, early in disease onset with limited or no presence of infiltrating lymphocytes (Cha, van Blockland et al. 2001). Our study establishes ETS1 as a driver of the pathologic MMP9 overexpression in the salivary epithelium of both pSS and non-pSS SGECs (0<FS<1). pSS pathogenesis involves a pre-inflammatory and immune phase, where the disorganization, breakdown, and reduced secretion (pre-inflammatory) of the salivary glands is exacerbated by lymphocytic infiltration (immune phase) (Hayashi 2011). Although the current classification criteria for pSS includes multiple clinical observations and a single assessment of LSG infiltrates (*i.e.*, focal scoring) when negative for serum Anti-SSA, pre-immune pSS bears significant value in preventive therapy development (Shiboski, Shiboski et al. 2017). pSS SGECs expressed MMP9 at higher levels compared to non-pSS FS=0 group, consistent with *in vivo* pathology disease (Figure 3.65.1). Moreover, non-pSS (0<FS<1) SGECs exhibited a similar increase in both MMP9 and ETS1 as the pSS FS≥1 group, which may be representative of a state of possible progression of sicca towards pSS.

3.4.2. Differences in ETS1 activity on the MMP9 promoter in iSGEC-nSS2 vs. -pSS1

The regulatory impact of ETS1 on MMP9 expression was present but reduced within the iSGEC-pSS1 cells when compared to iSGEC-nSS2 (intermediate non-pSS sicca) (Figure 3.5.1**,**

Figure 3.5.2**,** and Figure 3.5.3). This unanticipated observation might explain some of the discrepancies observed regarding MMP9 expression and its regulation in the pSS salivary gland epithelium (Azuma, Aota et al. 2000, Tandon, Perez et al. 2017, Aota, Ono et al. 2019). Transcriptional regulation of MMP9 is likely more dependent on ETS1 in sicca patients (non-pSS, 0<FS<1) when inflammation is limited. As the disease shifts to the immune-phase with lymphocytic infiltrates, other MMP9 regulators may play a role such as the inflammatory cytokines TNF-α or transcription factor NF-κβ (Azuma, Aota et al. 2000, Aota, Ono et al. 2019). The presence of other factors mediating ETS1 binding could explain smaller reduction in MMP9 promoter activity of iSGEC-pSS1 **(**Figure 3.5.3), although significant promoter binding by ETS1 was observed (Figure 3.5.3).

3.4.3. Modulation of ETS1 activity and function by cofactors or post-translational modification

The function and activity of ETS1 has been demonstrated to be heavily dependent on cooperative binding partners (Dittmer 2003, Garrett-Sinha 2013). ETS1 activity is further modulated by its phosphorylation status at different sites, such as ERK1/2 mediated Thr ^{38}/Thr ^{72} (Dittmer 2003, Garrett-Sinha 2013). The ERK1/2 pathway has been implicated in pSS SGEC cytokine production and EMT-mediated fibrosis of salivary gland tissue (Lisi, Sisto et al. 2014, Sisto, Lorusso et al. 2020). Post-translational modifications to ETS1 alongside cooperative binding partners could explain the difference in iSGEC-nSS2 and iSGEC-pSS1 MMP9 expression (Figure 3.5.1, Figure 3.5.2).

3.4.4. The potential role of LEF1 in the salivary epithelium

Although LEF1 was not overexpressed in the SGECs of either pSS or non-pSS (0<FS<1) patients when compared to the non-pSS sicca FS=0 group (Figure 3.5.1), our results showed significant correlation between ETS1 and LEF1 expression in SGECs. This suggests an impact

of the salivary inflamed environment on LEF1 expression and potential changes associated with explant culturing. In addition, since LEF1 is an architectural transcription factor involved in the formation of higher order structures, the effects of siRNA knockdown in our *in vitro* model systems may not be representative of the *in vivo* situation, where other factors play a role as a function of disease progression.

3.4.5. ETS1 and LEF1 alter the expression of EMT associated proteins

The effects of ETS1 and LEF1 on EMT associated proteins by Western blot (Figure 3.5.5) demonstrated an impact on epithelial/mesenchymal gene expression. LEF1 alone enhanced VIM expression greater than ETS1 or ETS1+LEF1 in iSGEC-nSS2, whereas either ETS1 or LEF1 increased VIM expression within iSGEC-pSS1. These results are consistent with previous studies highlighting the role of ETS1 in EMT where ETS1 itself was unable to induce EMT but potentiated and maintained the cells in an EMT-like state (Taki, Verschueren et al. 2006). iSGEC-pSS1 cells expressed VIM at higher basal levels than iSGEC-nSS2 cells and similarly responded greater to ETS1 overexpression. Despite the differences in basal expression of EMT-associated markers, both cell lines expressed K5 consistently, suggesting they possess features characteristic of progenitor cells of the basal epithelium (Figure 3.5.4) (Rios, Fu et al. 2014).

3.4.6. Caveats/pitfalls

It is important to note we did not assess the downstream effects of MMP9 inhibition by ETS1 such as MMP9-mediated downregulation of CXCL10 under IFN-γ stimulation (Aota, Ono et al. 2019). MMP9 has been previously demonstrated to mediate EMT in cell culture models (Li, He et al. 2020). However, the relationship between MMP9 and EMT-related genes within the salivary epithelium was not explored within this study. Additionally, we did not address possible mechanisms governing the overexpression of ETS1 within the epithelium of pSS patients.

Interestingly, LINE-1 ORF-1p, a retrotransposon element typically silenced through DNA methylation is overexpressed in pSS patients, interacts with ETS1 increasing nuclear concentrations and facilitates ETS1-DNA binding (Yang, Feng et al. 2013, Mavragani, Nezos et al. 2018). The series of etiologic events contributing/leading to pSS is not well understood, but hypomethylation has been reported as a potential causative agent (Mavragani, Nezos et al. 2018, Mougeot, Noll et al. 2018). Potential sources of non-immunologic LINE-1 ORF-1p hypomethylation could be due to improper X-chromosome inactivation where genes controlling methylation located on the X-chromosome are improperly silenced, leading to global methylation changes over time and an X-chromosome dose-effect (Mougeot, Noll et al. 2018).

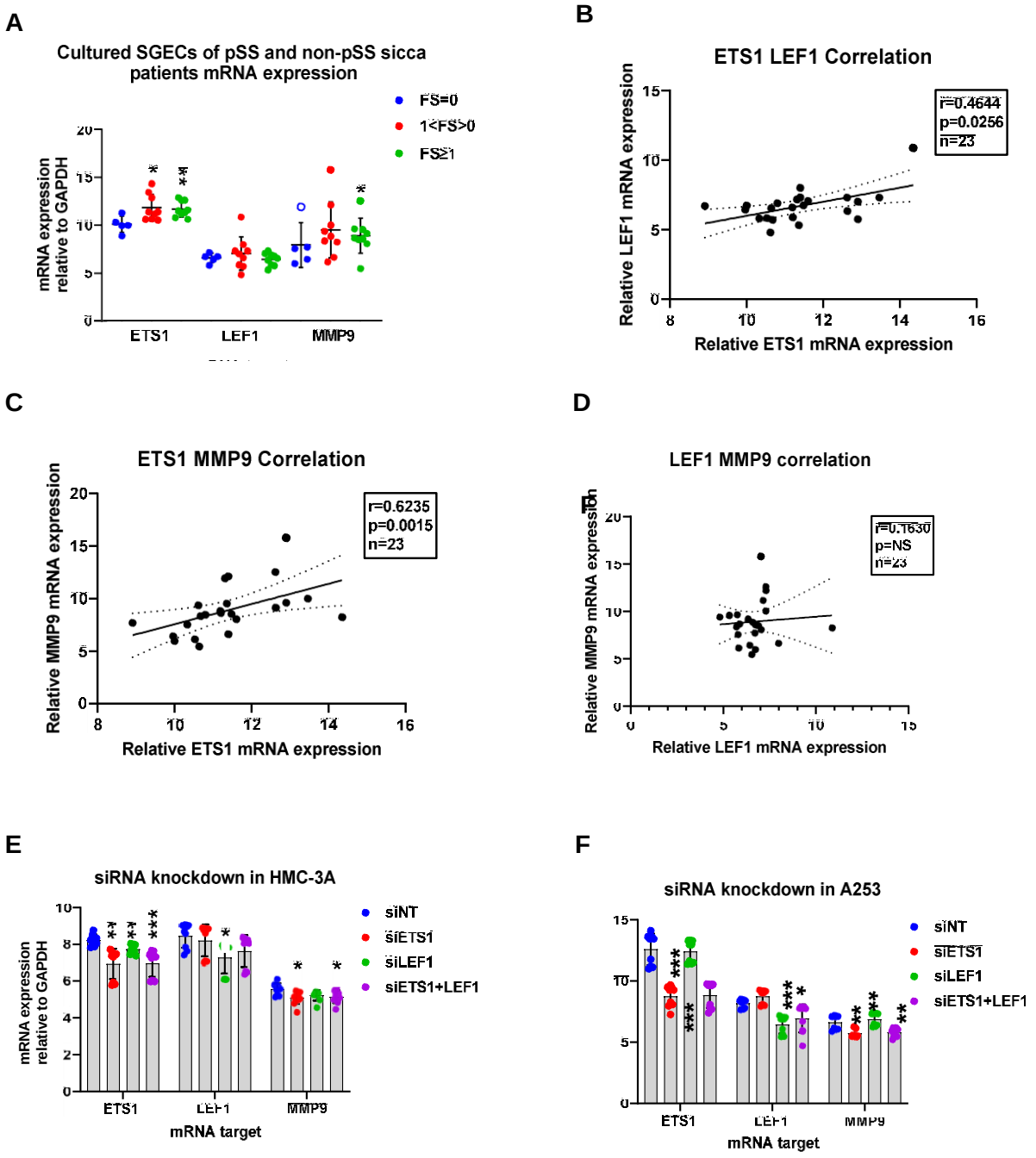

Figure 3.5.1: Effects of ETS1 and/or LEF1 siRNA mediated knockdown on MMP9 mRNA expression in salivary gland derived cell lines. Explant SGEC cultures were obtained from pSS (FS≥1) (n=9) (1<FS>0) (n=9), and non-pSS (FS=) (n=5) patients. (A) qRT-PCR expression of ETS1, LEF1, and MMP9 in primary SGECs was normalized to GAPDH and compared to FS=0 by Mann-Whitney U-test. One outlier was removed from the MMP9, FS=0 group using Grubb's analysis for statistical calculations (hollow circle). Error bars represent mean (+/-) standard deviation (SD). SGECs of pSS (FS≥1) overexpress both ETS1 (p=0.007) and MMP9 (p=0.0336) compared to non-pSS (FS=0) patients. Like pSS (FS≥1), non-pSS (1<FS>0) SGECs overexpressed ETS1 (p=0.0120) compared to the FS=0 group. (B-D) Spearman's rank correlation coefficient (rho) was used to assess correlations among ETS1, LEF1, and MMP9 mRNA expression in primary SGECs (n=23). (B-C) ETS1 expression correlated with both MMP9 (r=0.5120, p=0.0125, n=23) and LEF1 expression (r=0.5350; p=0.0085; n=23) (D). mRNA expression of ETS1, LEF1 and MMP9 was determined in the salivary gland derived cell lines HMC-3A (E), A253 (F), iSGEC-pSS1 (G), and iSGEC-nSS2 (H), 48hrs post-transfection with siRNA targeting ETS1 and/or LEF1, by qRT- PCR. Knockdown of ETS1 (siETS1), LEF1 (siLEF1), and ETS1+LEF1 (siETS1+LEF1) were compared to a non-targeting (siNT) control. qRT-PCR mRNA expression was normalized to the housekeeping gene GAPDH. Knockdown of ETS1 consistently led to a reduction of MMP9 mRNA expression. Data are presented as the mean+/- standard deviation (SD) (n=6): *p<0.05, **p<0.01, ***p<0.001.

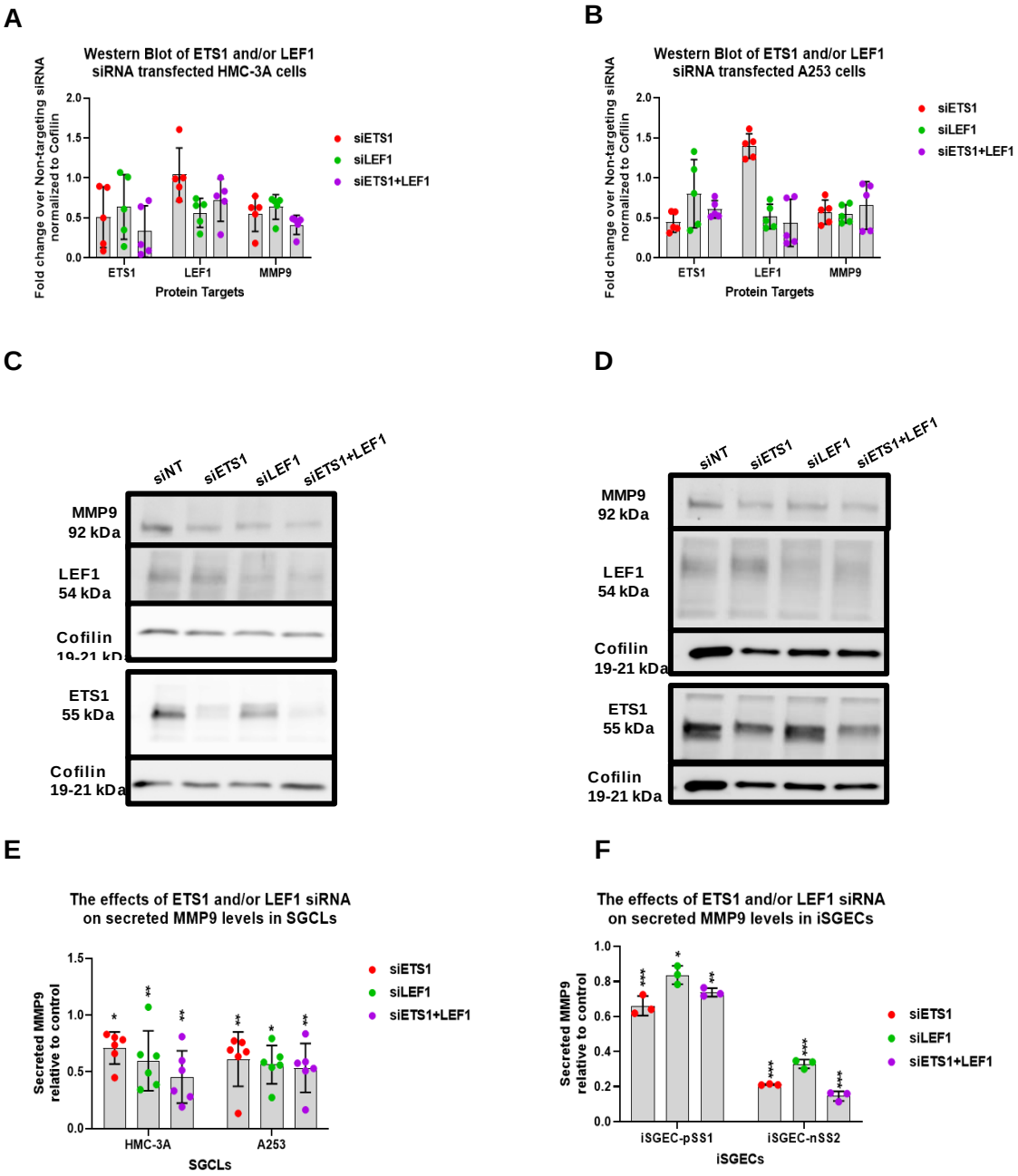

Figure 3.5.2: Effects of ETS1 and/or LEF1 siRNA-mediated knockdown on MMP9 protein expression in salivary gland derived cell lines. Semi-quantitative (densitometric) Western blot analysis (A/B) and representative Western blots (C/D) of siRNA knockdown experiments are shown. ETS1, LEF1, and MMP9 protein levels were determined 72hrs post-transfection with siRNA targeting ETS1 (siETS1), LEF1 (siLEF1), or ETS1+LEF1 (siETS1+siLEF1), relative to non-targeting siRNA (siNT) (control) in HMC-3A (A/C) and A253 (B/D) whole cell lysates. MMP9 protein levels were reduced in both A253 and HMC-3A cells when transfected with siETS1, siLEF1, or siETS1+LEF1. Equal protein amounts were loaded into each lane and respective target normalized to cofilin protein expression. Western blot sections corresponding to either (ETS1 and Cofilin) or (MMP9+LEF1 and Cofilin) were acquired from the same gel/ blot, per cell line, and processed identically from the same replicate sample, if possible. Loading controls and target proteins of the same gel/blot are imaged separately for optimized exposure requirements among the loading control vs. target protein(s). The effects of ETS1 (siETS1), LEF1 (siLEF1), and both ETS1+LEF1 (siETS1+siLEF1) siRNA knockdown on MMP9 protein secretion into culture media were also determined (E/F). Total MMP9 (active and inactive) was measured by ELISA and presented as fold-decrease of the non-targeting siRNA (siNT) control. In SGCLs HMC-3A (n=6) and A253 (n=6), there were significant reductions in total MMP9 protein supernatant levels after siRNA knockdown of ETS1 and/or LEF1 (E). Total MMP9 in the cell culture supernatant of iSGEC-pSS1 (n=3) and iSGEC-nSS2 (n=3) was significantly reduced by ETS1 and/or LEF1 knockdown (F). Mann-Whitney U-test was used to determine significant differences among the control (siNT) and siETS1, siLEF1, or siETS1+siLEF1. Results are presented as mean +/- standard deviation (SD). (***p<0.001), (**p<0.01), (*p<0.05).

A

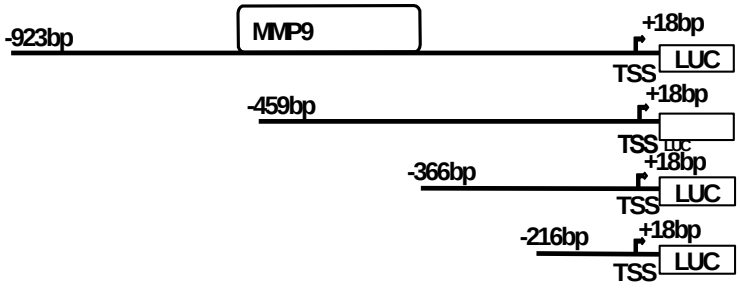
-923bp
MMP9
+18bp
LUC
TSS
-459bp
+18bp
TSS
-366bp
+18bp
LUC
TSS
-216bp
+18bp
LUC
TSS

B

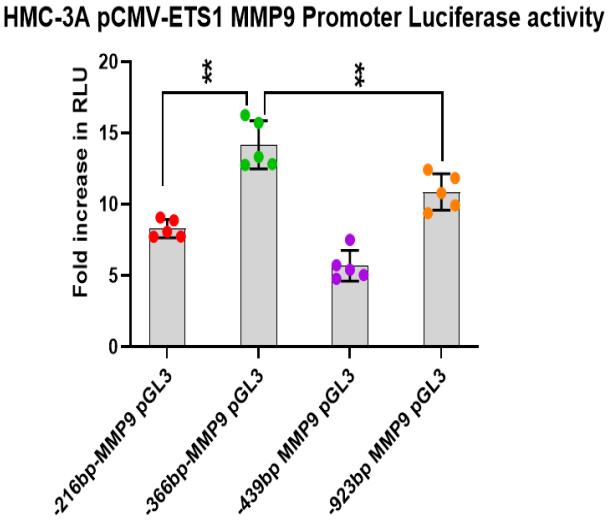
HMC-3A pCMV-ETS1 MMP9 Promoter Luciferase activity
Fold increase in RLU
20
15
10
5
0
**
**
-216bp-MMP9 pGL3
-366bp-MMP9 pGL3
-439bp MMP9 pGL3
-923bp MMP9 pGL3

C

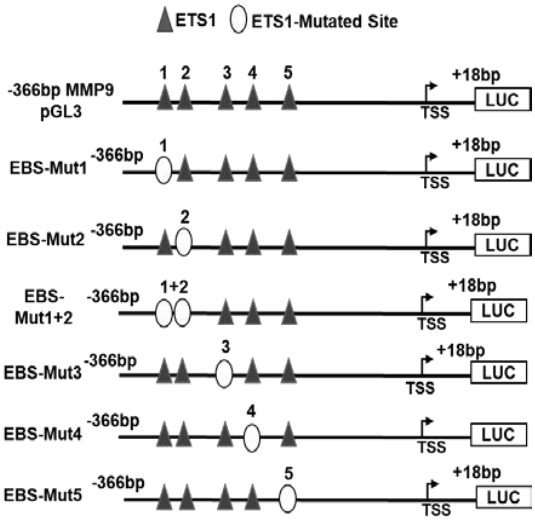
ETS1
ETS1-Mutated Site
-366bp MMP9 pGL3
1 2 3 4 5
+18bp
LUC
TSS
EBS-Mut1
-366bp
1
EBS-Mut2
2
EBS-Mut1+2
1+2
EBS-Mut3
3
EBS-Mut4
4
EBS-Mut5
5

D

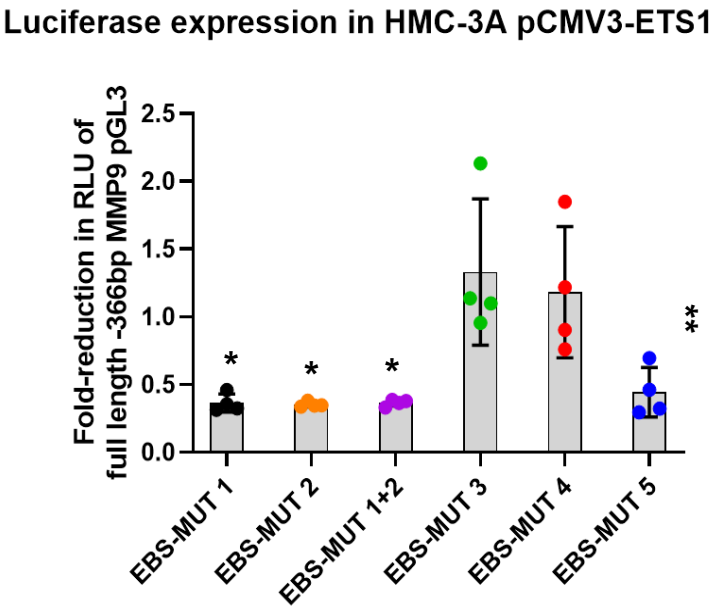
Luciferase expression in HMC-3A pCMV3-ETS1 clone (E6)
Fold-reduction in RLU of full length -366bp MMP9 pGL3
2.5
2.0
1.5
1.0
0.5
0.0
*
*
*
**
EBS-MUT 1
EBS-MUT 2
EBS-MUT 1+2
EBS-MUT 3
EBS-MUT 4
EBS-MUT 5

E

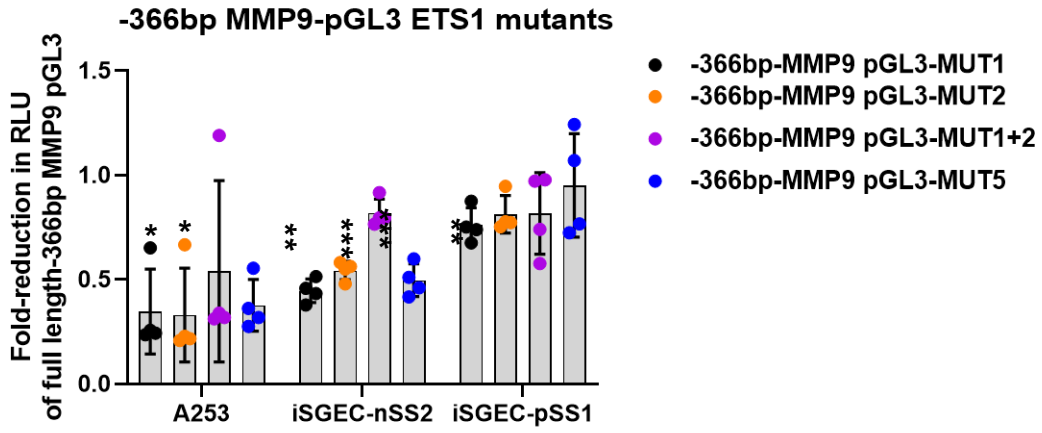
-366bp MMP9-pGL3 ETS1 mutants
Fold-reduction in RLU of full length-366bp MMP9 pGL3
1.5
1.0
0.5
0.0
A253
iSGEC-nSS2
iSGEC-pSS1
-366bp-MMP9 pGL3-MUT1
-366bp-MMP9 pGL3-MUT2
-366bp-MMP9 pGL3-MUT1+2
-366bp-MMP9 pGL3-MUT5

F

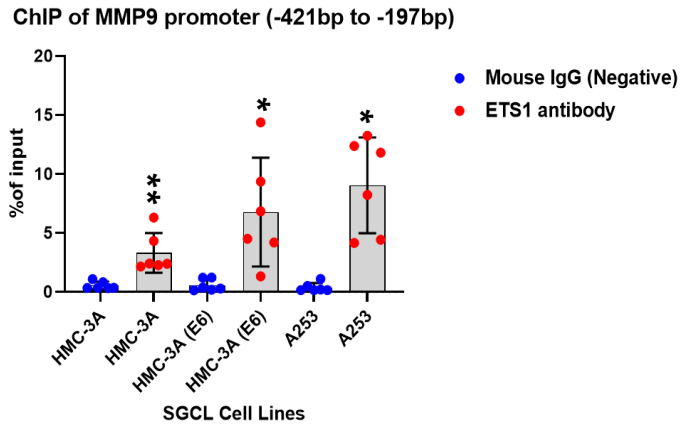

G

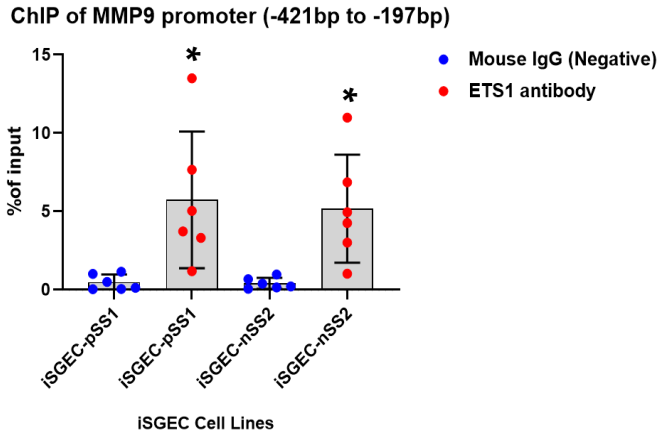

Figure 3.5.3: ETS1 binding and regulation of MMP9 promoter transcription in HMC-3A, A253, and iSGECs. (A) HMC-3A (E6) and control HMC-3A (EM) were transiently transfected with either 250ng of pGL3-basic MMP9 promoter full length (-923bp to +18bp) or 5'-deletion MMP9 promoter constructs and 30ng of control plasmid expressing renilla luciferase under the control of thymidine kinase promoter (pRL-TK). (B) Results were expressed as fold increase in RLU over the control normalized to pGL3-basic MMP9 expression. 5'-deletion constructs demonstrated significant increases in luciferase activity within the -366 to -216 promoter region of the MMP9 promoter. (C/D) EBS-MUT1/2/5 sites displayed significant reductions in luciferase activity compared to the full length -366bp-MMP9-pGL3 promoter plasmid. (E) Activity of the -366bp-MMP9-pGL3 ETS1 binding site mutants (EBS-MUT 1, 2, 1+2, and 5) were further investigated by transient transfection into A253 (n=6), iSGEC-nSS2 (n=6), and iSGEC-pSS1 (n=4). (F/G) ChIP-qPCR assay performed with SGCLs and iSGECs was utilized to assess the functional relevance of ETS1 interaction with the MMP9 promoter spanning across EBS-MUT1,2, and 5. Cell lysates immunoprecipitated with normal mouse IgG (negative control) (blue) or ETS1 (red) antibodies. Samples were normalized to 5% of sample input. Significant comparisons among control and ETS1 antibody were made by Mann-Whitney U-test with p-values indicated over their respective bars (***p<0.001), (**p<0.01), (*p<0.05). Error bars represent mean +/- standard deviation (SD).

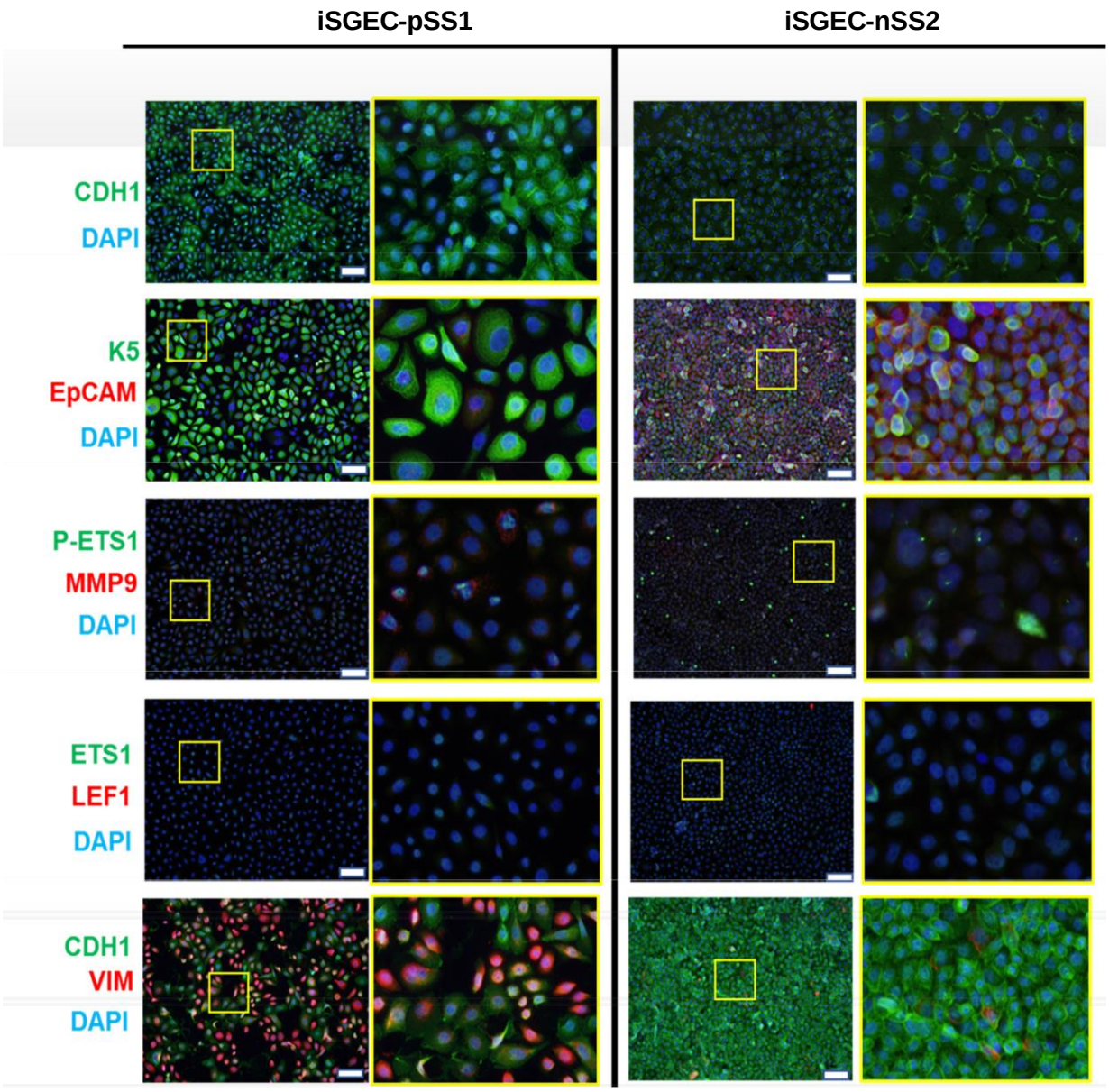

Figure 3.5.4: Characterization of epithelial and progenitor cell markers in iSGECs by immunofluorescence. iSGEC-pSS1 (left) and iSGEC-nSS2 (right) were cultured on gelatin coated 8-well tissue culture slides for 48-72 hrs. Epithelial marker (CDH1) was expressed ubiquitously throughout iSGEC-nSS2 cell junctions, whereas iSGEC-pSS1 displayed a mixed population of CDH1 expressing cell clusters. Progenitor cell markers (K5 and EpCAM) were expressed in both iSGECs, however, the localization of EpCAM in iSGEC-pSS1 was primarily found within the nucleus compared to membranous expression in iSGEC-nSS2. Phosphorylated ETS1 (Thr38) (P-ETS1) displayed greater overall nuclear localization and intensity in iSGEC-nSS2 and was co-expressed with increased MMP9 levels in iSGEC-pSS1. ETS1 and LEF1 demonstrated relatively low expression levels in iSGECs when assessed by IF. Both iSGEC cell lines contained co-expressing CDH1 and mesenchymal marker vimentin (VIM) expressing cells, although VIM was expressed at a much greater extent in iSGEC-pSS1. iSGEC-nSS2 cells expressed Phos(T38)-ETS1 uniformly as small nuclear bodies interspersed with high- expressing whole-cell localized Phos(T38)-ETS1, regardless of MMP9 levels. The overall intensity and localization of ETS1 and LEF1 was unremarkable in either cell line or highlighted obvious differences in some cells. Representative regions (yellow) are highlighted and displayed adjacent their respective image. Images were captured at 20x magnification and white scale bars represent 100µm.

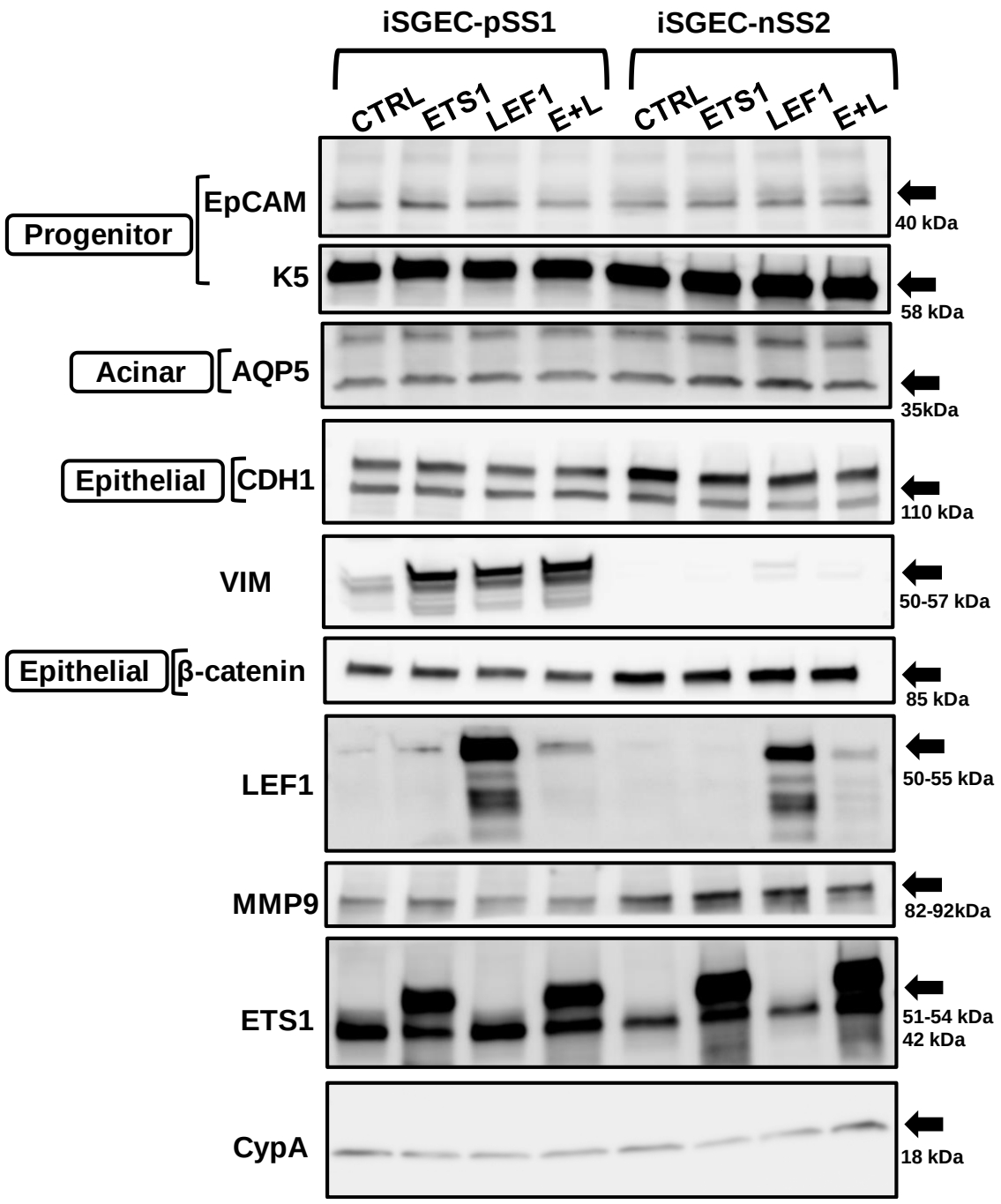

Figure 3.5.5: Effects of ETS1 and/or LEF1 protein expression of epithelial and mesenchymal cell markers in iSGECs. iSGECs were transiently transfected with 500ng of pCMV3 overexpressing plasmids and after 72hrs whole cell protein lysates were collected for Western blot analysis. Changes in the expression of progenitor cell markers EpCAM and K5, EMT epithelial markers CDH1 and β- catenin and mesenchymal VIM, and acinar AQP5 after overexpression of ETS1 and/or LEF1 were determined. Each lane was loaded with equal amounts of protein and Cyclophilin A (CyPA) used to compare loading among the experimental (pCMV3-ETS1/LEF1/E+L) and pCMV3-empty (CTRL). Expected protein sizes are listed under their respective arrow indicating the correct band. Protein targets are grouped according to their corresponding loading control (CyPA) ran on the same gel/blot. iSGECs exhibited differing levels of endogenous epithelial and mesenchymal markers with iSGEC-pSS1 displaying a greater mesenchymal-like profile. VIM expression was increased by both ETS1 and LEF1 overexpression in iSGEC-pSS1, whereas the presence of LEF1 was required for increasing VIM in iSGEC-nSS2. In contrast, the overexpression of either ETS1 or LEF1 reduced epithelial marker CDH1 expression in iSGEC- nSS2. AQP5 is aquaporin 5; CDH1 is cadherin 1; EpCAM is epithelial cell adhesion molecule; K5 is keratin 5; VIM is vimentin.

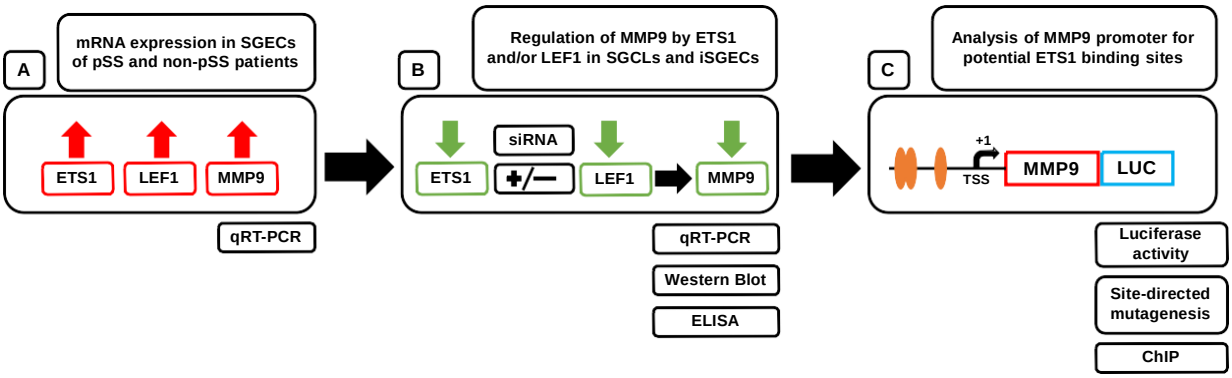

Figure 3.5.6: Experimental workflow for determination of regulation of MMP9 expression by transcription factors ETS1 and/or LEF1. Experimental strategy and assays used to determine ETS1 and/or LEF1 regulation of the MMP9 promoter in the pSS salivary gland epithelial cells. We have previously shown that transcription factors ETS1 and LEF1 are overexpressed in the epithelium of pSS labial salivary gland biopsies and that their expression correlates with MMP9 protein expression. Previous studies have demonstrated regulatory roles for both ETS1 and LEF1 in controlling MMP9 expression in T-Cells, however, their relationship to MMP9 expression has yet to be investigated in pSS epithelium. (A) We first investigated whether the overexpression of ETS1, LEF1, and MMP9 persisted in-vitro using SGEC explant cultures from LSG biopsies of pSS and non-pSS patients by qRT-PCR. (B) Due to the transient nature of primary SGEC cultures, two SGCLs HMC-3A, A253 of female and male origin, respectively, and two iSGEC lines of female origin were utilized as models to investigate the regulatory relationship among ETS1 and/or LEF1 with MMP9 at both mRNA and protein levels by siRNA knockdown. (C) To investigate regulation of MMP9 further, we generated an ETS1 overexpressing SGCL clone of HMC-3A to initially assess the direct transcriptional activity and binding of ETS1 on the MMP9 promoter.
The MMP9 promoter region (-914bp to +18bp) was inserted into a luciferase reporter plasmid to identify the significant DNA regulatory regions. These regions were narrowed down to individual ETS1 binding sites by a site directed mutagenesis approach. Lastly, the in-vitro binding of ETS1 onto the MMP9 promoter was confirmed by ChIP-qPCR on both iSGECs and SGCLs models.

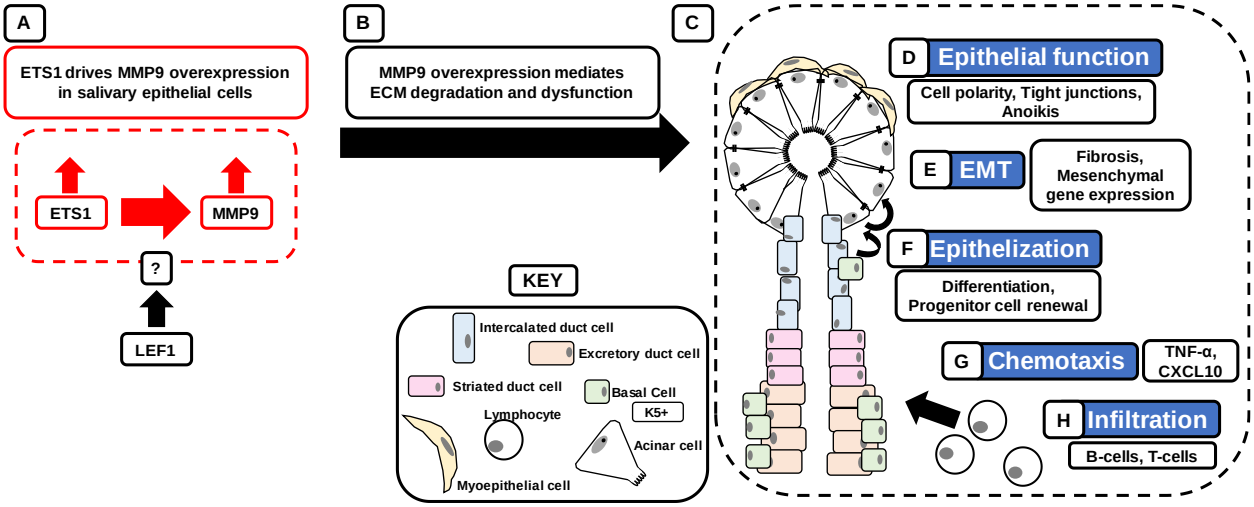

Figure 3.5.7: Proposed model for ETS1 mediated regulation of MMP9 expression and downstream effects of ECM degradation observed in pSS salivary glands. (A) Our in vitro experimental results presented in this study and previous work on salivary gland biopsies provide evidence that ETS1 regulates MMP9 overexpression in the salivary gland epithelium of non-pSS and pSS patients. LEF1 is overexpressed by the salivary gland epithelium in-vivo, however, due to the higher-structural DNA-bending properties of LEF1 as an accessory enhancer factor, its role in driving MMP9 expression could not be elicited using our model systems. (B) The overexpression of MMP9 within the salivary epithelium is a known pathological marker in pSS salivary gland dysfunction and is mainly driven by ETS1. (C) MMP9 targets a variety of ECM components with significant roles in maintaining glandular epithelial homeostasis and function. (D) MMP9 degrades tight junctions (cell-cell) and hemi-desmosomes (ECM-cell) within salivary glands, which disrupts epithelial cell polarity and directional secretion by acinar cells. Loss of ECM-cell connections leads to apoptosis of acinar cells through anoikis. (E) Disruption of ECM-cell connections within the epithelium promotes EMT and fibrosis. (F) Furthermore, re-epithelization and differentiation of resident progenitor cells rely on ECM components to direct movement and activity. Additionally, acinar cells rely on collagen for differentiation. The overabundance of K5+ progenitor cells, which normally can differentiate into both acinar and ductal cells during injury and stress, reflects the lack of a proper re-epithelization process occurring in pSS salivary glands, which is driven by MMP9 overexpression, thereby preventing ECM maturation. (G) MMP9 enhances chemotaxis and (H) infiltration of lymphocytes into the glandular tissue by degrading the ECM to facilitate lymphocyte migration. Meanwhile, cleavage-activation of variety of secreted and ECM-bound chemokines (CXCL10, TNFα) leads to increased inflammation.

3.6. Tables

Table 3.6.1. Demographics and clinical features of xerostomic patients from whom primary SGEC cultures were derived**.** Salivary gland epithelial cell cultures (SGECs) were derived from a total of N=23 patients receiving labial salivary gland biopsies as part of the routine diagnostic approach following the 2017 ACR-EULAR criteria. Patients were subdivided into three separate groups by focus score (FS) for comparisons (FS=0, 0<FS<1, and FS≥1). All SGEC cultures in this study were derived from female patients and treated identically following the same procedure. The presence of Anti-Ro (SSA) serum was not determined/ tested for in three FS≥1 patients. Of the remaining six FS≥1 patients, only two were positive (+) for the presence of serum Anti-Ro (SSA). Status was unavailable, due to lack of test or non-consent: *three patients; [$]one patient; [#]three patients; [&]one patient

Demographics	FS=0	0<FS<1	FS≥1
Subjects (N=23)	n=5	n=9	n=9
Age	31-69, AVG=44.4, SD+/- 14.3	38-78, AVG=59.1, SD+/- 11.7	36-70, AVG=54.6, SD+/- 9.9
Gender	5/5 Female	9/9 Female	9/9 Female
Clinical Features	**FS=0**	**0<FS<1**	**FS≥1**
Focus Score	0	0.16-0.9	1.0-3.52
Anti-Ro (SSA) positive	0/5	0/9	2/9*
Unstimulated Salivary Flow (Average <1.5mL/15min)	2.385[$]	1.34	1.67
Stimulated Salivary Flow (Average mL/min)	15.4225	14.32	15.85
Schirmer's positive	2/5	3/9[#]	2/9[&]

Table 3.6.2: Primers. Primers used for analyzing the expression of ETS1, LEF1, and MMP9 by qRT-PCR in SGECs, SGCLs, and iSGECs. The primers for the MMP9 promoter putative ETS1 binding sites are listed. Significant primers for ETS1 binding site mutagenesis to generate EBS-MUT constructs within the -366bp MMP9 promoter luciferase are listed. Nucleotide sequences altered within the 5'-GGAA/T-3' EBS binding motif of the constructs are shown in bold. Sanger sequencing and restriction digestion were performed to confirm mutagenesis.

Target	Primer Sequence
ETS1-F	5'-CTGCGCCCTGGGTAAAGA-3'
ETS1-R	5'-ACATCCTCTTTCTGCAGGATCT-3'
LEF1-F	5'-ACTCCAAACAAGGCATGTCCA-3'
LEF1-R	5'-GTGAGGATGGGTAGGGTTGC-3'
MMP9-F	5'-CCTGGGCAGATTCCAAACCT-3'
MMP9-R	5'-GCAAGTCTTCCGAGTAGTTTTGGAT-3'
GAPDH-F	5'-AGGGCTGCTTTTAACTCTGGT-3'
GAPDH-R	5'-CCCCACTTGATTTTGGAGGGA-3'
MMP9 CHIP-F	5'-AGGGGGATCATTAGTTTCAGAAA -3'
MMP9 CHIP-R	5'-ACTGCCAAGTCAGGCAAG-3'
-366bp-EBS-MUT1-F	5'-ACCAAG**TT**ATGGGGGATCCCTCCAGCTTC-3'
-366bp-EBS-MUT1-R	5'-CCCCCATAACTTGGTCTGAAAGCCTCCAGTGG-3'
-366bp-EBS-MUT2-F	5'- ATGGG**T**GAT**AA**CTCCAGCTTCATCCCCCTC-3'
-366bp-EBS-MUT2-R	5'- GGAGTTATCACCCATCCCTTGGTCTGAAAGC-3'
-366bp-EBS-MUT5-F	5'- TGCGGT**CGGG**TGCGGGTCTGGGGTCTTGC -3'
-366bp-EBS-MUT5-R	5'- CCGCACCCGACCGCAGGCCCTCAGGGG -3'

Table 3.6.3. Primary and Secondary Antibodies. Primary and secondary antibodies with their associated dilutions used for either Western blotting or immunofluorescence assays. Primary antibodies were diluted in TBS with 2% BSA, 0.1% Tween-20, and 0.05% sodium azide. Secondary antibodies were diluted in DPBS with 0.1% Tween-20.

Target	Assay	Species	Source	Cat#	Dilution
ETS1	WB	Mouse	SCBT	sc-55581	1:250
LEF1	WB, IF	Mouse	SCBT	sc-374412	1:250,1:100
MMP9	WB, IF	Mouse	SCBT	sc-393859	1:200, 1:100
ETS1	IF	Rabbit	Cell Signaling	14069S	1:200
Phospho-ETS1 (Thr38)	IF	Rabbit	Invitrogen	PA5-37572	1:200
EpCAM	WB, IF	Mouse	eBioscience	14-9326-82	1:400,1:300
K5	WB, IF	Rabbit	Biolegend	905504	1:500,1:300
AQP5	WB, IF	Mouse	SCBT	sc-514022	1:100
E-Cadherin	WB, IF	Rabbit	Proteintech	20874-1-AP	1:400, 1:300
B-Catenin	WB	Mouse	SCBT	sc-7963	1:300
Vimentin	WB, IF	Mouse	SCBT	sc-6260	1:500, 1:300
Cofilin	WB	Mouse	SCBT	sc-376476	1:1000
CyPA	WB	Mouse	SCBT	sc-134310	1:1000
Anti-mouse IgG-HRP	WB	Mouse	Cell Signaling	7076	1:2000
Anti-rabbit IgG-HRP	WB	Rabbit	Cell Signaling	7074	1:2000
Goat anti-rabbit IgG-Alexa-488	IF	Rabbit	Invitrogen	A32731	1:400
Goat anti-mouse IgG-Alexa-594	IF	Mouse	Invitrogen	A32742	1:400

CHAPTER 4: TELOMERE EROSION IN SJÖGREN'S SYNDROME: A MULTI-TISSUE COMPARATIVE ANALYSIS

Abstract

Background: Acinar progenitor cells within salivary glands have decreased regenerative capacity and exhibit shorter telomeres in primary Sjögren's syndrome (pSS) patients. We investigated whether DNA of saliva, PBMCs, and labial salivary gland (LSG) biopsy tissue have shorter telomeres in pSS compared to controls. mRNA expression of genes associated with pSS pathogenesis (ETS1, LEF1, MMP9), telomere DNA damage response (ATM), senescence (CDKN2A), telomerase inhibition (IFN-y, TGFβ1), and the shelterin complex (TPP1, POT1), were assessed in LSG tissue by qRT-PCR to examine potential defects in telomere maintenance.

Methods: Relative telomere length in DNA of saliva, PBMCs, and LSGs from non-pSS sicca and pSS patients was measured using qPCR. Saliva DNA telomere length was further compared to healthy controls. Expression of genes affecting telomere maintenance was analyzed in LSGs using qRT-PCR.

Results: pSS patients have shorter telomeres in saliva DNA (n=21) than healthy controls (n=27) ($p=0.0035$). ATM mRNA expression was higher in pSS LSG tissue (n=16) vs. non-pSS sicca patients (n=13) ($p=0.0283$) and strongly correlated with LEF1, TPP1, and POT1 ($p<0.01$, $r>0.6$).

Conclusions: Patients with pSS exhibited significant telomere erosion in saliva DNA. Overexpression of ATM in LSGs could represent a compensatory response to telomere shortening. The role of LEF1 in telomere erosion remains to be elucidated.

Key Words: Sjögren's syndrome, Autoimmune Disease, Telomere, Gene Expression

4.1 Rationale

Primary Sjögren's syndrome (pSS) is a chronic autoimmune disease primarily affecting salivary and lacrimal glands, resulting in dry eyes and mouth. The majority of pSS patients are female, diagnosed at the average age of 56 (Stefanski, Tomiak et al. 2017). pSS treatment involves the administration of immunosuppressants and agents inducing tear and saliva production (Stefanski, Tomiak et al. 2017). Patients with pSS exhibit systemic manifestations (e.g., arthralgia, interstitial lung disease, vasculitis) and have a greater risk of developing non-Hodgkin lymphoma (Stefanski, Tomiak et al. 2017).

Little is known about telomere dysfunction in pSS. Using lacrimal gland tissues, Kawashima et al., measured telomere length in pSS patients and dry mouth and/or eye controls (i.e., sicca) using quantitative fluorescent in situ hybridization (q-FISH) (Kawashima, Kawakita et al. 2011). pSS patients were found to have reduced telomere length within lacrimal gland epithelial cells, including areas without immune infiltrates. Similarly, Pringle et al., (Pringle, Wang et al. 2019) revealed telomere length in parotid gland stem cells of pSS patients were shorter than controls.

pSS patients overexpress various inflammatory cytokines within SGs potentially affecting telomere maintenance (Fox, Kang et al. 1994, Mason, Hamburger et al. 2003). For example, Tumor growth Factor Beta-1 (TGFβ1) and Interferon-Gamma (IFN-γ) can interfere with Telomerase Reverse Transcriptase (TERT) expression directly or indirectly.(Cong, Wright et al. 2002, Wang, Fu et al. 2017) The mechanism(s) affecting telomere maintenance and the ability of the shelterin complex to regulate telomere length in pSS needs to be elucidated (Denchi 2009, Diotti and Loayza 2011).

The Ataxia-Telangiectasia Mutated (ATM) gene is involved in DNA repair and regulates telomere length through interactions with the shelterin complex subunit Protection of Telomeres

1 protein (POT1) (Diotti and Loayza 2011, Lee, Bohrson et al. 2015). ATM is critical for preventing telomere shortening in certain biological systems and participates in directing cellular senescence, an important aspect of pSS pathogenesis (Herbig, Jobling et al. 2004, Lee, Bohrson et al. 2015, Pringle, Wang et al. 2019).

Lacrimal gland acinar cells with dysfunctional mitochondria have been observed in pSS, possibly corresponding to an early senescence phenotype (Kawashima, Kawakita et al. 2011). Mitochondrial dysfunction is characteristic of senescence and associated with shorter telomeres and increased reactive oxygen species (ROS) production (Passos, Saretzki et al. 2007). Elevated intracellular ROS could lead to increased apoptosis, as seen in pSS SG acinar cells (Ryo, Yamada et al. 2006, Kawashima, Kawakita et al. 2011, Rayess, Wang et al. 2012, Wakamatsu, Dogru et al. 2013). Telomere erosion in pSS acinar cells may involve ROS-related DNA damage and represent a key factor in senescence induction, thereby impairing SG renewal. Furthermore, oxidative stress influences expression of pSS pathogenic markers such as Matrix Metalloproteinase 9 (MMP9), which is overexpressed in SG acinar cells (Yu, Kamada et al. 2008, Tandon, Perez et al. 2017). MMP9 degrades tight junction proteins and type IV collagen, leading to extracellular matrix destabilization (Yu, Kamada et al. 2008).

We have previously determined pSS patients' SG cells overexpress transcription factors v-Ets Avian Erythroblastosis Virus E26 Oncogene Homolog 1 (ETS1) and Lymphoid Enhancer Binding Factor 1 (LEF1) (Shah, Noll et al. 2017, Shah, Noll et al. 2019). Protein and mRNA levels of ETS1 and LEF1 correlated with MMP9 expression (Shah, Noll et al. 2017, Shah, Noll et al. 2019). ETS1 and LEF1 likely upregulate MMP9 expression directly through the MMP9 promoter (Shah, Noll et al. 2019). Upregulation of ETS1 and LEF1 may be associated with oxidative stress and cell adhesion deficiencies beyond regulating MMP9 overexpression (Novak, Hsu et al. 1998, Barrera, Bahamondes et al. 2013, Wu, Zhang et al. 2013, O'Hara,

Splinter et al. 2017). Moreover, ETS1 may reduce glandular regeneration by direct transcriptional upregulation of Cyclin-dependent Kinase Inhibitor 2A (CDKN2A), contributing to cellular senescence (O'Hara, Splinter et al. 2017).

We compared relative telomere length (RTL) of DNA isolated from saliva, labial salivary gland (LSG) biopsies, and peripheral blood mononuclear cells (PBMCs) between pSS, non-pSS sicca, and/or healthy control (HC) subjects using a qPCR-based assay (Cawthon 2002). We also determined differences and correlations of mRNA expression levels between pSS and sicca patients for the telomere maintenance associated genes ATM, Tripeptidyl Peptidase 1 (TPP1) and POT1, the TERT direct/indirect effector cytokines TGFβ1 and IFN-γ, and the ETS1-regulated gene, CDKN2A.

4.2. Materials and Methods

Study population

This study was approved by Atrium Health institutional review board (Charlotte, NC, USA). All subjects gave informed consent. Using the 2016 ACR/EULAR-approved guidelines for classifying pSS, only patients negative for serum anti-SSA and positive for one or more objective test (Schirmer's dry eye test (strip absorption <5mm/5min) and unstimulated whole saliva flow test of ≤1.5ml/15min), were subjected to LSG biopsy, except for two previously recruited anti-SSA positive pSS patients (Shiboski, Shiboski et al. 2017). Stimulated salivary flow was also determined. Patient LSG biopsies were evaluated for immune infiltrates and focus score (FS) determination at University of North Carolina at Chapel Hill School of Dentistry, Pathology Department (Chapel Hill, NC, USA). A FS=1 is equivalent to one aggregate of ≥50 infiltrated lymphocytes per4mm2 section of LSG biopsy (Shiboski, Shiboski et al. 2017). Patients were considered pSS positive if FS ≥1 (Shiboski, Shiboski et al. 2017). Demographics

and/ or clinical characteristics of HCs, non-pSS sicca, and pSS patients are presented in Table 4.6.1.

Sample acquisition

During pSS diagnosis, excess LSG biopsy tissue was collected in RNAlater (Invitrogen, Carlsbad, CA, USA). At a two-week post-biopsy visit, saliva was collected in 50mL conical centrifuge tubes (Corning, Corning, NY, USA) and placed on ice. Blood was drawn after saliva collection into two 4.5mL sodium citrate (0.105M, 3.2%) buffered Vacutainer™ blood collection tubes (Becton Dickinson, Franklin, NJ, USA).

Saliva samples were collected from HCs without autoimmune disease or known oral complication (e.g., oral cancer and oral lichen planus). Samples were banked as either whole saliva or isolated DNA and stored at -80°C. Saliva samples requiring DNA isolation post-storage were processed at the same time to avoid batch effects.

DNA isolation of saliva, labial salivary gland and PBMCs

DNA was isolated from LSG tissues stored in RNAlater (Invitrogen, Carlsbad, CA, USA) using the Qiagen DNAeasy kit (Qiagen, Valencia, CA, USA) according to manufacturer's protocol. Whole blood PBMCs were isolated using LymphoprepTM-based density gradient centrifugation (Axis-Shield, Oslo, Norway) procedures. DNA was isolated using Qiagen DNAeasy kit (Qiagen, Valencia, CA, USA). Saliva DNA was isolated using DNA Genotek OG-500 kits (Oragene, Ontario, Canada). DNA quantity and quality were assessed using Nanodrop 1000 (Thermo Fisher Scientific, Waltham, MA, USA) and DNA concentration was standardized to 5ng/µL in nuclease-free water (Molecular Biologicals International, Irvine, CA, USA) for downstream RTL qPCR assay.

LSG biopsies RNA isolation and qRT-PCR

LSG biopsy RNA isolation was performed using the RNAeasy kit (Qiagen, Valencia, CA, USA). RNA concentration and purity were assessed using a Nanodrop 1000 (Thermo Fisher Scientific, Waltham, MA, USA). cDNA synthesis was carried out with random hexamers (Promega, Madison, WI, USA) and 500ng of total RNA as the starting material using the SmartScribe reverse transcription kit (Takara Bio, Mountain View, CA, USA). Primers were designed by using online tool NCBI Primer-BLAST and targeting a candidate gene's exon-exon junction. Relative mRNA gene expression values were determined by the ΔCT method. To calculate relative mRNA gene expression values, glyceraldehyde 3-phosphate dehydrogenase (GAPDH) internal control was used.

qPCR relative telomere length measurement

The RTL (i.e., average RTL of the LSG cell population analyzed) was calculated per Cawthon et al. and performed on a BioRad C1000 Touch Thermal Cycler (Biorad, Hercules, CA, USA). RTL assays were carried out in triplicate plates (Biorad, Hercules, CA, USA) for each sample and two sets of primers, "T" and "S". "T" primers, consisting of Tel1 and Tel2, bind to telomeric DNA on opposite strands and amplify the telomere TTAGGG and CCCTAA hexamer repeats (Cawthon 2002). "S" primers, consisting of 36B4U and 36B4D, bind to the Ribosomal Protein Lateral Stalk Subunit P0 (RPLP0) single copy reference gene (Cawthon 2002). The reaction included: DNA (5 ng/well), nuclease free water (5.5 µL) Qiagen RT2 SYBR Green Fast Master Mix (7.5 µL) (Qiagen, Valencia, CA, USA), and "T" primers consisting of 270 nM Tel-1 primer and 900 nM Tel-2 primer (1 µL each) (Cawthon 2009).

On a separate plate, an identical reaction was set up using "S" primers, consisting of 300 nM 36B4U primer and 500 nM 36B4D primer (1 µL each). The qPCR assays were as follows: one cycle (95°C; 5 min), and 40 cycles (95°C; 15 sec, 54°C; 2 min) for the reactions with "T" primers

and one cycle (95°C; 5 min), and 40 cycles (95°C;15 sec, 58°C; 70 sec) for “S” primers. Data outliers with >1cycle threshold (Ct) value variance from their two other replicates were removed from the analysis. Three replicates were performed on different days to assess batch variability.

RTL Calculation

To calculate RTL, the average “T” value was divided by the average “S” value for each sample and normalized using a pooled sample of each tissue type (LSG, PBMCs, saliva). For the sample analysis categories described in Supplementary Table 1, on each 96-well plate (per one plate batch), a pooled sample consisting of either LSG samples (n=20) for the LSG analysis or a pooled PBMC samples (n=20) for the PBMC analysis were included in the RTL assays. The average T/S ratio of pooled samples (3 wells) per plate (of 3 plates) was used to normalize each sample’s T/S ratio, per respective tissue type ((Tavg-sample/Savg-sample)/(Tavg-pooled/Savg-pooled)). Saliva DNA samples (n=27) were analyzed in two separate plate batches (instead of one batch, i.e., for LSGs and PBMCs), each with three 96-well qPCR plates. For saliva sample analysis, the pooled sample consisted of 13 saliva DNA samples (instead of 27, due to sample attrition). To normalize data across multiple saliva DNA batches, a normalization multiplication factor (MF) was determined by dividing the highest average pooled T/S by the average pooled sample T/S ratio per individual batch (Stout, Lin et al. 2017).

Formulas used were as follows (Stout, Lin et al. 2017):

Relative Telomere Length calculation of LSG and PBMCs DNA:

(Tavg-sample/Savg-sample)/(Tavg-pooled/Savg-pooled)

Relative Telomere Length calculation of saliva DNA:

((Tavg-sample/Savg-sample)/(Tavg-pooled/Savg-pooled)) x MF

MF=((Tavg(highest)-pooled /Savg(highest)-pooled)/(Tavg(Batch)-pooled /Savg(Batch)-pooled))

Statistical analysis

Statistical analyses and graphical representations were generated using GraphPad Prism v7.04 software (GraphPad software Inc., La Jolla, CA). Spearman's correlation test (α=0.05) was used to determine relationships among experimental variables mRNA expression of LSG tissue and RTL in DNA of saliva, PBMCs, and LSG) and with clinical characteristics. Spearman's correlation test was used to analyze LSG tissue mRNA expression data. LSG tissue mRNA correlations were corrected using Holm-Šídák post hoc test. To assess differences in clinical variables, the two-tailed, non-parametric Mann-Whitney U-test was used (α=0.05).

4.3. Results

4.3.1 Saliva, LSG, and PBMC RTL in pSS, non-pSS sicca, and healthy subjects

Demographics and FS of pSS and non-pSS sicca patients by sample/analysis-type is shown in Table 4.6.1. There were no significant differences in mean ages between subject groups per sample type. We determined RTL in DNA of LSGs, PBMCs, and saliva of pSS patients and non-pSS sicca controls. In addition, HC saliva DNA samples (n=27) were analyzed. HC saliva DNA RTL was longer than the RTL of pSS and non-pSS sicca patients combined (p=0.0372) (Figure 4.5.1 A-B). Moreover, saliva DNA RTL was shorter for pSS patients compared to HCs and non-pSS sicca patients (Figure 4.5.1 A-B). The HC group’s average age was 56.22 years (SD +/-10.68 years) compared to 52.59 years (SD +/-12.30 years) for the non-pSS sicca and pSS groups (p=0.477, Mann-Whitney U-test). This suggests that age was not a factor in the observed telomere length difference. We did not find a difference in saliva DNA RTL of non-pSS sicca patients (FS<1, n=6) vs. HCs(n=27) (p=0.6989) (Figure 4.5.1 A-B).

In addition, although a trend of difference in RTL between pSS to non-pSS sicca patients could be observed for PBMCs (Figure 4.5.1 C-D) and LSGs (Figure 4.5.1 C-D), we did not find it statistically significant, possibly due to higher variability in non-pSS sicca patients' samples. Indeed, pSS PBMCs showed a mean RTL increase and better clustered datapoints compared to non-pSS sicca (Figure 4.5.1 C-D), while LSGs RTL (Figure 4.5.1 C-D) followed the same trend as saliva DNA, i.e., mean reduction in pSS (Figure 4.5.1 A-B), and better datapoints clustering in pSS, similar to PBMCs (Figure 4.5.1 C-D). Assuming PBMCs of pSS patients have longer telomeres than non-pSS sicca and shorter telomeres than saliva DNA from HCs, the results cannot be simply interpreted as a "dilution" of telomere length due to infiltration of lymphocytes in saliva or LSGs, because pSS saliva DNA RTL datapoints (n=21) would be located between HCs (n=15) and non-pSS sicca (n=6) (Figure 4.5.1 A-B).

4.3.2. Expression of senescence markers, DNA damage response, and shelterin genes in pSS and non-pSS sicca LSG biopsies

ATM mRNA was overexpressed in LSG tissues of pSS patients (n=16) on average, when compared to non-pSS sicca patients (n=13) (p=0.0283) (Figure 4.5.2). CDKN2A expression was not significantly different between the pSS and non-pSS sicca patient groups (data not shown). In addition, ATM mRNA expression in LSG tissue correlated closely (p=0.003, r=0.6818, Figure 3A) with the expression of previously identified pSS associated marker LEF1 and the two shelterin complex genes, TPP1 (p=0.0024, r=0.6892, Figure 3B) and POT1 (p<0.0001, r=0.8232) (Figure 4.5.3) (Shah, Noll et al. 2017, Shah, Noll et al. 2019). Furthermore, ATM mRNA expression correlated with FS (n=28, p=0.0027, r=0.5449) (Data not shown).

4.3.3. ETS1, LEF1, and MMP9 mRNA correlation with FS in pSS and non-pSS sicca patients

With a larger sample size, we confirmed our previous findings showing that anti-SSA (+ and -) pSS patients (focus score (FS) ≥1) have an overall higher mRNA expression of ETS1, LEF1 and MMP9 in salivary gland biopsies compared to non-pSS sicca patient (Shah, Noll et al. 2017, Shah, Noll et al. 2019). As shown in Figure 4.5.2, LEF1 (n=29, p=0.0076, Figure 4.5.2) and MMP9 (n=29, p=0.0358, Figure 4.5.2) were overexpressed on average in pSS (FS≥1) compared to non-pSS sicca (FS<1) patients. Although the same trend was observed for ETS1 in these two groups, significance was only obtained when comparing the FS=0 group to the FS>0 group (non-pSS sicca and pSS patients combined, p=0.0161), as previously shown (Shah, Noll et al. 2019). Last, we confirmed correlation of FS with ETS1, LEF1, and MMP9 LSG mRNA expression in pSS and non-pSS sicca patients combined (Data not shown).

4.3.4. Correlation of relative telomere length in multiple tissues and LSG mRNA expression of genes influencing telomere length

To determine whether RTL correlated with factors influencing telomere maintenance, we measured LSG mRNA expression of TPP1, POT1, TGFβ1 and IFN-γ. We did not find a correlation between the mRNA expression of these genes and RTL (data not shown).

4.4. Discussion

This study is the first to investigate telomere length of saliva DNA, PBMCs, and labial salivary gland biopsies of pSS patients, simultaneously. We sought to determine whether telomere attrition could be assessed in multiple tissues of pSS patients and whether the expression of disease markers such as MMP9, ETS1, or LEF1 would potentially account for the outcome.

4.4.1. pSS RTL in saliva DNA is shorter than non-pSS sicca and HC subjects

We assessed RTL in multiple tissues of pSS and non-pSS sicca patients, i.e., saliva, LSG tissue, and PBMCs. We found saliva DNA RTL of pSS and non-pSS sicca patients to be shorter than a similar age- and gender-matched HC cohort (Figure 4.5.1 A-B). This result is analogous to Kawashima et al., regarding the telomere length of lacrimal glands tissues from a small sample size (Kawashima, Kawakita et al. 2011). Additionally, saliva DNA RTL of pSS patients was shorter than corresponding RTL of non-pSS sicca patients (FS<1), whereas the latter patients did not show a difference compared to HCs (Figure 4.5.1 A-B). Additionally, our results may only highlight differences in pSS anti-SSA (-) patients due to our sample population containing only two pSS anti-SSA (+) patients.

Saliva DNA originates from varying proportions of leukocytes and oral epithelial cells depending on age and disease status (Theda, Hwang et al. 2018). In pSS, novel approaches would be needed to determine the origins of saliva DNA and characterize oral cavity cell types and infiltrates, i.e., epithelial cells or lymphocytes originating from damaged LSGs. Alternatively, the observed difference may be due to increased DNA damage from chronic inflammation affecting lymphocytes and/or epithelial cells in the oral cavity, therefore perpetuating telomere loss in pSS patients. Overall, our findings corroborate the observed overexpression of ATM in the LSG tissue, connecting increased DNA damage to telomere attrition in pSS patients.

4.4.2 Damage to telomere DNA and ATM overexpression in pSS LSG tissue

Chronic inflammation related DNA damage is seen in a variety of pathologies (Kawanishi, Ohnishi et al. 2017). Damage to telomere DNA results in ATM expression and as telomeres are shortened, their ability to mitigate DNA damage is depleted (Diotti and Loayza 2011, Muraki, Nyhan et al. 2012). Our study found ATM mRNA expression to correlate significantly with FS

(p=0.0027, n=28, r=0.5449, data not shown) and displayed increased expression in LSG biopsies of the pSS patient group (p=0.0283, n=29).

mRNA expression of ATM strongly correlated with TPP1 and POT1 (Figure 4.5.3), potentially indicating a compensatory mechanism to the observed telomere shortening, where ATM activity influences interactions within the shelterin complex (Diotti and Loayza 2011, Lee, Bohrson et al. 2015). Telomere shortening induced senescence is mediated primarily by ATM and may involve expression of CDKN2A (Herbig, Jobling et al. 2004). Intercalated ductal cells of pSS patients overexpress CDKN2A, however, a measurable difference in whole LSG tissue was not uncovered in our study (Pringle, Wang et al. 2019). The fraction of senescent cells in tissue could be too insignificant for our approach. DNA damage leading to ATM overexpression may drive pSS SG tissue senescence.

Figure 4.5.4 proposes a model illustrating mechanisms of telomere attrition in pSS LSGs, possibly explaining our results, which do not contradict the results by Kawashima et al., 2011 and Pringle et al., 2019 (Kawashima, Kawakita et al. 2011, Pringle, Wang et al. 2019). Combining previous studies outlining telomere shortening in acinar cells of pSS patients and mechanisms proposed those studies, we outlined significant mechanisms potentially attributing to improper telomere maintenance outlined in Figure 4.5.4 (Kawashima, Kawakita et al. 2011, Pringle, Wang et al. 2019). Above all, multiple reports of increased ROS (and 8-OHdG) in pSS have been highlighted and may be the driver of ATM overexpression and telomere loss (Ryo, Yamada et al. 2006, Kawashima, Kawakita et al. 2011, Rayess, Wang et al. 2012, Wakamatsu, Dogru et al. 2013).

4.4.3. Overexpression of ETS1, LEF1, and MMP9 in the LSG tissue

In this study, we confirmed our previous results of the pSS pathogenic markers ETS1, LEF1, and MMP9. Moreover, ATM LSG mRNA expression strongly correlated with LEF1 (Figure 4.5.3). The mechanism(s) governing the correlation of LEF1, and ATM mRNA expression remain unexplained. Whether this correlation results from intracellular signals and/or interactions between infiltrating lymphocytes and SG acinar cells remains unanswered. One possibility is the impact of oxidative stress on LEF1 expression by reducing acinar cell adhesion. Indeed, oxidative stress has been previously suggested to play a role in pSS pathogenesis and could contribute to telomere attrition (Ryo, Yamada et al. 2006, Wakamatsu, Dogru et al. 2013).

4.4.4. Genes impacting telomere maintenance

We did not find a difference in expression of CDKN2A, TGFβ1, and IFN-γ in the pSS population compared to non-pSS sicca within analyzed tissues. The lack of significance could be due to LSG cellular heterogeneity. Indeed, the cytokines TGFβ1 and IFN-γ have been shown to be overexpressed in pSS ductal and acinar cells, respectively (Fox, Kang et al. 1994, Mason, Hamburger et al. 2003). Last, our pSS population did not encompass a significant proportion of anti-SSA (+) individuals and might represent a different pathogenic process where the influence of inflammatory cytokines is diminished.

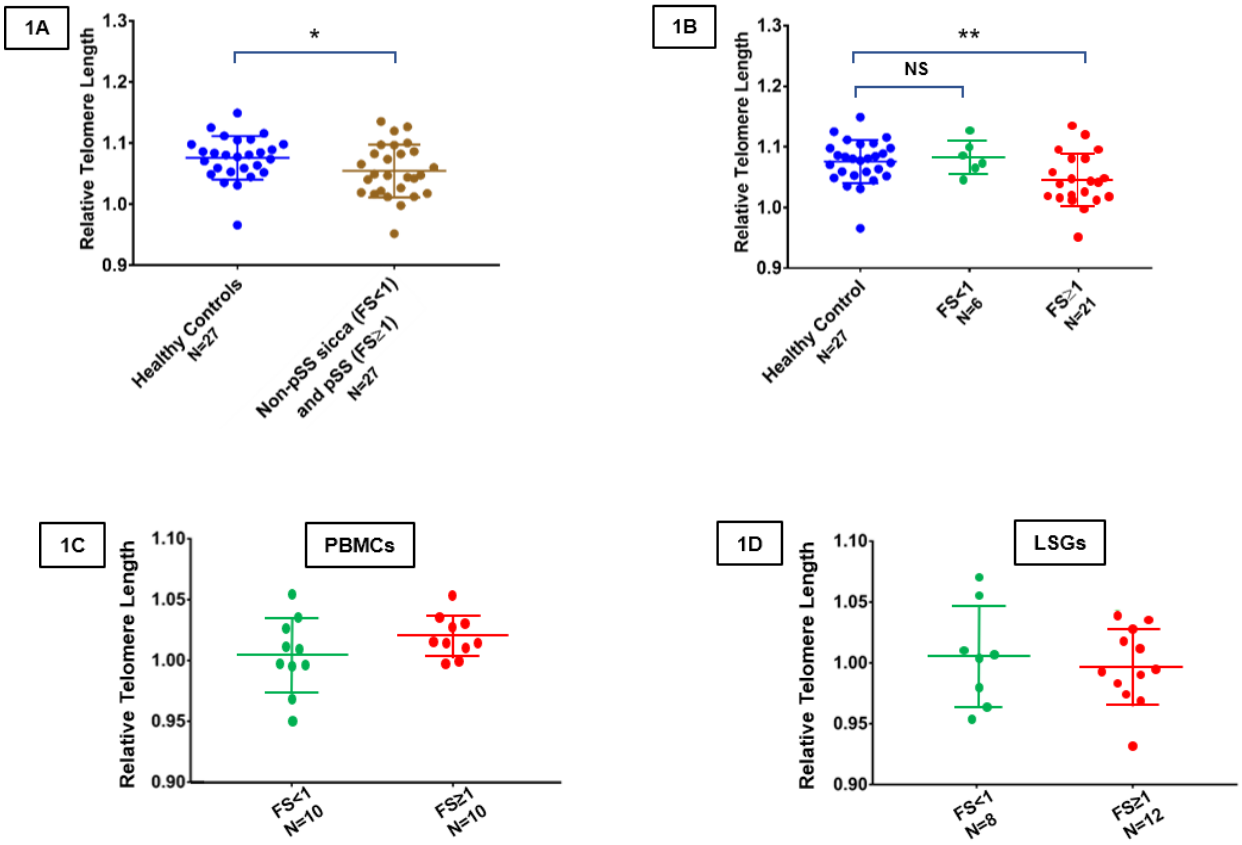

Figure 4.5.1: A-B. Relative Telomere Length (RTL) of saliva DNA of non-pSS sicca and pSS patients compared to healthy controls. Figure 4.5.1. (C-D) RTL in PBMCs and LSG tissue DNAs of non-pSS sicca (FS<1) and pSS (FS≥1) patients**.** (A) Saliva DNA samples from healthy controls, non-pSS sicca, and pSS patients were used to determine RTL. A significant difference in mean RTL was found between the healthy controls (n=27; blue) and the non-pSS sicca (FS<1) + pSS (FS≥1) groups combined (p=0.0372; brown). (B) When the non-pSS sicca group (FS<1, n=6, green) was separated from the pSS group (FS>1, n=21, red), a larger significant difference (p=0.0035) in RTL was observed between healthy controls (blue) and pSS group (red). There was no significant difference in means between the healthy control group (n=27, blue) and the non-pSS sicca group (FS>1, n=6, p=0.6989, green). Significance was determined using the Mann-Whitney U-test (**p<0.01, *p<0.05, NS=Not Significant (p>0.05)). Bars represent mean (+/- SD). Figure 4.5.1 (C-D) RTL measurements of PBMCs (**C**) and LSG tissue biopsies (**D**) from non-pSS sicca (green) and pSS patients (red) is shown. Although a trend of higher mean RTL for PBMCs and lower mean RTL for LSGs in pSS compared to non-pSS sicca was observed, differences were not found statistically significant, possibly due to higher variability in non-pSS sicca samples (poor clustering of data). Significance was calculated using the Mann-Whitney U-test. Bars represent mean (+/- SD).

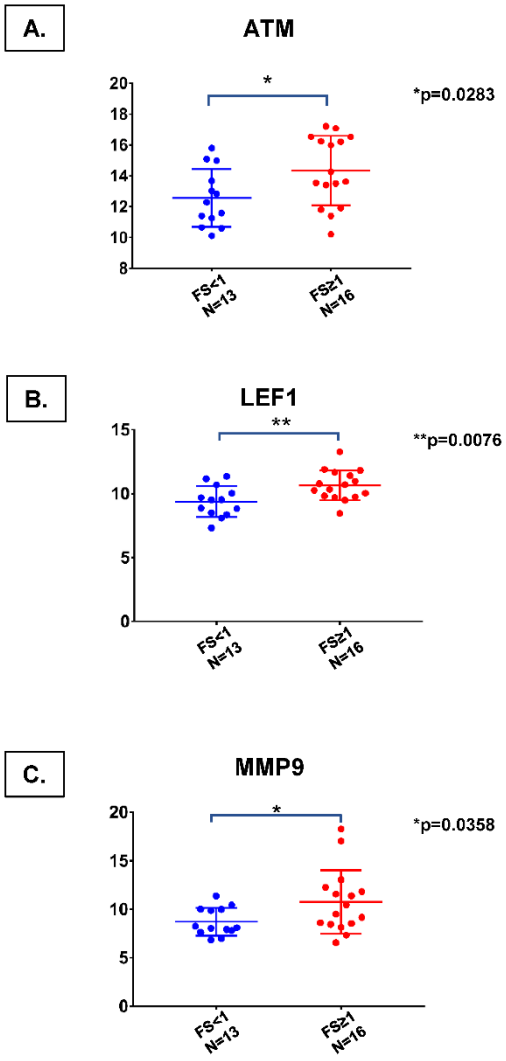

Figure 4.5.2: Comparison of ATM, LEF1, and MMP9 mRNA expression in LSG tissue of non-pSS sicca and pSS patients**.** ATM mRNA was overexpressed in the pSS patients (n=16) LSG tissue compared to non-pSS sicca patients (n=13) (A). We also confirmed the overexpression of LEF1 and MMP9 in the LSG tissue of pSS patients (n=16) as compared to non-pSS sicca patients (n=13) (B and C), as previously published (Shah, Noll et al. 2019). Significance was calculated using the Mann-Whitney U-test (**p<0.01, *p<0.05). Bars represent mean (+/- SD).

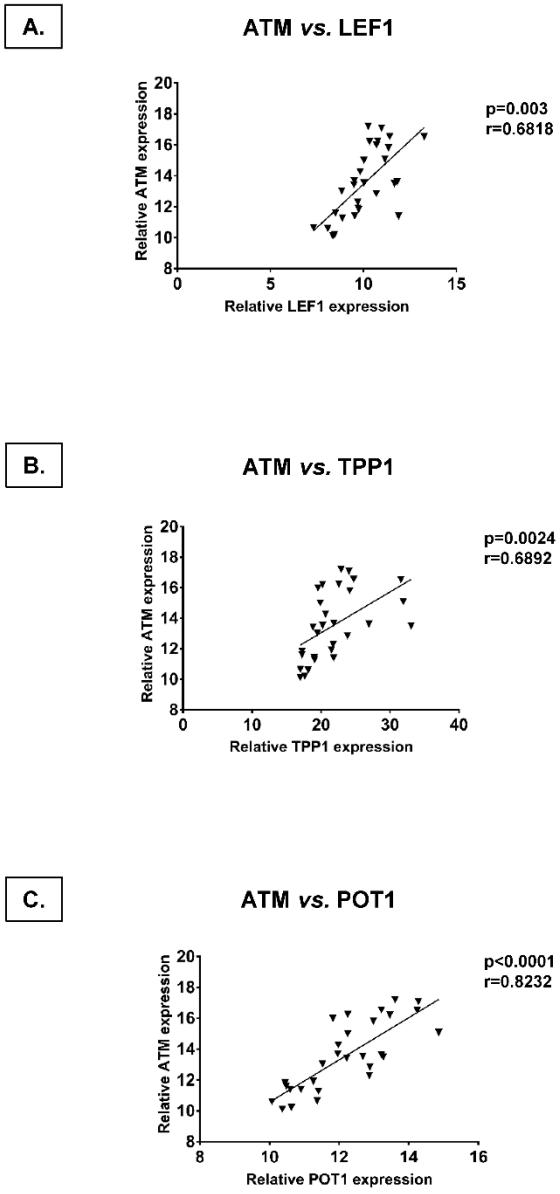

Figure 4.5.3: Correlation of ATM mRNA expression with that of LEF1, TPP1, and POT1. Relative mRNA expression of ATM correlated strongly with that of transcription factor LEF1, and the telomere maintenance associated genes, TPP1 and POT1, in the labial salivary gland tissue of pSS and non-pSS sicca patients (n=29 total) (A, B and C). The Spearman's coefficient (rho) and respective p-value are shown.

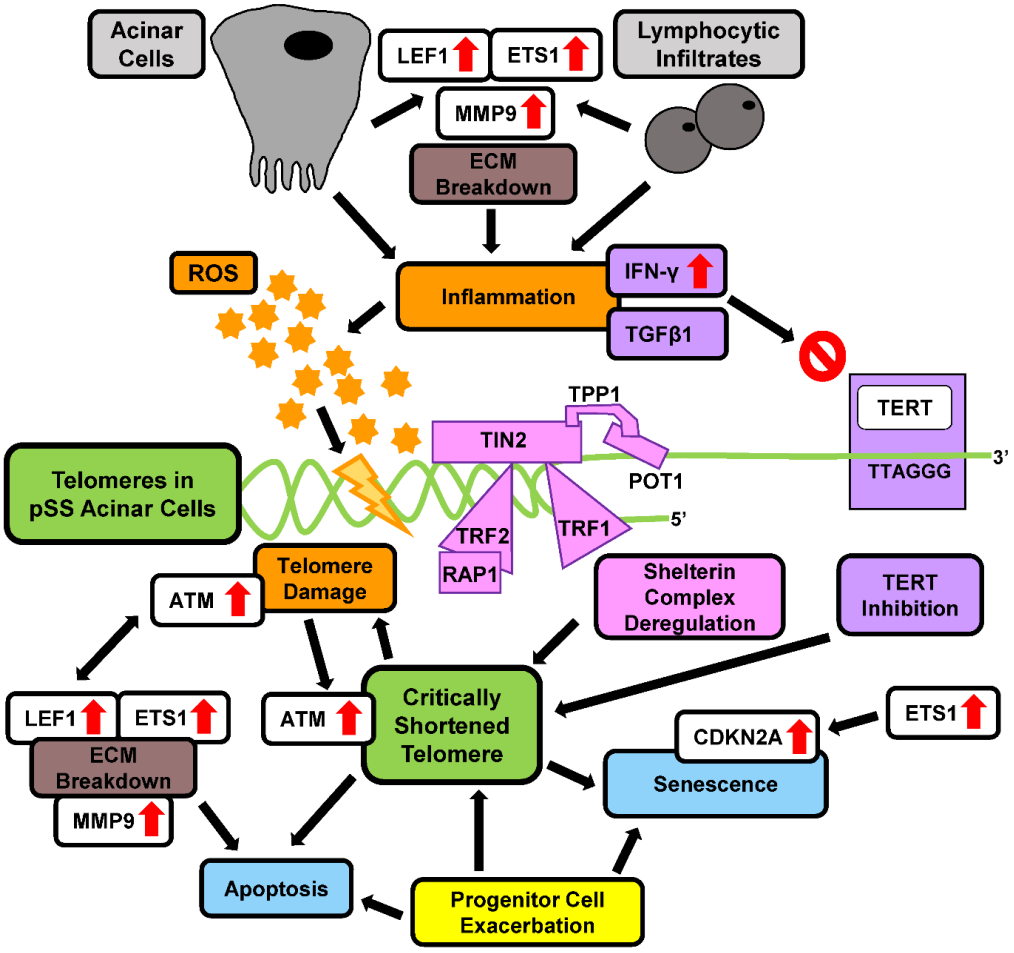

Figure 4.5.4: Possible mechanisms explaining telomere attrition in pSS**.** Telomere attrition in pSS salivary gland (SG) cells likely follows a multifaceted progression. Overexpression of genes (red arrows) combined with dysregulation of telomere maintenance processes may result in downstream effects (black arrows), including telomere erosion. Acinar cells and lymphocytic infiltrates (grey) drive local inflammatory conditions and exacerbate glandular destruction/disintegration (brown box) through expression of inflammatory cytokines (TGFβ1, IFN-γ) and the collagenase, MMP9. Breakdown of glandular integrity by MMP9 can lead to anoikis, a form of apoptosis. TGFβ1 and IFN-γ can directly or indirectly inhibit TERT (purple items), thereby affecting telomere maintenance. Additionally, inflammation drives the production of reactive oxygen species (ROS), which can damage telomere DNA, leading to a DNA damage response primarily mediated through ATM (orange items). The shelterin complex (pink items) regulates telomere length through TERT recruitment to telomere ends. This complex also prevents unnecessary ATM recognition of uncapped telomere ends (Denchi 2009). Dysregulation of the shelterin complex can arise from different sources, where expression changes in its subunits may hinder TERT recruitment. In addition, progenitor cells (yellow box) in pSS SGs have significantly shorter telomeres in pSS and a potentially exacerbated replicative capacity. Shorter telomeres in pSS progenitor cells are an impending product of exhaustive over-replication from continued replenishment of acinar cell populations. Shortening of telomeres reduces their ability to mitigate DNA damage and the downstream ATM response, furthering cell senescence or apoptosis. Critically shortened telomeres (green) in SG cells can promote apoptosis or senescence (blue boxes). Additionally, the transcription factors ETS1 and LEF1 are expressed at higher levels in both lymphocytic and acinar cells of pSS SGs compared to SGs of non-pSS sicca patients (Shah, Noll et al. 2017, Shah, Noll et al. 2019). ETS1 may have a direct role in generation of senescent progenitor cells through the direct upregulation of CDKN2A. In our study, LEF1 mRNA expression strongly correlated with that of ATM (Spearman $r>0.6$, $p<0.01$). Assuming mRNA levels correlate with functional protein levels, the significance and origin of such relationship in telomere attrition remain to be determined.

4.6 Tables

Table 4.6.1: Clinical characteristics and demographics of healthy control subjects, non-pSS sicca, and pSS patients. *Patients are Schirmers (+) if the value is ≤5mm/ 5min. **A value of ≤1.5ml/ 15min for unstimulated salivary flow was considered low, per ACR-EULAR criteria. ***/*Saliva or tear samples unavailable for one patient in the pSS group and two patients in the non-pSS sicca group.

	Healthy Controls	**non-pSS sicca 0≤FS<1**	**pSS FS≥1**
Patients-Ct (M/F)	27 (8/19)	15 (0/15)	29 (1/28)
Age: Mean (SD)	56.2 (9.9)	50.2 (13.0)	57.7 (10.5)
Range	40-84	33-71	26-74
Median	55	48	58
Dry Eyes (Yes/No)	NA	13/2	27/2
Dry Mouth (Yes/No)	NA	13/2	29/29
Schirmer's (+)*-Ct	NA	12	18
Schirmer's (+)-Saliva mm/5min: Mean (SD)	NA	3.0 (1.4)	3.0 (1.6)
Range	NA	1.0-5.0	0-5.0
Median	NA	2.5	3.0
Unstimulated Whole Salivary Flow mL/15min**/***: Mean (SD)	NA	2.7 (2.9)	2.1 (2.4)
Range	NA	0-9.6	0-8.1
Median	NA	1.5	1.5
Stimulated Whole Salivary Flow mL/15min***: Mean (SD)	NA	17.6 (11.7)	9.1 (6.5)
Range	NA	2.1-34.8	1.1-23.1
Median	NA	17.5	7.5
Serum Anti-SSA (+)-Ct	NA	None	2

CHAPTER 5: CONCLUSIONS AND FUTURE DIRECTIONS

5.1. Generation of novel iSGECs: Utility and impacts in pSS research

The iSGECs generated in our study represent a preliminary model system for the development of therapies targeting salivary gland dysfunction. We have demonstrated iSGEC-nSS2 cells derived from a sicca female patient, retained the ability to form spheroids with differentiated cell types at late passages (p-80) and exhibited a significant proliferation capacity (>100 passages) when cultured as a monolayer. Overall, iSGECs could be used as an alternative to currently available cell culture models in salivary gland research.

5.2 ETS1 regulates MMP9 in the salivary epithelium of pSS and non-pSS patients

We have shown that ETS1 is able to upregulate MMP9 expression in non-pSS sicca derived iSGECs and to a lesser extent in pSS derived iSGECs. Additionally, we found differences in the expression of EMT factors possibly contributing to fibrosis of the salivary gland. Also, differences in MMP9 regulation might reflect progression of the salivary gland ECM destruction towards a pro-inflammatory stage. Using both non-pSS and pSS iSGEC cell culture models, ETS1 was determined to bind at three separate locations on the MMP9 promoter, providing a non-immunologic mediated mechanism of MMP9 expression in-vitro. Investigating the mechanisms governing ETS1 expression promoting pSS pathogenesis through MMP9 upregulation could provide new therapeutic targets to reduce salivary gland degradation and improve acinar function.

5.3 ROS could promote telomere-induced senescence within the pSS salivary epithelium

Chronic DNA damage may lead to ATM mRNA overexpression due to compromised telomere maintenance observed in pSS. Shorter saliva DNA RTL in anti-SSA (-) pSS patients might result from multiple convergent mechanisms, which would need to be addressed on a cell-specific

level in future studies. Gene expression correlation between telomere maintenance genes and pSS pathogenic marker(s) suggests a link between telomere attrition and disease progression, representing a potential avenue in anti-SSA (-) pSS diagnosis and therapeutic interventions. Moreover, our investigation strengthened the connection among telomere attrition and progenitor cell renewal by revealing the significant correlation among relative telomere length and the expression of LEF1.

5.4 Summary and Future Directions

At the forefront of epithelial dysfunction in pSS, understanding the role in which ETS1, LEF1, and MMP9 play in glandular homeostasis and disease onset could align future research targets for epithelial-centered treatment. The significance of “pre-immune” pSS is currently complex concept but is better defined and understood could promote new avenues to disease prevention by targeting the onset of salivary dysfunction early in disease pathogenesis.

Based on our extensive bioinformatics analysis across multiple autoimmune diseases, we specifically highlighted the importance of ETS1, LEF1, and MMP9 as differentially expressed candidate gene targets contributing to the disruption of the pSS salivary epithelium. Previously, limitations in investigating “pre-immune” pSS hampered progress due to the lack of relevant cell culture and mouse models. Primary SGEC cell culture from labial salivary gland biopsies is one of the current standard approaches to in-vitro analysis of pathogenic mechanisms in the pSS epithelium. In our laboratory, I was the first scientist to isolate and culture SGECs from LSG biopsies from both non-pSS and pSS patients. Unfortunately, primary SGEC culture has several limitations described earlier, reducing its utility in pSS research. To circumvent some limitations with SGEC-based model systems of pSS, I produced three novel immortalized salivary gland epithelial cell lines derived from two non-pSS “sicca” and one pSS patient. These three cell lines

were the first immortalized non-pSS sicca and pSS SGECs of female origin, which have now been commercialized.

After demonstrating both tissue and disease relevancy of iSGECs through the expression of markers pertinent to the salivary epithelium and pSS pathogenesis, I investigated the relationship between ETS1 and/or LEF1 andMMP9. Secondarily we also determined relationship between ETS1 and LEF1, since tandem binding sites are present in MMP9 promoter. We found that ETS1 and MMP9 retained their overexpression after explant, furthering their relationship and providing supportive evidence towards my iSGEC models. On the other hand, after extensive primary SGEC culture, we were unable to confirm the in-vitro pSS overexpression of LEF1, which was previously observed within pSS LSG biopsies by IF. The expression of LEF1 was most likely altered during SGEC explant as a product of extensive environmental changes and cell-cell communication and involvement of the immune response. Thus, using a variety of molecular biology techniques, I was able to first demonstrate the regulation of MMP9 by ETS1 in both our cell culture models and salivary gland cell lines. Originally, I believed the relationship among ETS1 and MMP9 would prove relatively linear, where increases in expression regulation and disease progression were directly correlated. However, as I made progress in my investigations, the relationship among ETS1 and MMP9 proved to be more complex. Although MMP9 is expressed highest in primary SGECs of pSS patients, the direct regulation of MMP9 by ETS1 was markedly reduced when compared among our non-pSS sicca (iSGEC-nSS2) and pSS (iSGEC-pSS) models. The effect of ETS1 on MMP9 expression was more drastic in iSGEC-nSS2 cells, as demonstrated in both the MMP9 luciferase reporter assay and ETS1 siRNA knockdown experiments. Interestingly, using MMP9 luciferase reporter assays, we were able to uncover three ETS1 binding sites, potentially representing two different regulatory binding motifs for ETS1 on the MMP9 promoter. These two binding motifs provide insights into the progression of pSS and the differential regulation of

MMP9 by ETS1. I also demonstrated the potential for shifts in mechanisms governing salivary epithelial disfunction in pSS, which opens the future towards targeting treatments during early “pre-immune” and post-lymphocytic infiltration stages. Lastly, while uncovering the roles of ETS1 and LEF1 within the epithelium, I provide evidence of their roles in driving a dysfunctional wound healing process mediated through epithelial-mesenchymal transition (EMT). Both ETS1 and LEF1 positively contributed to regulating the expression of EMT markers in iSGECs. These results provide strong evidence of their role in epithelial disruption during early pSS pathogenesis. Targeting the initial loss of epithelial homeostasis in pSS is a favorable approach to mitigating future damage to epithelia within the acinus structures, since most current treatment strategies target either immune system or geared at symptom mitigation. My work has provided evidence for at least two separate mechanisms driven by ETS1 and/or LEF1 which impact salivary epithelial function and EMT in both non-pSS and pSS patients alongside generating novel cell models for future drug testing and high throughput screening.

REFERENCES

Ahuja, D., M. T. Sáenz-Robles and J. M. Pipas (2005). "SV40 large T antigen targets multiple cellular pathways to elicit cellular transformation." Oncogene 24(52): 7729-7745.

Alevizos, I., C. Zheng, A. P. Cotrim, S. Liu, L. McCullagh, M. E. Billings, C. M. Goldsmith, M. Tandon, E. J. Helmerhorst, M. A. Catalan, S. J. Danielides, P. Perez, N. P. Nikolov, J. A. Chiorini, J. E. Melvin, F. G. Oppenheim, G. G. Illei and B. J. Baum (2017). "Late responses to adenoviral-mediated transfer of the aquaporin-1 gene for radiation-induced salivary hypofunction." Gene Ther 24(3): 176-186.

ATCC. (2020). "A-253 (ATCC® HTB-41™)." 2020, from https://www.atcc.org/Global/Products/D/9/3/3/HTB-41.aspx.

Azuma, M., T. Tamatani, Y. Kasai and M. Sato (1993). "Immortalization of normal human salivary gland cells with duct-, myoepithelial-, acinar-, or squamous phenotype by transfection with SV40 ori- mutant deoxyribonucleic acid." Lab Invest 69(1): 24-42.

Baker, O. J. (2010). "Tight junctions in salivary epithelium." Journal of biomedicine & biotechnology 2010: 278948-278948.

Ayesha B, Fernandez-Ruiz R, Shrock D, Snyder BM, Lieberman SM, Tuetken R, Field E, Singh N. Clinical and laboratory features of patients with focal lymphocytic sialadenitis on minor salivary gland biopsy for sicca symptoms: A single-center experience. Medicine (Baltimore). 2021 Apr 2;100(13):e25325. doi: 10.1097/MD.0000000000025325. PMID: 33787627; PMCID: PMC8021287.

Alunno A, Leone MC, Giacomelli R, Gerli R and Carubbi F (2018) Lymphoma and Lymphomagenesis in Primary Sjögren's Syndrome. Front. Med. 5:102. doi: 10.3389/fmed.2018.00102

Arce-Franco, M., Dominguez-Luis, M., Pec, M.K. et al. Functional effects of proinflammatory factors present in Sjögren's syndrome salivary microenvironment in an in vitro model of human salivary gland. Sci Rep 7, 11897 (2017). https://doi.org/10.1038/s41598-017-12282-x

Azuma M, Aota K, Tamatani T, Motegi K, Yamashita T, Harada K, et al. Suppression of tumor necrosis factor alpha-induced matrix metalloproteinase 9 production by the introduction of a super-repressor form of inhibitor of nuclear factor kappaBalpha complementary DNA into immortalized human salivary gland acinar cells. Prevention of the destruction of the acinar structure in Sjögren's syndrome salivary glands. Arthritis Rheum. 2000;43(8):1756-67.

Ambudkar I. Calcium signaling defects underlying salivary gland dysfunction. Biochim Biophys Acta Mol Cell Res. 2018 Nov;1865(11 Pt B):1771-1777. doi: 10.1016/j.bbamcr.2018.07.002. Epub 2018 Jul 10. PMID: 30006140.

Alessandro Furlan Albin Pourtier. Ets-1 activation, when tumors crosstalk with their microenvironment Cancer Cell & Microenvironment 2015; 2: e494. doi: 10.14800/ccm.494;

Aqrawi, L.A., Galtung, H.K., Guerreiro, E.M. et al. Proteomic and histopathological characterisation of sicca subjects and primary Sjögren's syndrome patients reveals promising tear, saliva and extracellular vesicle disease biomarkers. Arthritis Res Ther 21, 181 (2019). https://doi.org/10.1186/s13075-019-1961-4

Alexandra Zervoudaki, Emanuel Economou, Christos Pitsavos, Karmen Vasiliadou, Constantina Aggeli, Konstantinos Tsioufis, Marina Toutouza, Christodoulos Stefanadis, Pavlos Toutouzas, The effect of Ca2+ channel antagonists on plasma concentrations of matrix metalloproteinase-2 and -9 in essential hypertension, American Journal of Hypertension, Volume 17, Issue 3, March 2004, Pages 273–276, https://doi.org/10.1016/j.amjhyper.2003.11.007

Baum, B. J., I. Alevizos, C. Zheng, A. P. Cotrim, S. Liu, L. McCullagh, C. M. Goldsmith, P. D. Burbelo, D. E. Citrin, J. B. Mitchell, L. K. Nottingham, S. F. Rudy, C. Van Waes, M. A. Whatley, J. S. Brahim, J. A. Chiorini, S. Danielides, R. J. Turner, N. J. Patronas, C. C. Chen, N. P. Nikolov and G. G. Illei (2012). "Early responses to adenoviral-mediated transfer of the aquaporin-1 cDNA for radiation-induced salivary hypofunction." Proc Natl Acad Sci U S A 109(47): 19403-19407.

Baum, B. J., J. A. Ship and A. J. Wu (1992). "Salivary gland function and aging: a model for studying the interaction of aging and systemic disease." Crit Rev Oral Biol Med 4(1): 53-64.

Bruno, S. and Z. Darzynkiewicz (1992). "Cell cycle dependent expression and stability of the nuclear protein detected by Ki-67 antibody in HL-60 cells." Cell Prolif 25(1): 31-40.

Baum Bruce, J., et al. (2012). "Early responses to adenoviral-mediated transfer of the aquaporin-1 cDNA for radiation-induced salivary hypofunction." Proceedings of the National Academy of Sciences 109(47): 19403-19407.

Berardicurti O, Ruscitti P, Di Benedetto P, D'Andrea S, Navarini L, Marino A, Cipriani P and Giacomelli R (2021) Association Between Minor Salivary Gland Biopsy During Sjögren's

Syndrome and Serologic Biomarkers: A Systematic Review and Meta-Analysis. Front. Immunol. 12:686457. doi: 10.3389/fimmu.2021.686457

Bharaj, T. K., Aqrawi, L. A., Fromreide, S., Jonsson, R., Brun, J. G., Appel, S., & Skarstein, K. (2021). Inflammatory Stratification in Primary Sjögren's Syndrome Reveals Novel Immune Cell Alterations in Patients' Minor Salivary Glands. Frontiers in immunology, 12, 701581. https://doi.org/10.3389/fimmu.2021.701581

Bookman AA, Shen H, Cook RJ, Bailey D, McComb RJ, Rutka JA, Slomovic AR, Caffery B. Whole stimulated salivary flow: correlation with the pathology of inflammation and damage in minor salivary gland biopsy specimens from patients with primary Sjögren's syndrome but not patients with sicca. Arthritis Rheum. 2011 Jul;63(7):2014-20. doi: 10.1002/art.30295. PMID: 21337320.

Barrera MJ, Bahamondes V, Sepulveda D, Quest AF, Castro I, Cortes J, et al. Sjogren's syndrome and the epithelial target: a comprehensive review. J Autoimmun. 2013;42:7-18.

Baumeister, P., Hollmann, A., Kitz, J., Afthonidou, A., Simon, F., Shakhtour, J., Mack, B., Kranz, G., Libl, D., Leu, M., Schirmer, M. A., Canis, M., Belka, C., Zitzelsberger, H., Ganswindt, U., Hess, J., Jakob, M., Unger, K., & Gires, O. (2018). High Expression of EpCAM and Sox2 is a Positive Prognosticator of Clinical Outcome for Head and Neck Carcinoma. Scientific reports, 8(1), 14582. https://doi.org/10.1038/s41598-018-32178-8

Costa, A. F., A. Altemani and M. Hermsen (2011). "Current Concepts on Dedifferentiation/High-Grade Transformation in Salivary Gland Tumors." Pathology Research International 2011: 325965.

Christodoulou MI, Kapsogeorgou EK, Moutsopoulos HM. Characteristics of the minor salivary gland infiltrates in Sjögren's syndrome. J Autoimmun. 2010 Jun;34(4):400-7. doi: 10.1016/j.jaut.2009.10.004. Epub 2009 Nov 3. PMID: 19889514

Corden, A., Handelman, B., Yin, H. et al. Neutralizing antibodies against adeno-associated viruses in Sjögren's patients: implications for gene therapy. Gene Ther 24, 241–244 (2017). https://doi.org/10.1038/gt.2017.1

Carubbi F, Alunno A, Cipriani P, Bartoloni E, Baldini C, Quartuccio L, Priori R, Valesini G, De Vita S, Bombardieri S, Gerli R, Giacomelli R. A retrospective, multicenter study evaluating the prognostic value of minor salivary gland histology in a large cohort of patients with primary Sjögren's syndrome. Lupus. 2015 Mar;24(3):315-20. doi: 10.1177/0961203314554251. Epub 2014 Oct 8. PMID: 25297554.

Chen, L., Lu, D., Yu, K., He, S., Liu, L., Zhang, X., Feng, B., & Wang, X. (2021). Bioinformatics Analysis for Identification of Key Genes in Salivary Gland and the Potential of a Combination of Biomarkers for the Diagnosis of SS. Journal of inflammation research, 14, 4143–4153. https://doi.org/10.2147/JIR.S322318

Czuwara-Ladykowska, Joanna et al . Ets1 Is an Effector of the Transforming Growth Factor β (TGF-β) Signaling Pathway and an Antagonist of the Profibrotic Effects of TGF-β. Journal of Biological Chemistry, Volume 277, Issue 23, 20399 – 20408

Chen, M., Sinha, M., Luxon, B. A., Bresnick, A. R., & O'Connor, K. L. (2009). Integrin alpha6beta4 controls the expression of genes associated with cell motility, invasion, and

metastasis, including S100A4/metastasin. The Journal of biological chemistry, 284(3), 1484–1494. https://doi.org/10.1074/jbc.M803997200

Chin, V. L., & Lim, C. L. (2019). Epithelial-mesenchymal plasticity-engaging stemness in an interplay of phenotypes. Stem cell investigation, 6, 25. https://doi.org/10.21037/sci.2019.08.08

Cox TR, Erler JT. Remodeling and homeostasis of the extracellular matrix: implications for fibrotic diseases and cancer. Dis Model Mech. 2011;4(2):165-78.

Cha S, Brayer J, Gao J, Brown V, Killedar S, Yasunari U, et al. A dual role for interferon-gamma in the pathogenesis of Sjogren's syndrome-like autoimmune exocrinopathy in the nonobese diabetic mouse. Scand J Immunol. 2004;60(6):552-65.

D'Agostino, C., O. A. Elkashty, C. Chivasso, J. Perret, S. D. Tran and C. Delporte (2020). "Insight into Salivary Gland Aquaporins." Cells 9(6): 1547.

Daniels, T. E., Cox, D., Shiboski, C. H., Schiødt, M., Wu, A., Lanfranchi, H., Umehara, H., Zhao, Y., Challacombe, S., Lam, M. Y., De Souza, Y., Schiødt, J., Holm, H., Bisio, P. A., Gandolfo, M. S., Sawaki, T., Li, M., Zhang, W., Varghese-Jacob, B., Ibsen, P., … Sjögren's International Collaborative Clinical Alliance Research Groups (2011). Associations between salivary gland histopathologic diagnoses and phenotypic features of Sjögren's syndrome among 1,726 registry participants. Arthritis and rheumatism, 63(7), 2021–2030.

Dorian Parisis, Clara Chivasso, Jason Perret, Muhammad Shahnawaz Soyfoo, and Christine Delporte.. 2020. Current State of Knowledge on Primary Sjögren’s Syndrome, an Autoimmune Exocrinopathy.

Didier K, Bolko L, Giusti D, Toquet S, Robbins A, Antonicelli F and Servettaz A (2018) Autoantibodies Associated With Connective Tissue Diseases: What Meaning for Clinicians? Front. Immunol. 9:541. doi: 10.3389/fimmu.2018.00541

Dittmer J. The biology of the Ets1 proto-oncogene. Mol Cancer. 2003;2:29.

Delannoy-Courdent A, Fauquette W, Dong-Le Bourhis XF, Boilly B, Vandenbunder B, Desbiens X. Expression of c-ets-1 and uPA genes is associated with mammary epithelial cell tubulogenesis or neoplastic scattering. Int J Dev Biol. 1996 Dec;40(6):1097-108. PMID: 9032015.

Delli K, Vissink A, Spijkervet FK. Salivary gland biopsy for Sjögren's syndrome. Oral Maxillofac Surg Clin North Am. 2014 Feb;26(1):23-33. doi: 10.1016/j.coms.2013.09.005. PMID: 24287191.

Delaleu, N., Mydel, P., Kwee, I., Brun, J.G., Jonsson, M.V. and Jonsson, R. (2015), High Fidelity Between Saliva Proteomics and the Biologic State of Salivary Glands Defines Biomarker Signatures for Primary Sjögren's Syndrome. Arthritis & Rheumatology, 67: 1084-1095. https://doi.org/10.1002/art.39015

Dimitriou, I. D., E. K. Kapsogeorgou, R. F. Abu-Helu, H. M. Moutsopoulos and M. N. Manoussakis (2002). "Establishment of a convenient system for the long-term culture and study of non-neoplastic human salivary gland epithelial cells." European Journal of Oral Sciences 110(1): 21-30.

Draeger, A., W. B. Nathrath, E. B. Lane, B. E. Sundström and T. I. Stigbrand (1991). "Cytokeratins, smooth muscle actin and vimentin in human normal salivary gland and pleomorphic adenomas. Immunohistochemical studies with particular reference to myoepithelial and basal cells." Apmis 99(5): 405-415.

Emmerson, E., A. J. May, S. Nathan, N. Cruz-Pacheco, C. O. Lizama, L. Maliskova, A. C. Zovein, Y. Shen, M. O. Muench and S. M. Knox (2017). "SOX2 regulates acinar cell development in the salivary gland." eLife 6: e26620.

Ewert P, Aguilera S, Alliende C, Kwon YJ, Albornoz A, Molina C, Urzúa U, Quest AF, Olea N, Pérez P, Castro I, Barrera MJ, Romo R, Hermoso M, Leyton C, González MJ. Disruption of tight junction structure in salivary glands from Sjögren's syndrome patients is linked to proinflammatory cytokine exposure. Arthritis Rheum. 2010 May;62(5):1280-9. doi: 10.1002/art.27362. PMID: 20131287.

Frucht-Pery J, Sagi E, Hemo I, Ever-Hadani P. Efficacy of doxycycline and tetracycline in ocular rosacea. Am J Ophthalmol. 1993 Jul 15;116(1):88-92. doi: 10.1016/s0002-9394(14)71750-7. PMID: 8328549

Fafeur V, Tulasne D, Quéva C, Vercamer C, Dimster V, Mattot V, Stéhelin D, Desbiens X, Vandenbunder B. The ETS1 transcription factor is expressed during epithelial-mesenchymal transitions in the chick embryo and is activated in scatter factor-stimulated MDCK epithelial cells. Cell Growth Differ. 1997 Jun;8(6):655-65. PMID: 9185999.

Fox RI, Stern M. Sjögren's syndrome: mechanisms of pathogenesis involve interaction of immune and neurosecretory systems. Scand J Rheumatol Suppl. 2002;116:3-13. PMID: 12109541.

Fayyaz, A., Kurien, B. T., & Scofield, R. H. (2016). Autoantibodies in Sjögren's Syndrome. Rheumatic diseases clinics of North America, 42(3), 419–434. https://doi.org/10.1016/j.rdc.2016.03.002

Fujita-Yoshigaki J, Matsuki-Fukushima M, Sugiya H. Inhibition of Src and p38 MAP kinases suppresses the change of claudin expression induced on dedifferentiation of primary cultured parotid acinar cells. Am J Physiol Cell Physiol. 2008 Mar;294(3):C774-85. doi: 10.1152/ajpcell.00472.2007. Epub 2008 Jan 30. PMID: 18234848.

Fujita-Yoshigaki, J. (2010). "Plasticity in Differentiation of Salivary Glands: The Signaling Pathway That Induces Dedifferentiation of Parotid Acinar Cells." Journal of Oral Biosciences 52(2): 65-71.

Fujita-Yoshigaki, J., M. Matsuki-Fukushima and H. Sugiya (2008). "Inhibition of Src and p38 MAP kinases suppresses the change of claudin expression induced on dedifferentiation of primary cultured parotid acinar cells." Am J Physiol Cell Physiol 294(3): C774-785.

Gilboe IM, Kvien TK, Uhlig T, Husby G. Sicca symptoms and secondary Sjögren's syndrome in systemic lupus erythematosus: comparison with rheumatoid arthritis and correlation with disease variables. Ann Rheum Dis. 2001 Dec;60(12):1103-9. doi: 10.1136/ard.60.12.1103. PMID: 11709451; PMCID: PMC1753445.

Gervais, E.M., Desantis, K.A., Pagendarm, N., Nelson, D.A., Enger, T., Skarstein, K., Liaaen Jensen, J. and Larsen, M. (2015), Changes in the Submandibular Salivary Gland Epithelial Cell Subpopulations During Progression of Sjögren's Syndrome-Like Disease in the NOD/ShiLtJ Mouse Model. Anat. Rec., 298: 1622-1634. https://doi.org/10.1002/ar.23190

Garreto L, Charneau S, Mandacaru SC, Nóbrega OT, Motta FN, de Araújo CN, Tonet AC, Modesto FMB, Paula LM, de Sousa MV, Santana JM, Acevedo AC, Bastos IMD. Mapping Salivary Proteases in Sjögren's Syndrome Patients Reveals Overexpression of Dipeptidyl Peptidase-4/CD26. Front Immunol. 2021 Jun 17;12:686480. doi: 10.3389/fimmu.2021.686480. PMID: 34220840; PMCID: PMC8247581.

Goicovich E, Molina C, Pérez P, Aguilera S, Fernández J, Olea N, et al. Enhanced degradation of proteins of the basal lamina and stroma by matrix metalloproteinases from the salivary glands of Sjögren's syndrome patients: Correlation with reduced structural integrity of acini and ducts. Arthritis & Rheumatism. 2003;48(9):2573-84.

Gábor Varga, Physiology of the salivary glands, Surgery (Oxford), Volume 30, Issue 11, 2012, Pages 578-583,ISSN 0263-9319,https://doi.org/10.1016/j.mpsur.2012.09.010.

Gervais, E.M., Desantis, K.A., Pagendarm, N., Nelson, D.A., Enger, T., Skarstein, K., Liaaen Jensen, J. and Larsen, M. (2015), Changes in the Submandibular Salivary Gland Epithelial Cell Subpopulations During Progression of Sjögren's Syndrome-Like Disease in the NOD/ShiLtJ Mouse Model. Anat. Rec., 298: 1622-1634. https://doi.org/10.1002/ar.23190

Guo S, Dipietro LA. Factors affecting wound healing. J Dent Res. 2010 Mar;89(3):219-29. doi: 10.1177/0022034509359125. Epub 2010 Feb 5. PMID: 20139336; PMCID: PMC2903966.

Giannandrea, M., & Parks, W. C. 2014. Diverse functions of matrix metalloproteinases during fibrosis. Disease models & mechanisms, 7(2), 193–203. https://doi.org/10.1242/dmm.012062

Gao Y, Chen Y, Zhang Z, Yu X and Zheng J (2020) Recent Advances in Mouse Models of Sjögren's Syndrome. Front. Immunol. 11:1158. doi: 10.3389/fimmu.2020.01158

Giard, D. J., S. A. Aaronson, G. J. Todaro, P. Arnstein, J. H. Kersey, H. Dosik and W. P. Parks (1973). "In Vitro Cultivation of Human Tumors: Establishment of Cell Lines Derived From a Series of Solid Tumors2." JNCI: Journal of the National Cancer Institute 51(5): 1417-1423.

Guchelaar, H. J., A. Vermes and J. H. Meerwaldt (1997). "Radiation-induced xerostomia: pathophysiology, clinical course and supportive treatment." Support Care Cancer 5(4): 281-288.

Hosseini, Z. F., D. A. Nelson, N. Moskwa, L. M. Sfakis, J. Castracane and M. Larsen (2018). "FGF2-dependent mesenchyme and laminin-111 are niche factors in salivary gland organoids." Journal of cell science 131(4): jcs208728.

Humphreys-Beher MG, Yamachika S, Yamamoto H, Maeda N, Nakagawa Y, Peck AB, Robinson CP. Salivary gland changes in the NOD mouse model for Sjögren's syndrome: is there a non-immune genetic trigger? Eur J Morphol. 1998 Aug;36 Suppl:247-51. PMID: 9825931.

Holdgate, N., & St Clair, E. W. (2016). Recent advances in primary Sjogren's syndrome. F1000Research, 5, F1000 Faculty Rev-1412. https://doi.org/10.12688/f1000research.8352.1

Hiroe Tada, Hideyuki Takahashi, Shota Ida, Yurino Nagata, Kazuaki Chikamatsu. Epithelial–Mesenchymal Transition Status of Circulating Tumor Cells Is Associated With Tumor Relapse in Head and Neck Squamous Cell Carcinoma. Anticancer Research Jun 2020, 40 (6) 3559-3564; DOI: 10.21873/anticanres.14345

Hai, B., Yang, Z., Millar, S. E., Choi, Y. S., Taketo, M. M., Nagy, A., & Liu, F. (2010). Wnt/β-catenin signaling regulates postnatal development and regeneration of the salivary gland. Stem cells and development, 19(11), 1793–1801. https://doi.org/10.1089/scd.2009.0499

Iris L A Bodewes, Shereen Al-Ali, Cornelia G van Helden-Meeuwsen, Naomi I Maria, Jessica Tarn, Dennis W Lendrem, Marco W J Schreurs, Eline C Steenwijk, Paul L A van Daele, Tim Both, Simon J Bowman, Bridget Griffiths, Wan-Fai Ng, UK Primary Sjögren's Syndrome registry, Marjan A Versnel, Systemic interferon type I and type II signatures in primary Sjögren's syndrome reveal differences in biological disease activity, Rheumatology, Volume 57, Issue 5, May 2018, Pages 921–930, https://doi.org/10.1093/rheumatology/kex490

Ikeura, K., T. Kawakita, K. Tsunoda, T. Nakagawa and K. Tsubota (2016). "Characterization of Long-Term Cultured Murine Submandibular Gland Epithelial Cells." PloS one 11(1): e0147407-e0147407.

Ittah, M., C. Miceli-Richard, J. Eric Gottenberg, F. Lavie, T. Lazure, N. Ba, J. Sellam, C. Lepajolec and X. Mariette (2006). "B cell-activating factor of the tumor necrosis factor family (BAFF) is expressed under stimulation by interferon in salivary gland epithelial cells in primary Sjögren's syndrome." Arthritis Res Ther 8(2): R51.

Jang, S. I., H. L. Ong, A. Gallo, X. Liu, G. Illei and I. Alevizos (2015). "Establishment of functional acinar-like cultures from human salivary glands." J Dent Res 94(2): 304-311.

Jang, S. I., H. L. Ong, X. Liu, I. Alevizos and I. S. Ambudkar (2016). "Up-regulation of Store-operated Ca2+ Entry and Nuclear Factor of Activated T Cells Promote the Acinar Phenotype of the Primary Human Salivary Gland Cells." J Biol Chem 291(16): 8709-8720.

Jordan NV, Johnson GL, Abell AN. Tracking the intermediate stages of epithelial-mesenchymal transition in epithelial stem cells and cancer. Cell Cycle. 2011;10(17):2865-73.

Kratochwil K, Galceran J, Tontsch S, Roth W, Grosschedl R. FGF4, a direct target of LEF1 and Wnt signaling, can rescue the arrest of tooth organogenesis in Lef1(-/-) mice. Genes Dev. 2002 Dec 15;16(24):3173-85. doi: 10.1101/gad.1035602. PMID: 12502739; PMCID: PMC187508.

Konsta OD, Charras A, Le Dantec C, Kapsogeorgeou E, Bordron A, Brooks WH, Tzioufas AG, Pers JO, Renaudineau Y. Epigenetic modifications in salivary glands from patients with Sjögren's syndrome affect cytokeratin 19 expression. Bull Group Int Rech Sci Stomatol Odontol. 2016 Jun 28;53(1):e01. PMID: 27352422.

Kassan SS, Moutsopoulos HM. Clinical Manifestations and Early Diagnosis of Sjögren Syndrome. Arch Intern Med. 2004;164(12):1275–1284. doi:10.1001/archinte.164.12.1275

Kalluri R, Weinberg RA. The basics of epithelial-mesenchymal transition. J Clin Invest. 2009 Jun;119(6):1420-8. doi: 10.1172/JCI39104. Erratum in: J Clin Invest. 2010 May 3;120(5):1786. PMID: 19487818; PMCID: PMC2689101.

Kalk WW, Vissink A, Stegenga B, Bootsma H, Nieuw Amerongen AV, Kallenberg CG. Sialometry and sialochemistry: a non-invasive approach for diagnosing Sjögren's syndrome. Ann Rheum Dis. 2002 Feb;61(2):137-44. doi: 10.1136/ard.61.2.137. PMID: 11796400; PMCID: PMC1754002.

Kawanami, T., T. Sawaki, T. Sakai, M. Miki, H. Iwao, A. Nakajima, T. Nakamura, T. Sato, Y. Fujita, M. Tanaka, Y. Masaki, T. Fukushima, Y. Hirose, M. Taniguchi, N. Sugimoto, T. Okazaki and H. Umehara (2012). "Skewed production of IL-6 and TGFβ by cultured salivary gland epithelial cells from patients with Sjögren's syndrome." PloS one 7(10): e45689-e45689.

Knox, S. M., I. M. A. Lombaert, C. L. Haddox, S. R. Abrams, A. Cotrim, A. J. Wilson and M. P. Hoffman (2013). "Parasympathetic stimulation improves epithelial organ regeneration." Nature communications 4: 1494-1494.

Knox, S. M., I. M. A. Lombaert, X. Reed, L. Vitale-Cross, J. S. Gutkind and M. P. Hoffman (2010). "Parasympathetic Innervation Maintains Epithelial Progenitor Cells During Salivary Organogenesis." Science 329(5999): 1645.

Kwak, M., N. Ninche, S. Klein, D. Saur and S. Ghazizadeh (2018). "c-Kit+ Cells in Adult Salivary Glands do not Function as Tissue Stem Cells." Scientific Reports 8(1): 14193.

Lin, L. C., O. Elkashty, M. Ramamoorthi, N. Trinh, Y. Liu, G. Sunavala-Dossabhoy, T. Pranzatelli, D. G. Michael, C. Chivasso, J. Perret, J. A. Chiorini, C. Delporte and S. D. Tran (2018). "Cross-contamination of the human salivary gland HSG cell line with HeLa cells: A STR analysis study." Oral Dis 24(8): 1477-1483.

Lombaert, I. M. A., J. F. Brunsting, P. K. Wierenga, H. Faber, M. A. Stokman, T. Kok, W. H. Visser, H. H. Kampinga, G. de Haan and R. P. Coppes (2008). "Rescue of Salivary Gland Function after Stem Cell Transplantation in Irradiated Glands." PLOS ONE 3(4): e2063.

Maria, O. M., A. Zeitouni, O. Gologan and S. D. Tran (2011). "Matrigel improves functional properties of primary human salivary gland cells." Tissue Eng Part A 17(9-10): 1229-1238.

Liao R, Yang H-T, Li H, Liu L-X, Li K, Li J-J, Liang J, Hong X-P, Chen Y-L and Liu D-Z (2022) Recent Advances of Salivary Gland Biopsy in Sjögren's Syndrome. Front. Med. 8:792593. doi: 10.3389/fmed.2021.792593

Li N, Li L, Wu M, Li Y, Yang J, Wu Y, Xu H, Luo D, Gao Y, Fei X and Jiang L (2021) Integrated Bioinformatics and Validation Reveal Potential Biomarkers Associated With Progression of Primary Sjögren's Syndrome. Front. Immunol. 12:697157. doi: 10.3389/fimmu.2021.697157

Lu, P., Takai, K., Weaver, V. M., & Werb, Z. (2011). Extracellular matrix degradation and remodeling in development and disease. Cold Spring Harbor perspectives in biology, 3(12), a005058. https://doi.org/10.1101/cshperspect.a005058

Li Y, He J, Wang F, Wang X, Yang F, Zhao C, et al. Role of MMP-9 in epithelial-mesenchymal transition of thyroid cancer. World Journal of Surgical Oncology. 2020;18(1):181.

Leehan, K. M., Pezant, N. P., Rasmussen, A., Grundahl, K., Moore, J. S., Radfar, L., Lewis, D. M., Stone, D. U., Lessard, C. J., Rhodus, N. L., Segal, B. M., Scofield, R. H., Sivils, K. L., Montgomery, C., & Farris, A. D. (2018). Minor salivary gland fibrosis in Sjögren's syndrome is

elevated, associated with focus score and not solely a consequence of aging. Clinical and experimental rheumatology, 36 Suppl 112(3), 80–88.

Li N, Li L, Wu M, Li Y, Yang J, Wu Y, Xu H, Luo D, Gao Y, Fei X and Jiang L (2021) Integrated Bioinformatics and Validation Reveal Potential Biomarkers Associated With Progression of Primary Sjögren's Syndrome. Front. Immunol. 12:697157. doi: 10.3389/fimmu.2021.697157

Min, H.K., Moon, SJ., Park, KS. et al. Integrated systems analysis of salivary gland transcriptomics reveals key molecular networks in Sjögren's syndrome. Arthritis Res Ther 21, 294 (2019). https://doi.org/10.1186/s13075-019-2082-9

May, A. J., N. Cruz-Pacheco, E. Emmerson, E. A. Gaylord, K. Seidel, S. Nathan, M. O. Muench, O. D. Klein and S. M. Knox (2018). "Diverse progenitor cells preserve salivary gland ductal architecture after radiation-induced damage." Development 145(21): dev166363.

Min, S., E.-A. C. Song, A. Oyelakin, C. Gluck, K. Smalley and R.-A. Romano (2018). "Functional characterization and genomic studies of a novel murine submandibular gland epithelial cell line." PLOS ONE 13(2): e0192775.

Nam, H., J.-H. Kim, J.-Y. Hwang, G.-H. Kim, J.-W. Kim, M. Jang, J.-H. Lee, K. Park and G. Lee (2018). "Characterization of Primary Epithelial Cells Derived from Human Salivary Gland Contributing to in vivo Formation of Acini-like Structures." Molecules and cells 41(6): 515-522.

Mavragani CP, Tzioufas AG, Moutsopoulos HM. Sjögren's syndrome: autoantibodies to cellular antigens. Clinical and molecular aspects. Int Arch Allergy Immunol. 2000 Sep;123(1):46-57. doi: 10.1159/000024423. PMID: 11014971.

Molina, C., Alliende, C., Aguilera, S., Kwon, Y. J., Leyton, L., Martínez, B., Leyton, C., Pérez, P., & González, M. J. (2006). Basal lamina disorganisation of the acini and ducts of labial salivary glands from patients with Sjogren's syndrome: association with mononuclear cell infiltration. Annals of the rheumatic diseases, 65(2), 178–183. https://doi.org/10.1136/ard.2004.033837

Mignogna MD, Fedele S, Lo Russo L, Lo Muzio L, Wolff A. Sjögren's syndrome: the diagnostic potential of early oral manifestations preceding hyposalivation/xerostomia. Journal of oral pathology & medicine: official publication of the International Association of Oral Pathologists and the American Academy of Oral Pathology. 2005;34(1):1-6.

Maimets, M., Rocchi, C., Bron, R., Pringle, S., Kuipers, J., Giepmans, B. N., Vries, R. G., Clevers, H., de Haan, G., van Os, R., & Coppes, R. P. (2016). Long-Term In Vitro Expansion of Salivary Gland Stem Cells Driven by Wnt Signals. Stem cell reports, 6(1), 150–162. https://doi.org/10.1016/j.stemcr.2015.11.009

Martinez ML, Lopes LF, Coelho EB, Nobre F, Rocha JB, Gerlach RF, Tanus-Santos JE. Lercanidipine reduces matrix metalloproteinase-9 activity in patients with hypertension. J Cardiovasc Pharmacol. 2006 Jan;47(1):117-22. doi: 10.1097/01.fjc.0000196241.96759.71. PMID: 16424795.

Nakamura Y, Esnault S, Maeda T, Kelly EA, Malter JS, Jarjour NN. Ets-1 regulates TNF-alpha-induced matrix metalloproteinase-9 and tenascin expression in primary bronchial fibroblasts. J Immunol. 2004;172(3):1945-52.

Nazir SU, Kumar R, Singh A, Khan A, Tanwar P, Tripathi R, et al. Breast cancer invasion and progression by MMP-9 through Ets-1 transcription factor. Gene. 2019;711:143952.

Novak, A., Hsu, S. C., Leung-Hagesteijn, C., Radeva, G., Papkoff, J., Montesano, R., Roskelley, C., Grosschedl, R., & Dedhar, S. (1998). Cell adhesion and the integrin-linked kinase regulate the LEF-1 and beta-catenin signaling pathways. Proceedings of the National Academy of Sciences of the United States of America, 95(8), 4374–4379. https://doi.org/10.1073/pnas.95.8.4374

Nisticò, P., Bissell, M. J., & Radisky, D. C. (2012). Epithelial-mesenchymal transition: general principles and pathological relevance with special emphasis on the role of matrix metalloproteinases. Cold Spring Harbor perspectives in biology, 4(2), a011908. https://doi.org/10.1101/cshperspect.a011908

Nikolov NP, Illei GG. Pathogenesis of Sjögren's syndrome. Curr Opin Rheumatol. 2009 Sep;21(5):465-70. doi: 10.1097/BOR.0b013e32832eba21. PMID: 19568172; PMCID: PMC2766246.

Nguyen, V. T., P. Dawson, Q. Zhang, Z. Harris and K. H. Limesand (2018). "Administration of growth factors promotes salisphere formation from irradiated parotid salivary glands." PloS one 13(3): e0193942-e0193942.

Noll, B., F. Bahrani Mougeot, M. T. Brennan and J. C. Mougeot (2020). "Telomere erosion in Sjögren's syndrome: A multi-tissue comparative analysis." J Oral Pathol Med 49(1): 63-71.
Patel, R. and A. Shahane (2014). "The epidemiology of Sjögren's syndrome." Clinical epidemiology 6: 247-255.

Noll B, Bahrani Mougeot F, Brennan MT, Mougeot JC. Telomere erosion in Sjögren's syndrome: A multi-tissue comparative analysis. J Oral Pathol Med. 2020 Jan;49(1):63-71. doi: 10.1111/jop.12961. Epub 2019 Sep 29. PMID: 31529714.

Noll BD, Grdzelishvili A, Brennan MT, Mougeot FB, Mougeot JC. Immortalization of Salivary Gland Epithelial Cells of Xerostomic Patients: Establishment and Characterization of Novel Cell Lines. J Clin Med. 2020 Nov 25;9(12):3820. doi: 10.3390/jcm9123820. PMID: 33255850; PMCID: PMC7768371.

Narayanan V, Schappell LE, Mayer CR, Duke AA, Armiger TJ, Arsenovic PT, Mohan A, Dahl KN, Gleghorn JP, Conway DE. Osmotic Gradients in Epithelial Acini Increase Mechanical Tension across E-cadherin, Drive Morphogenesis, and Maintain Homeostasis. Curr Biol. 2020 Feb 24;30(4):624-633.e4. doi: 10.1016/j.cub.2019.12.025. Epub 2020 Jan 23. PMID: 31983640; PMCID: PMC7153951.

Okumura K, Nakamura K, Hisatomi Y, Nagano K, Tanaka Y, Terada K, Sugiyama T, Umeyama K, Matsumoto K, Yamamoto T, Endo F. Salivary gland progenitor cells induced by duct ligation differentiate into hepatic and pancreatic lineages. Hepatology. 2003 Jul;38(1):104-13. doi: 10.1053/jhep.2003.50259. PMID: 12829992.

Pringle, S., X. Wang, H. Bootsma, F. K. L. Spijkervet, A. Vissink and F. G. M. Kroese (2019). "Small-molecule inhibitors and the salivary gland epithelium in Sjögren's syndrome." Expert Opin Investig Drugs 28(7): 605-616.

Pringle, S., X. Wang, G. Verstappen, J. H. Terpstra, C. K. Zhang, A. He, V. Patel, R. E. Jones, D. M. Baird, F. K. L. Spijkervet, A. Vissink, H. Bootsma, R. P. Coppes and F. G. M. Kroese (2019). "Salivary Gland Stem Cells Age Prematurely in Primary Sjogren's Syndrome." Arthritis Rheumatol 71(1): 133-142.

Pedersen, A.M.L., Bardow, A. & Nauntofte, B. Salivary changes and dental caries as potential oral markers of autoimmune salivary gland dysfunction in primary Sjögren's syndrome. BMC Clin Pathol 5, 4 (2005). https://doi.org/10.1186/1472-6890-5-4

Porcheri, C., & Mitsiadis, T. A. (2019). Physiology, Pathology and Regeneration of Salivary Glands. Cells, 8(9), 976. https://doi.org/10.3390/cells8090976

Pringle S, Wang X, Verstappen GMPJ, Terpstra JH, Zhang CK, He A, Patel V, Jones RE, Baird DM, Spijkervet FKL, Vissink A, Bootsma H, Coppes RP, Kroese FGM. Salivary Gland Stem Cells Age Prematurely in Primary Sjögren's Syndrome. Arthritis Rheumatol. 2019 Jan;71(1):133-142. doi: 10.1002/art.40659. PMID: 29984480; PMCID: PMC6607019.

Peck AB, Saylor BT, Nguyen L, Sharma A, She JX, Nguyen CQ, et al. Gene expression profiling of early-phase Sjögren's syndrome in C57BL/6.NOD-Aec1Aec2 mice identifies focal adhesion maturation associated with infiltrating leukocytes. Invest Ophthalmol Vis Sci. 2011;52(8):5647-55.

Perez P, Kwon YJ, Alliende C, Leyton L, Aguilera S, Molina C, et al. Increased acinar damage of salivary glands of patients with Sjogren's syndrome is paralleled by simultaneous imbalance of matrix metalloproteinase 3/tissue inhibitor of metalloproteinases 1 and matrix

metalloproteinase 9/tissue inhibitor of metalloproteinases 1 ratios. Arthritis Rheum. 2005;52(9):2751-60.

Pertovaara, M., Korpela, M., Uusitalo, H., Pukander, J., Miettinen, A., Helin, H., & Pasternack, A. (1999). Clinical follow up study of 87 patients with sicca symptoms (dryness of eyes or mouth, or both). Annals of the rheumatic diseases, 58(7), 423–427. https://doi.org/10.1136/ard.58.7.423

Quartuccio L, Baldini C, Bartoloni E, Priori R, Carubbi F, Corazza L, Alunno A, Colafrancesco S, Luciano N, Giacomelli R, Gerli R, Valesini G, Bombardieri S, De Vita S. Anti-SSA/SSB-negative Sjögren's syndrome shows a lower prevalence of lymphoproliferative manifestations, and a lower risk of lymphoma evolution. Autoimmun Rev. 2015 Nov;14(11):1019-22. doi: 10.1016/j.autrev.2015.07.002. Epub 2015 Jul 8. PMID: 26162302.

Roescher, N., Lodde, B., Vosters, J., Tak, P., Catalan, M., Illei, G. and Chiorini, J. (2012), Temporal changes in salivary glands of non-obese diabetic mice as a model for Sjögren's syndrome. Oral Diseases, 18: 96-106. https://doi.org/10.1111/j.1601-0825.2011.01852.x

Robinson, C. P., Yamachika, S., Alford, C. E., Cooper, C., Pichardo, E. L., Shah, N., Peck, A. B., & Humphreys-Beher, M. G. (1997). Elevated Levels of Cysteine Protease Activity in Saliva and Salivary Glands of the Nonobese Diabetic (NOD) Mouse Model for Sjögren Syndrome. Proceedings of the National Academy of Sciences of the United States of America, 94(11), 5767–5771. http://www.jstor.org/stable/42150

Risselada AP, Kruize AA, Goldschmeding R, et al. The prognostic value of routinely performed minor salivary gland assessments in primary Sjögren's syndrome Annals of the Rheumatic Diseases 2014;73:1537-1540.

Radfar L, Kleiner DE, Fox PC, Pillemer SR. Prevalence and clinical significance of lymphocytic foci in minor salivary glands of healthy volunteers. Arthritis Rheum. (2002) 47:520–4. doi: 10.1002/art.10668

Risselada AP, Looije MF, Kruize AA, Bijlsma JW, van Roon JA. The role of ectopic germinal centers in the immunopathology of primary Sjögren's syndrome: a systematic review. Semin Arthritis Rheum. 2013 Feb;42(4):368-76. doi: 10.1016/j.semarthrit.2012.07.003. Epub 2012 Sep 18. PMID: 22995442.

Radfar, L., Kleiner, D.E., Fox, P.C. and Pillemer, S.R. (2002), Prevalence and clinical significance of lymphocytic foci in minor salivary glands of healthy volunteers. Arthritis & Rheumatism, 47: 520-524. https://doi.org/10.1002/art.10668

Robinson CP, Yamamoto H, Peck AB, Humphreys-Beher MG. Genetically programmed development of salivary gland abnormalities in the NOD (nonobese diabetic)-scid mouse in the absence of detectable lymphocytic infiltration: a potential trigger for sialoadenitis of NOD mice. Clinical immunology and immunopathology. 1996;79(1):50-9.

Schindelin, J., I. Arganda-Carreras, E. Frise, V. Kaynig, M. Longair, T. Pietzsch, S. Preibisch, C. Rueden, S. Saalfeld, B. Schmid, J. Y. Tinevez, D. J. White, V. Hartenstein, K. Eliceiri, P. Tomancak and A. Cardona (2012). "Fiji: an open-source platform for biological-image analysis." Nat Methods 9(7): 676-682.

Satyanarayana, A., R. A. Greenberg, S. Schaetzlein, J. Buer, K. Masutomi, W. C. Hahn, S. Zimmermann, U. Martens, M. P. Manns and K. L. Rudolph (2004). "Mitogen stimulation cooperates with telomere shortening to activate DNA damage responses and senescence signaling." Molecular and cellular biology 24(12): 5459-5474.

Shiboski CH, Shiboski SC, Seror R, Criswell LA, Labetoulle M, Lietman TM, et al. 2016 American College of Rheumatology/European League Against Rheumatism Classification Criteria for Primary Sjogren's Syndrome: A Consensus and Data-Driven Methodology Involving Three International Patient Cohorts. Arthritis Rheumatol. 2017;69(1):35-45

Shiboski, C. H., Baer, A. N., Shiboski, S. C., Lam, M., Challacombe, S., Lanfranchi, H. E., Schiødt, M., Shirlaw, P., Srinivasan, M., Umehara, H., Vivino, F. B., Akpek, E., Bunya, V., Vollenweider, C. F., Greenspan, J. S., Daniels, T. E., Criswell, L. A., & Sjögren's International Collaborative Clinical Alliance Research Groups (2018). Natural History and Predictors of Progression to Sjögren's Syndrome Among Participants of the Sjögren's International Collaborative Clinical Alliance Registry. Arthritis care & research, 70(2), 284–294. https://doi.org/10.1002/acr.23264

Scott LE, Weinberg SH and Lemmon CA (2019) Mechanochemical Signaling of the Extracellular Matrix in Epithelial-Mesenchymal Transition. Front. Cell Dev. Biol. 7:135. doi: 10.3389/fcell.2019.00135

Singh, N., & Cohen, P. L. (2012). The T cell in Sjogren's syndrome: force majeure, not spectateur. Journal of autoimmunity, 39(3), 229–233. https://doi.org/10.1016/j.jaut.2012.05.019

Solans-Laqué R, López-Hernandez A, Bosch-Gil JA, Palacios A, Campillo M, Vilardell-Tarres M. Risk, predictors, and clinical characteristics of lymphoma development in primary Sjögren's syndrome. Semin Arthritis Rheum. 2011 Dec;41(3):415-23. doi: 10.1016/j.semarthrit.2011.04.006. Epub 2011 Jun 12. PMID: 21665245.

Sebastian, A., Sebastian, M., Misterska-Skóra, M., Woytala, P., Jakuszko, K., & Wiland, P. (2018). How to Distinguish Patients with pSS among Individuals with Dryness without Invasive Diagnostic Studies. Journal of immunology research, 2018, 1060421. https://doi.org/10.1155/2018/1060421

Srivastava, A., & Makarenkova, H. P. (2020). Innate Immunity and Biological Therapies for the Treatment of Sjögren's Syndrome. International journal of molecular sciences, 21(23), 9172. https://doi.org/10.3390/ijms21239172

Schenke-Layland K, Xie J, Angelis E, Starcher B, Wu K, Riemann I, et al. Increased degradation of extracellular matrix structures of lacrimal glands implicated in the pathogenesis of Sjögren's syndrome. Matrix Biol. 2008;27(1):53-66.

Sequeira SJ, Larsen M, DeVine T. Extracellular matrix and growth factors in salivary gland development. Frontiers of oral biology. 2010;14:48-77.

Santiago L, Daniels G, Wang D, Deng F-M, Lee P. Wnt signaling pathway protein LEF1 in cancer, as a biomarker for prognosis and a target for treatment. Am J Cancer Res. 2017;7(6):1389-406.

Shah NR, Noll BD, Stevens CB, Brennan MT, Mougeot FB, Mougeot JC. Biosemantics guided gene expression profiling of Sjogren's syndrome: a comparative analysis with systemic lupus erythematosus and rheumatoid arthritis. Arthritis Res Ther. 2017;19(1):192.

Shah NR, Noll BD, Padilla RJ, Brennan MT, Mougeot FB, Mougeot J-LC. Expression of ETS1 and LEF1 in salivary glands of Sjögren syndrome patients. Oral Diseases. 2019;25(1):164-73.

Sisto M, Lisi S, Ribatti D. The role of the epithelial-to-mesenchymal transition (EMT) in diseases of the salivary glands. Histochem Cell Biol. 2018 Aug;150(2):133-147. doi: 10.1007/s00418-018-1680-y. Epub 2018 May 23. PMID: 29789993.

Sullivan KE, Piliero LM, Dharia T, Goldman D, Petri MA. 3' polymorphisms of ETS1 are associated with different clinical phenotypes in SLE. Hum Mutat. 2000;16(1):49-53. doi: 10.1002/1098-1004(200007)16:1<49::AID-HUMU9>3.0.CO;2-Z. PMID: 10874305.

Suh Y, Yoon CH, Kim RK, Lim EJ, Oh YS, Hwang SG, An S, Yoon G, Gye MC, Yi JM, Kim MJ, Lee SJ. Claudin-1 induces epithelial-mesenchymal transition through activation of the c-Abl-ERK signaling pathway in human liver cells. Oncogene. 2013 Oct 10;32(41):4873-82. doi: 10.1038/onc.2012.505. Epub 2012 Nov 19. Erratum in: Oncogene. 2017 Feb 23;36(8):1167-1168. PMID: 23160379.

Shin, H.-S., H. J. Hong, W.-G. Koh and J.-Y. Lim (2018). "Organotypic 3D Culture in Nanoscaffold Microwells Supports Salivary Gland Stem-Cell-Based Organization." ACS Biomaterials Science & Engineering 4(12): 4311-4320.

Shirasuna, K., M. Sato and T. Miyazaki (1981). "A neoplastic epithelial duct cell line established from an irradiated human salivary gland." Cancer 48(3): 745-752.

Shubin, A. D., A. Sharipol, T. J. Felong, P.-L. Weng, B. E. Schutrum, D. S. Joe, M. H. Aure, D. S. W. Benoit and C. E. Ovitt (2020). "Stress or injury induces cellular plasticity in salivary gland acinar cells." Cell and Tissue Research 380(3): 487-497.

Sisto, M., R. Tamma, D. Ribatti and S. Lisi (2020). "IL-6 Contributes to the TGF-β1-Mediated Epithelial to Mesenchymal Transition in Human Salivary Gland Epithelial Cells." Arch Immunol Ther Exp (Warsz) 68(5): 27.

Su, L., P. R. Morgan, D. L. Harrison, A. Waseem and E. B. Lane (1993). "Expression of keratin mRNAS and proteins in normal salivary epithelia and pleomorphic adenomas." The Journal of Pathology 171(3): 173-181.

Tandon M, Perez P, Burbelo PD, Calkins C, Alevizos I. Laser microdissection coupled with RNA-seq reveal cell-type and disease-specific markers in the salivary gland of Sjogren's syndrome patients. Clin Exp Rheumatol. 2017;35(5):777-85.

Tanner RM, Lynch AI, Brophy VH, Eckfeldt JH, Davis BR, et al. (2011) Pharmacogenetic Associations of MMP9 and MMP12 Variants with Cardiovascular Disease in Patients with Hypertension. PLOS ONE 6(8): e23609. https://doi.org/10.1371/journal.pone.0023609

Taco A van der Meulen, Hermie J M Harmsen, Hendrika Bootsma, Silvia C Liefers, Arnau Vich Vila, Alexandra Zhernakova, Jingyuan Fu, Cisca Wijmenga, Fred K L Spijkervet, Frans G M Kroese, Arjan Vissink, Dysbiosis of the buccal mucosa microbiome in primary Sjögren’s

syndrome patients, Rheumatology, Volume 57, Issue 12, December 2018, Pages 2225–2234, https://doi.org/10.1093/rheumatology/key215

Teos, L., Zhang, Y., Cotrim, A. et al. IP3R deficit underlies loss of salivary fluid secretion in Sjögren's Syndrome. Sci Rep 5, 13953 (2015). https://doi.org/10.1038/srep13953

Taki M, Verschueren K, Yokoyama K, Nagayama M, Kamata N. Involvement of Ets-1 transcription factor in inducing matrix metalloproteinase-2 expression by epithelial-mesenchymal transition in human squamous carcinoma cells. International journal of oncology. 2006;28(2):487-96.

Teng, Y., Cang, B., Mao, F. et al. Expression of ETS1 in gastric epithelial cells positively regulate inflammatory response in Helicobacter pylori-associated gastritis. Cell Death Dis 11, 498 (2020). https://doi.org/10.1038/s41419-020-2705-8

Theander E, Jonsson R, Sjostrom B, Brokstad K, Olsson P, Henriksson G. Prediction of Sjogren's Syndrome Years Before Diagnosis and Identification of Patients With Early Onset and Severe Disease Course by Autoantibody Profiling. Arthritis Rheumatol. 2015;67(9):2427-36

Wang, Y., S. Chen, Z. Yan and M. Pei (2019). "A prospect of cell immortalization combined with matrix microenvironmental optimization strategy for tissue engineering and regeneration." Cell & bioscience 9: 7-7.

Vu TH, Werb Z. Matrix metalloproteinases: effectors of development and normal physiology. Genes Dev. 2000 Sep 1;14(17):2123-33. doi: 10.1101/gad.815400. PMID: 10970876.

Verstappen, G. M., Gao, L., Pringle, S., Haacke, E. A., van der Vegt, B., Liefers, S. C., Patel, V., Hu, Y., Mukherjee, S., Carman, J., Menard, L. C., Spijkervet, F., Vissink, A., Bootsma, H., & Kroese, F. (2021). The Transcriptome of Paired Major and Minor Salivary Gland Tissue in Patients With Primary Sjögren's Syndrome. Frontiers in immunology, 12, 681941. https://doi.org/10.3389/fimmu.2021.681941

Velozo J, Aguilera S, Alliende C, et alSevere alterations in expression and localisation of α6β4 integrin in salivary gland acini from patients with Sjögren syndrome. Annals of the Rheumatic Diseases 2009;68:991-996.

Werner MH, Burley SK. Architectural transcription factors: proteins that remodel DNA. Cell. 1997;88(6):733-6.

Wang D, John SA, Clements JL, Percy DH, Barton KP, Garrett-Sinha LA. Ets-1 deficiency leads to altered B cell differentiation, hyperresponsiveness to TLR9 and autoimmune disease. Int Immunol. 2005 Sep;17(9):1179-91. doi: 10.1093/intimm/dxh295. Epub 2005 Jul 28. PMID: 16051621.

Wei, P., Li, C., Qiang, L., He, J., Li, Z., & Hua, H. (2015). Role of salivary anti-SSA/B antibodies for diagnosing primary Sjögren's syndrome. Medicina oral, patologia oral y cirugia bucal, 20(2), e156–e160. https://doi.org/10.4317/medoral.20199

Wiseman BS, Sternlicht MD, Lund LR, Alexander CM, Mott J, Bissell MJ, Soloway P, Itohara S, Werb Z. Site-specific inductive and inhibitory activities of MMP-2 and MMP-3 orchestrate mammary gland branching morphogenesis. J Cell Biol. 2003 Sep 15;162(6):1123-33. doi: 10.1083/jcb.200302090. PMID: 12975354; PMCID: PMC2172848.

Wu D, Witt RL, Harrington DA and Farach-Carson MC (2019) Dynamic Assembly of Human Salivary Stem/Progenitor Microstructures Requires Coordinated α1β1 Integrin-Mediated Motility. Front. Cell Dev. Biol. 7:224. doi: 10.3389/fcell.2019.00224

Wakako Kobayashi, Masayuki Ozawa. The epithelial-mesenchymal transition induced by transcription factor LEF-1 is independent of β-catenin, Biochemistry and Biophysics Reports, Volume 15, 2018, Pages 13-18, ISSN 2405-5808, https://doi.org/10.1016/j.bbrep.2018.06.003.

Weng PL, Aure MH, Maruyama T, Ovitt CE. Limited Regeneration of Adult Salivary Glands after Severe Injury Involves Cellular Plasticity. Cell Rep. 2018 Aug 7;24(6):1464-1470.e3. doi: 10.1016/j.celrep.2018.07.016. PMID: 30089258; PMCID: PMC6350767.

Warner, K. A., A. Adams, L. Bernardi, C. Nor, K. A. Finkel, Z. Zhang, S. A. McLean, J. Helman, G. T. Wolf, V. Divi, L. Queimado, F. J. Kaye, R. M. Castilho and J. E. Nör (2013). "Characterization of tumorigenic cell lines from the recurrence and lymph node metastasis of a human salivary mucoepidermoid carcinoma." Oral oncology 49(11): 1059-1066.

Wise CM, Woodruff RD. Minor salivary gland biopsies in patients investigated for primary Sjögren's syndrome. A review of 187 patients. J Rheumatol. 1993 Sep;20(9):1515-8. PMID: 8164207.

Yang, Ling-Xiaa; Guo, Hu-Bingb; Liu, Sui-Yuana; Feng, Hong-Pinga; Shi, Jina ETS1 promoted cell growth, metastasis and epithelial–mesenchymal transition process in melanoma by regulating miR-16-mediated SOX4 expression, Melanoma Research: August 2021 - Volume 31 - Issue 4 - p 298-308 doi: 10.1097/CMR.0000000000000743

Yang, J., Antin, P., Berx, G. et al. Guidelines and definitions for research on epithelial–mesenchymal transition. Nat Rev Mol Cell Biol 21, 341–352 (2020).

You, S., Avidan, O., Tariq, A., Ahluwalia, I., Stark, P. C., Kublin, C. L., & Zoukhri, D. (2012). Role of epithelial-mesenchymal transition in repair of the lacrimal gland after experimentally induced injury. Investigative ophthalmology & visual science, 53(1), 126–135.

Yoshimi, R., Ueda, A., Ozato, K., & Ishigatsubo, Y. (2012). Clinical and pathological roles of Ro/SSA autoantibody system. Clinical & developmental immunology, 2012, 606195.

Zhang J, Jamaluddin M, Zhang Y, Widen SG, Sun H, Brasier AR, Zhao Y. Type II Epithelial-Mesenchymal Transition Upregulates Protein N-Glycosylation to Maintain Proteostasis and Extracellular Matrix Production. J Proteome Res. 2019 Sep 6;18(9):3447-3460. doi: 10.1021/acs.jproteome.9b00342. Epub 2019 Aug 28. PMID: 31424945; PMCID: PMC7195216

Zhang K, Zhou Y, Cheng X, Fu X, Du W, Feng Y, Jia J, Yang X, Xiao G, Zheng Z, Zhu P, Wu Z. Epithelial Cell Adhesion Molecule in Primary Sjögren's Syndrome Patients: Characterization and Evaluation of a Potential Biomarker. J Immunol Res. 2019 Dec 5;2019:3269475. doi: 10.1155/2019/3269475. PMID: 31886299; PMCID: PMC6915146

Zervoudaki, A., Economou, E., Stefanadis, C. et al. Plasma levels of active extracellular matrix metalloproteinases 2 and 9 in patients with essential hypertension before and after antihypertensive treatment. J Hum Hypertens 17, 119–124 (2003).

APPENDIX A: Publications

Publications:

1. **Braxton Noll**, Farah Bahrani Mougeot, Michael T Brennan, Jean-Luc C Mougeot. 2022. **“**Dissecting the salivary gland: epithelial-centered dysfunction in primary Sjögren’s Syndrome.” Manuscript in preparation.
2. **Braxton Noll**, Farah Bahrani Mougeot, Michael T Brennan, Jean-Luc C Mougeot. 2022. “Regulation of MMP9 transcription by ETS1 in immortalized salivary gland epithelial cells of xerostomic and primary Sjögren’s syndrome patients.” Manuscript in Review.
3. **Noll BD**, Bahrani Mougeot F, Brennan MT, Mougeot JC. Telomere erosion in Sjögren's syndrome: A multi-tissue comparative analysis. J Oral Pathol Med. 2020 Jan;49(1):63-71. doi: 10.1111/jop.12961. Epub 2019 Sep 29. PMID: 31529714.
4. **Noll BD**, Grdzelishvili A, Brennan MT, Mougeot FB, Mougeot JC. Immortalization of Salivary Gland Epithelial Cells of Xerostomic Patients: Establishment and Characterization of Novel Cell Lines. J Clin Med. 2020 Nov 25;9(12):3820. doi: 10.3390/jcm9123820. PMID: 33255850; PMCID: PMC7768371.
5. Mougeot JL, **Noll BD**, Bahrani Mougeot FK. Sjögren's syndrome X-chromosome dose effect: An epigenetic perspective. Oral Dis. 2019 Mar;25(2):372-384. doi: 10.1111/odi.12825. Epub 2018 Apr 19. PMID: 29316023.
6. Shah NR, **Noll BD**, Padilla RJ, Brennan MT, Mougeot FB, Mougeot JC. Expression of ETS1 and LEF1 in salivary glands of Sjögren syndrome patients. Oral Dis. 2019 Jan;25(1):164-173. doi: 10.1111/odi.12985. Epub 2018 Oct 22. PMID: 30270548.
7. Shah NR, **Noll BD**, Stevens CB, Brennan MT, Mougeot FB, Mougeot JC. Biosemantics guided gene expression profiling of Sjögren's syndrome: a comparative analysis with systemic lupus erythematosus and rheumatoid arthritis. Arthritis Res Ther. 2017 Aug 17;19(1):192. doi: 10.1186/s13075-017-1400-3. PMID: 28818099; PMCID: PMC5561593.

APPENDIX B: Supplementary Methods

Salivary gland cell lines: HMC-3A, A253, iSGEC-nSS2, and iSGEC-pSS1

A253 cells were purchased from the ATCC and cultured in McCoys 5A media (Lonza/ Hyclone) supplemented with 10% fetal bovine serum (FBS) and 2mM L-glutamine (Corning). HMC-3A cells were cultured in DMEM (High glucose + sodium pyruvate) (Lonza/ Hyclone) supplemented with (final concentration): 10% FBS (VWR), 20ng/mL EGF (Gibco), 5µg/mL insulin (MP Bio), 400ng/mL hydrocortisone (Sigma), and 2mM L-glutamine (Corning). Cells were grown (37°C; 5% CO2) for routine passaging in T-75 flask until 80-90% confluency. Trypsinization was completed using 0.25% Trypsin+ .053mM EDTA (Corning). Cultures were serum starved for 24hrs prior experimentation. Transfection experiments were carried out in basal media for HMC-3A and iSGEC cells, whereas after the 24hr serum starvation, Human Keratinocyte Growth Supplement (HKGS) (1x) (Gibco, Catalog# S0015) was added to the A253 basal media as a source of EGF to ensure consistency among experimental cell lines and their respective growth media. Both media formulations for HMC-3A and iSGEC's contain EGF, which is known to affect MMP9 expression as assessed by O-Charoenrat, P *et al*., (Overexpression of epidermal growth factor receptor in human head and neck squamous carcinoma cell lines correlates with matrix metalloproteinase-9 expression and in vitro invasion. (2000) Int. J. Cancer, 86: 307-317.).

Primary culture of salivary gland epithelial cells

Excess labial salivary gland (LSG) biopsy tissue was placed in basal epithelial media (1:3 DMEM/Ham's F12) supplemented with 5x antibiotic/ antimycotic (stock concentration= 100x) (Gibco), 2.5% FBS, insulin (500ng/ mL), hydrocortisone (400ng/ mL), epidermal growth factor (10ng/ mL), for transport to the laboratory. LSG tissue was washed (2x) in PBS containing 1x antibiotic/ antimycotic and minced into approximately 0.5-1mm^2 pieces with multiple fragments seeded into T-75 flask. Cell were cultured in basal media (with antibiotic/ antimycotic reduced to

1x) for approximately two weeks or until reaching 70-80% confluency. Cells were washed with DPBS and removed from the flask using 0.05% trypsin+ EDTA. Trypsin was inactivated using soybean trypsin inhibitor (1:1) and the supernatant removed by centrifugation (6min, 600xg). SGECs were transferred into T-75 collagen coated flask and media switched to EpiLife Basal media (Gibco, Catalog# MEPI500CA) supplemented with HKGS (1x) (Gibco). SGECs were cultured until 70-80% confluency with residual fibroblast removed using 0.02% EDTA in DPBS. Morphologically consistent SGEC cultures were trypsinized (0.05% trypsin+ EDTA) between passages 2-4 and transferred to collagen coated 6-well tissue culture treated plates for mRNA isolation. SGECs were routinely plated on collagen-coated coverslips for epithelial confirmation by IF expression of Cytokeratin 8/18.

siRNA knockdown and transient transfection

A253 and HMC-3A cells were plated in 6-well plates 24hrs prior transfection at a concentration of 0.3-.5 x 10^6 cells per well. siRNA was transfected at a concentration of 50nM using 3µL of Lipofectamine 3000 suspended in opti-MEM (ThermoFisher) at a volume of 200µL. A concentration of 50nM ETS1 siRNA and LEF1 siRNA each were used for dual knockdown and did not indicate increased toxicity when compared to 50nM or 100nM of non-targeting siRNA control. The transfection mixture was added dropwise to each well containing 1.8mL of media. iSGECs were plated in 6-well plates 24-hrs prior transfection at a concentration of 8x105 cells per well. siRNA was transfected at a concentration of 25nM using 1.5µL of Lipofectamine 3000 with opti-MEM at a volume of 200µL. The transfection mixture was added dropwise to each well containing 1.8mL of media.

Western blot

Proteins were isolated using Mammalian Protein Extraction Buffer (M-PER) (Pierce) following the manufacturers' recommended protocol with the addition of protease inhibitor cocktail (Millipore-Sigma). Protein extracts were briefly sonicated, and the insoluble lysate fraction removed by centrifugation (5000xg, 5min). Samples were first measured by Bradford assay and then mixed with 6x Laemmli buffer. After boiling (5min, 95°C), equal protein concentrations were loaded into and resolved by SDS-polyacrylamide gel electrophoresis (Biorad). Proteins were transferred and visualized on nitrocellulose membranes blocked with 5% nonfat dried skim milk in TBS with 0.1% Tween-20 for 1hr at RT. Primary antibodies were added at concentrations listed in Table 3.6.3 and incubated overnight at 4°C. Membranes were washed (3x, 5min each) and incubated with the appropriate HRP-conjugated secondary antibody for 1hr at RT. Samples were normalized to either cofilin or cyclophilin A expression and visualized with an ImageQuant-LS4000 (GE). Densitometric measurements were acquired using Li-COR Image Studio Lite software (Ver. 5.2). Due to the overlapping sizes and cross-reactivity of antibodies, blots were frequently cut into horizontal, transverse sections corresponding to their target's size before incubation with primary antibodies. Western blot images displayed as separate sections originate from the same experiment. Furthermore, to alleviate the cross-reactivity of secondary antibodies, blots were incubated with 30% H_2O_2 for 10 min, and then washed with TBST (3x, 5min each) to inhibit residual HRP-conjugated secondary for any subsequent blotting.

Chromatin immunoprecipitation (CHIP) assays

ChIP assays were performed using the EpiQuick Tissue Chromatin Immunoprecipitation Kit (Epigentek, Catalog# P-2003) following the manufactures recommended protocol with slight modifications. Cells were fixed with 1% formaldehyde for 12min at RT. After decrosslinking, nuclear extracts were sonicated on ice (8x, 20sec, 1min rest on ice in-between each cycle) to generate roughly 200-1000bp sized fragments. Antibodies (2µg of ETS1 antibody or mouse IgG (negative control)) were added to wells and allowed to bind for 1hr at RT before blocking with

2% BSA+ calf thymus DNA (100µg/ml) in PBS (4hrs, 4°C). Prior to immunoprecipitation, cell lysates were precleared in a single unblocked well (4hrs, 4°C). Samples were split equally among the negative control (mouse IgG) and experimental (ETS1 antibody) blocked wells for incubation overnight at 4°C. Wells were extensively washed before subsequent elution, decrosslinking, and DNA purification. qPCR was performed using standard methods with primers targeting the MMP9 promoter region from -197bp to -421bp . Experimental samples and controls (mouse IgG) were normalized to 5% of the initial input of non-immunoprecipitated DNA.

ELISA

MMP9 secretion into media was measured by QuickZYME MMP9 (Quicktime Biosciences) assay following the manufactured recommended protocol. Briefly, cells were cultured in serum free media (without HKGS) for 24hrs, washed with PBS, and replaced with complete media before subjection to siRNA knockdown using the methods previously outlined. After 72hrs media was harvested for total MMP9 quantification and normalized to total cellular protein, as determined by Bradford assay (Thermo). Experimental fold changes were determined by comparison to the non-targeting siRNA control.

Promoter truncates and site directed mutagenesis

Preliminary putative ETS1 transcription factor binding sites on the MMP9 proximal promoter region were determined initially using the online tools ALGEN-PROMO. Mutations of five consensus ETS1 (5'-GGA/T-3') binding sites (EBS) between -216bp to -366bp: EBS-MUT1 (-336bp to -332bp), EBS-MUT2 (-329bp to -323bp), EBS-MUT1+2 (-336bp to -332bp and -329bp to -323bp), EBS-MUT3 (-313bp to -309bp), EBS-MUT4, (-288bp to -284bp), EBS-MUT5 (-233bp to -229bp) were generated using the Site Directed Mutagenesis Kit (NEB) following the manufacturers' recommended protocol. Mutant plasmids and constructs were verified by sanger sequencing and restriction digestion.

Detection of iSGECs protein markers by Immunofluorescence

iSGECs were cultured on 8-well chambered slides (Thermo) coated with gelatin (0.2%) for 24-48hrs prior fixation with 4% PFA in PBS (12min, RT). Fixed cells were permeabilized with 0.2% Triton X-100 in PBS supplemented with 2% BSA for 25min. Slides were subsequently blocked with 5% BSA and 0.1% Tween-20 in PBS (1hr, RT). Cells were incubated with primary antibodies overnight (4°C). Following incubation, cells were washed 3x for 15min (total) at RT in PBS and incubated with secondary antibodies conjugated to fluorescent probes (1hr, RT). Cells were mounted with fluoroshield aqueous mounting media with DAPI (AbCAM) to counterstain nuclei. Slides were viewed on an Olympus BX51 fluorescence microscope (Shinjuku City, Tokyo, Japan) and photographs taken using a mounted Olympus DP70 camera (Shinjuku City, Tokyo, Japan).